In presenting the dissertation as a partial fulfillment of the requirements for an advanced degree from the Georgia Institute of Technology, I agree that the Library of the Institute shall make it available for inspection and circulation in accordance with its regulations governing materials of this type. I agree that permission to copy from, or to publish from, this dissertation may be granted by the professor under whose direction it was written, or, in his absence, by the Dean of the Graduate Division when such copying or publication is solely for scholarly purposes and does not involve potential financial gain. It is understood that any copying from, or publication of, this dissertation which involves potential financial gain will not be allowed without written permission.

[redacted]

7/25/68

LOCALIZED SCOUR AROUND A VERTICAL CIRCULAR PILE IN OSCILLATORY FLOW

A THESIS

Presented to

The Faculty of the Graduate Division

by

Hilmi Dogan Altinbilek

In Partial Fulfillment

of the Requirements for the Degree

Doctor of Philosophy

In the School of Civil Engineering

Georgia Institute of Technology

October, 1969

LOCALIZED SCOUR AROUND A VERTICAL

CIRCULAR PILE IN OSCILLATORY FLOW

Approved:

Chairman

Date approved by Chairman: Oct 22, 1969

ACKNOWLEDGMENTS

The writer would like to express his gratitude to Dr. M. R. Carstens for his valuable guidance, criticisms, and patience throughout the duration of this study; he initially suggested the problem, supervised the work and served as the chairman of the thesis reading committee. The other members of the reading committee, to whom the writer is also thankful, were Dr. C. S. Martin and Dr. R. D. Barksdale. Mr. Homer Bates, senior laboratory technician, provided expert assistance in carrying out the experimental program. Assistance from Miss Judy Wilkinson in typing the original manuscript is also acknowledged.

This study was carried out under the sponsorship of the U. S. Army Coastal Engineering Research Center, Contract No. DACW72-67-0017. The Georgia Institute of Technology has provided the large amount of computer time necessary for the analysis of the data.

TABLE OF CONTENTS

TABLE OF CONTENTS (Continued)

LIST OF TABLES

LIST OF FIGURES

Figure Page

TEXT

LIST OF FIGURES (Continued)

NOMENCLATURE

TEXT

Symbol	Quantity	Dimensions (F,L,T)
a	Amplitude of water motion (2a is total amplitude)	L
a_c	Amplitude of water motion at deformed-bed incipient-motion condition	L
B	Width of the channel	L
C_D'	Coefficient of drag of particle falling in a quiescent infinite fluid	None
D	Cylinder diameter	L
D_g	Geometric-mean sediment diameter	L
$f\ (\ )$	Function of	None
g	Magnitude of acceleration of gravity	LT^{-2}
H	Wave height	L
h	Distance from mean water level to bottom	L
K_0, K_1, K_2, K_3	Dimensionless coefficients	None
L	Length, Wave Length	L
N_s	Sediment number $(U_m / \sqrt{(s-1)g\ D_g})$	None
Q_{si}	Sediment discharge into scour hole (solids plus voids)	L^3T^{-1}
Q_{so}	Sediment discharge out of scour hole (solids plus voids)	L^3T^{-1}
Q_s'	Sediment discharge (solids)	L^3T^{-1}

NOMENCLATURE (Continued)

Symbol	Quantity	Dimensions (F,L,T)
R	Sediment Reynold's number (UD_g/ν)	None
S	Scour depth	L
s	Ratio of solids density to water density	None
S_T	Terminal scour depth	L
T	Period of oscillation	T
t	Time	T
U	Mean velocity	LT^{-1}
u	Velocity at particle level	LT^{-1}
u_e	Pickup velocity	LT^{-1}
U_m	Maximum velocity of oscillatory flow above the bed	LT^{-1}
V	Volume	L^3
α	Angle of inclination of the bed from the horizontal	None
γ	Specific weight of the fluid	FL^{-3}
γ_s	Specific weight of the bed material	FL^{-3}
σ_g	Geometric standard deviation of bed material as to size	None
ν	Kinematic viscosity	L^2T^{-1}
ϕ	Angle of repose	None
	APPENDIX	
C_D	Coefficient of drag on a particle lying on the surface of the bed	None
C_D'	Coefficient of drag on a particle falling in a quiescent fluid	None

NOMENCLATURE (Continued)

Symbol	Quantity	Dimensions (F,L,T)
C_L	Coefficient of lift on a particle lying on the surface of the bed	None
D_g	Geometric mean diameter of sediment particles	L
F_D	Drag force on a typical particle lying on the surface of the bed	F
F_L	Lift force on a typical particle lying on the surface of the bed	F
F_N	Summation of the external forces on a particle in a direction normal to the bed (+ downward)	F
F_T	Summation of the external forces on a particle in a direction parallel to the bed (+ in direction of flow)	F
g	Magnitude of the acceleration of gravity	LT^{-2}
K	$2\ k_3/k_1k_2$	None
k_1, k_2	Particle-shape coefficient (Projected area)	None
k_3	Particle-shape coefficient (volume)	None
k_4	C_D/C_D'	None
s	Specific-weight ratio, γ_s/γ	None
U	Mean velocity in the test section	LT^{-1}
u	Velocity at particle level	LT^{-1}
u_c	Value of u at beginning of particle motion	LT^{-1}
u_d	Deposit velocity, that is, the velocity that the bed surface moves due to deposition	LT^{-1}

NOMENCLATURE (Concluded)

Symbol	Quantity	Dimensions (F,L,T)
u_e	Pickup velocity, that is, the velocity that the bed surface moves due to scour	LT^{-1}
u_t	Velocity of bed movement, $u_d - u_e$	LT^{-1}
W	Submerged weight of a typical particle	F
x	Distance from the sediment-supply tube to the virtual origin of the laminar boundary layer	L
y	Coordinate normal to bed (+ upward)	L
α	Angle of inclination of the bed from the horizontal;	None
γ	Specific weight of the fluid;	FL^{-3}
γ_s	Specific weight of the bed material;	FL^{-3}
ν	Kinematic viscosity;	L^2T^{-1}
ρ	Fluid density	FT^2L^{-4}
σ_g	Geometric standard deviation of bed material as to size;	None
τ	Boundary shear stress;	FL^{-2}
ϕ	Angle of repose	None

SUMMARY

A method has been presented for analyzing the localized scour which develops around a single vertical circular cylinder in a cohesionless bed under the action of first-order Stokian water waves. The analysis of localized scour is based upon the conservation of mass with the scour hole as the control volume. The total differential equation is separable in which the differential time is equal to the differential volume divided by the difference in volume rate of flow of sediment out of and into the scour hole. The approach is to analyze the three terms (differential volume, sediment-transport rate in, and sediment-transport rate out) separately and then to integrate the differential equation to obtain scour depth as a function of time.

Scour-hole geometry in unconsolidated bed material is closely approximated by an inverted frustum of a right circular cone because the sides of the scour hole are inclined at about the angle of repose of the bed material. The differential volume in terms of the scour depth is determined from the configuration of the scour hole.

The rate that sediment is transported out of the scour hole is assumed to be proportional to a product of two subfunctions. The first subfunction is a sediment-pickup function of coefficient of drag, particle diameter, bed slope, angle of repose and fluid density in the vicinity of the particle. The variables of the first subfunction are established by consideration of the forces acting on a typical surface particle. The functional relationship is established by the results of

LeFeuvre's experimental study. The sediment-pickup function is assumed to be applicable to all localized scouring situations. The second subfunction is a function of the scour-hole geometry, sediment-grain geometry and scour depth.

The rate that sediment is transported into the scour hole from upstream is also assumed to be a product of two subfunctions. The first subfunction which is a bed-load transport function of flow, fluid and sediment variables, is established by consideration of the surface forces acting on a typical surface particle on a flat bed. The work of others, principally Stein, Rathbun and Guy, and work at Colorado State University are used to determine the functional relationship of first subfunction in unidirectional flow. Bed-load transport functions of oscillatory flow are written using analogous functions of unidirectional flow. The second subfunction is a function of the scour-hole geometry.

Model tests were used to determine the second subfunctions of input and output sediment-transport rates. Model tests were performed utilizing the oscillatory-flow water tunnel of Hydraulics Laboratory of Georgia Institute of Technology. The amplitude of water motion was a controlled variable. The period of oscillation is essentially constant in all runs. Two sizes of bed material and six sizes of cylindrical pile are tested. Model tests are performed without dunes on the bed because dunes alter the flow pattern in the model. The gap in model tests is bridged using the similarity laws.

Measured scour depth is compared with the predicted scour depth for 13 model tests. Preparation of general scour-depth-versus-time

curves is demonstrated. The terminal scour depth, and the influence of the bed forms upon the localized scour around a circular cylinder are discussed. To illustrate the application of the similarity criterion to realistic situations, numerical examples are presented.

CHAPTER I

INTRODUCTION

Definition of the Problem

The subject of this study is an investigation of the localized scour which develops in a cohesionless bed around a single vertical circular pile subjected to first-order Stokian water waves. The object is to establish similarity relations for localized scour by means of rational analysis and experiments involving localized scour.

Local scour is the local erosion phenomena as around bridge piers or at the base of outlet structures. The prevention of damaging scour and prediction of the extent of local scour are important in the design of the hydraulic structures.

Localized scour will occur where the water has been accelerated as it moves past the obstruction in the stream or where large vortices are generated as the flow separates from the obstruction. Localized scouring situations are characterized by continual change of boundary geometry with time. The changes in flow boundary are accompanied with alterations in flow pattern and in capacity of flow to excavate and remove the sediment. A theoretical analysis of local scour would have to combine a prediction of flow pattern and a prediction of the local transport capacity of the flow. The problem is to obtain rational functions for rate of sediment transport into and out of a scour hole. These functions can then be incorporated into the equation of continuity of sediment for the scour hole in order to obtain the change in scour hole

volume with time.

Review of Literature

Localized scour around bridge piers or at the base of outlet structures in unidirectional flow has been investigated by many researchers, but no study has been reported concerning the scour which develops around a single vertical pile which is subjected to wave action. The following discussion will be limited to the localized scour studies along vertical piles and piers. For a more complete review of localized scour, the reader is referred to Karaki and Haynie (1).

Schneible (2), Borhek (3), Hubbard (4), and Anderson (5), among many others, have made many field investigations on scour problems near bridge piers. Due to the overall complexity of field conditions and numerous variables involved, no generally accepted principles (not even rules of thumb) for the prediction of scour around bridge piers have evolved from prototype studies alone. It is interesting to note the recommendation that is given by Peck, Hanson, and Thornburn (6) on the design of piles in sand in their book on foundation engineering:

> No universal rule can be given for estimating the maximum depth of scour in a stream with a bottom of sand or silt. Several records indicate depth of as much as 4 ft for each foot of rise of water and in some streams the ratio is known to be as great as 7. On the other hand, in the majority of rivers the depth is much less. Experience with a given stream is the best guide in estimating the depth of scour.

The earlier experimental approach has also had limited success because the goal was restricted to a particular installation or to some special phase of the problem. One such study is reported by Engels (7) at Dresden, Germany, as early as in 1893. In recent years a considerable

effort has been made to understand the mechanics of local scour. The functional relationship between the various parameters affecting the scour such as sediment size, pier shape, and flow velocity was investigated by several researchers in the laboratory flumes where factors affecting the scour can be controlled. Laursen (8) found that the effect of sediment size on the magnitude of maximum scour depth was very small when sediment was continuously supplied to scour hole by the upstream flow. Laursen and Toch (9) concluded from their experiments that the maximum scour depth depended only on the initial depth of flow and was independent of both the mean velocity and the sediment characteristics. Chitale (10) and Marin (11) found that the ratio of maximum scour depth to the approach flow depth was a function of the Froude number of the approach flow. Tarapore (12) concluded from his experiments of local scour around a vertical cylinder in an open channel that maximum scour depth was a function of the width of the cylinder alone. Other investigators stressed the effect of the pier shape on the magnitude of maximum scour depth. Chabert and Engeldinger (13) made an extensive study of the scour around single vertical cylinders in a flume. They have found for a given sand and pier size that the scour depth reached a maximum for velocities approximately corresponding to beginning of bed transport (dunes), but their results could not be related to the prototype because of the lack of a similarity criteria. Shen, Schneider and Karaki (14) have recently studied the scour around a vertical circular pile in a recirculating flume. Although their findings were short of an expression for maximum scour depth, they found that the maximum depth of scour is a function of the pier Reynolds number and is inde-

pendent of sediment size for sands whose median diameter is less than 0.52 mm. In the absence of similarity criteria for localized scour to relate experiments to prototype, neither early model tests nor subsequent experimental studies by various investigators have been successful in obtaining the means of predicting scour around a pile in the field.

Very little material appears in the literature to explain the local scour phenomenon theoretically. In his work on the nature of scour, Laursen (15) offered some general principles based on the equation of continuity of sediment to analyze the localized scour. He stated that the rate of scour will equal the difference between the capacity for transport out of the scoured area and the rate of supply to the area. Laursen has predicted a limiting extent of scour that will be approached automatically.

Tarapore (12) has applied the principle of sediment continuity to analyze the scour around a vertical circular pier in an alluvial channel. He assumed a particular velocity distribution in the scour hole that is analogous to a two-dimensional jet issuing into an infinite fluid and used the experimental results to obtain certain experimental constants. However, his assumption of the velocity distribution in the scour hole does not seem to be realistic.

Carstens (16) attempted to develop similarity criteria for scour depth in localized scour situations. Carstens' analysis is based upon the conservation of mass with the scour hole as the control volume. Assuming that in an area of localized scour, the velocity and velocity distribution are the results of the disturbance element around which scour is occurring, the total differential equation is separable in which

the differential time is equal to the differential volume divided by the difference in volume rate of flow of sediment (plus voids) out of and into the scour hole. The approach is to analyze the three terms (differential volume, sediment transport in, and sediment transport rate out) separately and then to integrate the differential equation to obtain scour depth as a function of time. A minimum of two model tests is required to evaluate the numerical coefficients in the separate terms for the rate of sediment transport out of and into the scour hole.

Using the experimental data of Chabert and Engeldinger (13) of scour around a vertical cylinder, Carstens formulated a scour function to obtain scour depth as a function of time in the absence of transport into the scour hole from upstream. Without sediment transport into the hole, the scour hole never attains a terminal depth. The effect of dunes moving past the cylinder (and scour hole) was also considered. When sediment was being transported into the scour hole from upstream, a terminal scour depth was predicted. Carstens stated that the terminal depth of scour was too poorly defined to be useful as an experimental variable. The ratio of the terminal depth of the scour to the pier width was found to be independent of the magnitudes of approach velocity and sediment size, if the approach velocity (cm/sec) was equal to or greater than 200 times the square root of the median sediment diameter (diameter in cm). Carstens' conclusion is in agreement with the conclusion of Laursen and Toch (9). In a later publication, Carstens (17) used the same method of analysis for the localized scour around a horizontal cylinder lying on the bed in oscillatory flow.

Grodowczyk, Maggiola, and Folguera (30) recently proposed an

analytical-numerical approach based on shallow-water theory for localized scour around isolated obstacles located in an erodible-bed channel in unidirectional flow. The physical obstacle is replaced by an imaginary obstacle that is bounded by the surface of separation of flow. Assuming that each streamtube outside the imaginary obstacle (surface of separation) behaves as a single "erodible-bed-channel", the equations of motion and continuity of the one-dimensional erodible-bed channel are applied to each streamtube. The rate of bed-load transportation is assumed to be the same as the general form of the Meyer-Peter formula. The equations of motion and continuity are integrated numerically to obtain scour depth as a function of time. Also the asymptotic solution of equation of motion and continuity was obtained for an estimate of maximum scour depth. The maximum value of the depth of scour was found to be a function of the submerged density of the bed material, particle mean diameter as well as a function of the Froude number, shear stress and a modified Reynolds number.

Gradowczyk, Maggiolo, and Folguera stated that in the absence of sediment transport into the scour hole from upstream, scour process can not reach equilibrium in a finite time. On the contrary, in experiments where sediment was transported into the scour hole from upstream (while the bed was flat) an equilibrium depth was reached. This equilibrium scour depth was generally smaller than the maximum scour depth. Since the mathematical model was proposed for flat bed conditions, the effects of dunes moving past the obstruction were not considered. Furthermore, since the vortex in front of the cylinder could not be taken into account in the mathematical model, the scour depth at the upstream nose of the

cylinder could not be determined. The maximum scour depth was found at the side of the cylinder along the axis transversal to the flow.

CHAPTER II

THEORETICAL ANALYSIS OF THE PROBLEM

When an obstruction, such as a pile, is placed in a flow, the flow pattern in the vicinity of that obstruction will be altered. As a result, the capacity of the flow to carry sediment is altered. In any area where the capacity for the transport out of the area is greater than the transport into the area, local scour will occur. Conversely, where the transport out of the area is less than the rate of supply, fill will occur. The resultant changes in the flow boundary will further alter the flow pattern (and the rate of transport out) until equilibrium between scour and fill is achieved. An analytical solution for localized scour would, therefore, have to combine a prediction of flow pattern and a prediction of the local transport capacity of the flow.

In the case of localized scour around a pile, knowledge of the velocity distribution and of the flow pattern involving vortices is only qualitative. Oscillatory-flow condition introduces further complications. In addition, the variables influencing the sediment transport rate are numerous. Consequently, a rigorous mathematical solution for transport capacity appears hopeless.

One approach is to use an analysis of the forces on surface grains in the formulation of a rational scour development function and then to use model-test results for the determination of various constants in that function. The analysis of scour-hole development is based upon a separate determination of two of the three terms in the equation of

continuity for scour-hole volume, that is, rate of sediment transport in and rate of sediment transport out. Then rate of change of scour-hole volume can be derived from continuity relations. Model tests can be utilized to provide the values of the constants needed by development and to provide a check on the theory as to the effect of various factors such as the pile diameter and sediment characteristics.

The Equation of Sediment Continuity

A general mathematical expression for localized scour can be given in the form of a differential equation that is based upon the principle of conservation of mass. The mass under consideration is the mass of sand removed from the scour hole. Since the scour hole volume is enlarging with time, the rate form of the equation is needed. For convenience a volume-rate equation is utilized rather than the mass-rate equation. The equation of continuity for the scour hole volume can be written as:

$$\frac{dV}{dt} = Q_{so} - Q_{si} \tag{1}$$

in which dV/dt is the rate of change of the scour hole volume, V, with respect to time, t; Q_{so} is the volume rate of sediment being carried out; and Q_{si} is the volume rate of sediment being carried into the scour hole.

In the analysis, it is assumed that the two transport processes involving (a) transport from the scour hole by localized scour and (b) transport into the scour hole from the surrounding bed are independent and that the net rate of transport is the sum of the two independent

processes. If Q_{so}, Q_{si}, and V are functions of scour hole geometry, Equation 1 is separable and integrable as follows:

$$t = \int_{o}^{S} \frac{dV}{Q_{so} - Q_{si}} \tag{2}$$

Output Sediment-Transport Function

In an attempt to derive a rational function for the rate of transport out of the scour hole, Q_{so}, the studies of other investigators had to be utilized. For this purpose, experimental studies were sought in which the rate of supply into the scoured area, Q_{si}, was zero and bed forms did not exist.

Experiments on the local scour of a sand bed downstream of an outlet by a horizontal jet have been reported by Laursen (15), Tsuchiya and Iwagaki (18), and Tarapore (19). All these studies involved a jet which flowed over an initially flat bed. These reported scour situations were free from incoming sediment and the bed forms (dunes) were nonexistent, but in each case, the scour hole was enlarging with time. Since the flow pattern is different at every value of scour depth, S, the rate of transport out, Q_{so}, has to be evaluated as a function of S. Furthermore, the rate of change in scour depth, dS/dt, has to be determined from experimentally determined graphs of S as a function of t in order to calculate Q_{so}. To avoid these complications, a steady-state scour study was sought with a constant flow pattern over the scoured area.

In his doctoral research study, A. R. LeFeuvre (20) determined the sand transport from a small area of flat bed. The sediment was

forced into a flow section through a vertical supply tube. The end of the supply tube formed a small sediment bed at the wall of the main-flow section. During a run, the sediment supply rate was constant. LeFeuvre's experiments were ideal in formulation of a sediment pickup function from a flat bed because (a) the dunes were nonexistent, (b) no sediment was transported into the scour hole from upstream, and (c) the rate of scour was constant. The experimental results of LeFeuvre's flat-bed transport study has been reanalyzed. The rate of sediment pickup can be expressed as follows:

$$\frac{u_e}{u} = 1(10^{-3}) \left(\frac{C_D'}{8.2 \cos \alpha} \frac{u^2}{(s-1)g D_g} - \tan \alpha - \tan \phi \right)^{5/2} \quad (3)$$

in which u_e/u is the ratio of the pickup velocity, u_e, to the mean velocity at particle level, u; s is the specific-weight ratio; D_g is the geometric mean diameter of sediment particles; C_D' is the coefficient of drag on a particle falling quiescent fluid, g is the magnitude of acceleration of gravity, ϕ is the angle of repose of bed material; and α is the angle of inclination of the bed from the horizontal. Pickup velocity, u_e, is a transport velocity which is the volume rate (solids plus voids) of bed removal per unit area of bed in the absence of deposition.

Derivation of Equation 3 and underlying assumptions are included in a yet unpublished paper by LeFeuvre, Altinbilek and Carstens presented in the Appendix. In Equation 3, the value of the flow parameter $u/\sqrt{(s-1)g D_g}$ is called the sediment number, N_s. The sediment number is a form of Froude number, being proportional to the square root of the ratio of the fluid inertial force per unit volume to the submerged weight

of the sand per unit volume. Sediment number, N_s, is a convenient flow variable by which the geometry of the bed forms is characterized.

Because of the fundamental similarity of all localized-scouring situations, the rate of sediment pickup expressed in Equation 3 can be expected to be applicable in other situations even though the constant of proportionality will differ from one localized scour to another depending upon the disturbance geometry and the reference velocity, u, used in evaluating N_s. The output sediment transport function, Q_{so}, can, then, be formulated as:

$$\frac{Q_{so}}{uD_g B} = \left\{ f\left(\begin{array}{l} \text{scour-hole geometry,} \\ \text{sediment-grain geometry,} \end{array} \quad \frac{S}{D} \right) \right\} \qquad (4)$$

$$\left\{ \frac{C_D'}{8.2 \cos\alpha} N_s^2 - \tan\phi - \tan\alpha \right\}^{5/2}$$

In the above equation the velocity, u, used in evaluating N_s, is taken in the vicinity of the particles in order that the sediment-pickup function can be used without regard to the particular flow situation. Accordingly, determination of u as scour develops, is an independent problem. In Equation 4, the term B represents the pertinent dimension of the obstruction along which the sediment pickup occurs.

For the case of localized scour around a vertical circular pile, the length B will be proportional to pile diameter D. The reference velocity, u, in Equation 4 is taken to be the maximum velocity of oscillatory flow, U_m. The maximum velocity of oscillatory flow instead of local velocity at the particle level is chosen as the reference velocity inasmuch as the angular velocity of a vortex at the particle level is

expected to be proportional to the velocity of the main flow section that generates the vortex. The functional coefficient of f of Equation 4 includes not only the variables involving the scour-hole geometry and sediment-grain geometry but also a geometric variable S/D which is necessary to establish the stage of scour-hole development. Sediment-grain geometry should include the variables involving the size, shape and gradation of the bed material. Since there is no direct or quantitative way to assess the particle shape, the geometric mean diameter, D_g, (or D_g/D in nondimensional form) is the most important single parameter to represent the effects of the sediment-grain geometry in Equation 4. Scour-hole geometry involves the angle of repose, ϕ, of the sand which is also a function of sediment-grain geometry. The angle of repose approximates the angle that the wall slope of the scour hole makes with the horizontal.

Using the above considerations and assuming that all scoured material are picked up from a relatively flat area in the immediate vicinity of the pile at the bottom of the scour hole where the angle of inclination, α, is zero, Equation 4 can be written as follows:

$$Q_{so} = K_O \, D \, D_g \, U_m \left(\frac{C_D'}{8.2} N_s^2 - \tan\phi \right)^{5/2} \qquad (5)$$

in which $K_O \propto f\,(S/D, D_g/D, \phi)$ is a functional coefficient to be determined experimentally. Equation 5 expresses the rate of sediment transport out of the scour hole around a vertical circular pile in oscillatory flow.

Input Sediment-Transport Functions

The net rate of sediment transport is zero with symmetric oscillatory flow over a homogeneous level bed. Either the bed must be inhomogeneous or the water motion must be asymmetric for a net transport of sediment to occur with oscillatory flow. The sediment will be transported into an inhomogenity such as a scour hole on the bed, and conversely will be transported out of an inhomogenity such as a mound on the bed.

Although Manohar (21) performed some experiments to measure sediment transport over a level bed with asymmetric water oscillations, no experiments have been reported with oscillatory flow which involve sediment transport into an inhomogeneous area of the bed, such as into a hole. Due to a lack of such experimental information, the formulation of input sediment-transport functions for the rate that sediment is transported into a scour hole must be based upon the transport functions which are experimentally determined for the unidirectional flow.

The description of the process by which a duned bed evolves from an initially flat bed in oscillatory flow has been reported by Carstens, Neilson and Altinbilek (29). The four different stages of bed-form development on a flat bed in oscillatory flow are characterized as follows:

(1) no movement of bed material, $a/D_g < a_c/D_g$,

(2) two-dimensional dunes, $a_c/D_g < a/D_g < 775$,

(3) three-dimensional dunes, $775 < a/D_g < 1700$,

(4) flat bed with sediment transport, $a/D_g > 1700$,

in which a is the amplitude of water motion, and a_c is the amplitude of water motion at deformed-bed incipient-motion condition.

The upper limit of the first stage is distinguished by the incipient-motion condition which is defined as the flow condition at which an appreciable number of particles laying on the surface of a bed are in motion. The first movement of surface particles occurs at about the time of maximum velocity. Incipient motion will occur at different values of water-motion amplitude depending upon whether the bed is flat or deformed. A deformed-bed, incipient-motion condition occurs on a previously duned bed or when a flow disturbance is placed on the bed.

The water motion amplitude, a_c, associated with the deformed-bed incipient-motion condition is the lower limit of ripple propagation. The upper limit of the ripple propagation, a_s, at which ripples form spontaneously and simultaneously all over the flat bed, is at an amplitude slightly larger than the amplitude for flat-bed incipient-motion. Determination of water-motion amplitudes, a_c, at incipient-motion condition, and a_s, at the upper limit of propagating ripples for a given sand and flow conditions is shown in Reference 29. Neither the incipient-motion condition, $\frac{a_c}{D_g}$, nor the upper limit of propagating ripples, $\frac{a_s}{D_g}$, appears to have any effect upon the geometry of equilibrium dunes.

If the value of $\frac{a}{D_g}$ is less than 775, the dune system is two-dimensional. The crests of the dunes are unbroken and are essentially constant in elevation. The crests of the dunes are perpendicular to the direction of the water motion at bed level. Dunes are essentially

symmetrical with the crests moving slightly back and forth as the scour and deposition occur on each side of the crest. The dune amplitude increases until $\frac{a}{D_g}$ is approximately 775. The ratio of the amplitude-to-wave length of the dunes is approximately constant.

If the value of $\frac{a}{D_g}$ is greater than 775, the bed forms are no longer two-dimensional in character. The breakdown of the two-dimensional dune system is progressive. Initially, the dunes are sand hills with valleys both across and along the flow direction. With increasing water-motion amplitude, the entire surface of the bed is in motion resembling a second fluid under the water. The amplitude of three-dimensional dunes decreases linearly with increasing water-motion amplitude. In contrast, the wave length of three-dimensional dunes is nearly independent of the water-motion amplitude.

The upper limit of three-dimensional dunes is defined by formation of a flat bed and by the sediment transport over the flat bed at the value of $\frac{a}{D_g}$ equal to about 1700.

The dune systems of unidirectional flow are in some respects quite similar to those of oscillatory flow even though the shape of a dune is quite different. Like two-dimensional dunes in oscillatory flow, the dune systems of unidirectional flow show a linear variation in amplitude for the values of sediment number less than 6.5. The variation of the boundary-drag coefficient of the bed with N_s in unidirectional flow is also indicative of a change in dune geometry at a value of N_s of 6.5. The mean velocity of flow rather than the velocity at particle level is used in computation of the sediment number, N_s.

When the value of sediment number, N_s, is larger than 6.5, the dune systems of unidirectional flow become three-dimensional. The upper limit of three-dimensional dunes from experimental results appears to be in the range $12 < N_s < 15$. Carstens (17) has chosen the value of $N_s = 15$ as the upper limit of the three-dimensional dunes by giving greater credence to the experimental data obtained with larger depths of the unidirectional flow.

The flat-bed region, $N_s > 15$, is complicated in unidirectional flow experiments by the appearance of antidunes. Antidunes are bed forms that occur in trains that are in phase with and strongly interact with gravity water-surface waves (25). The strong interaction between the waves on the bed and the surface wave occurs when the Froude number is about unity. Antidunes would not exist with oscillatory flow at the sea bed which is generated by a train of moving surface waves.

Inasmuch as bed-form geometry in oscillatory flow is characterized by four distinct stages, different sediment transport functions should exist in each stage in which transport occurs, that is, in stages (2), (3), and (4). Because of the basic similarity of phenomena (except antidunes) the functional form of the transport equations in stages (2) and (3) are presumed to be similar for oscillatory flow as for unidirectional flow. In the stage (4), flat bed with sediment movement, the Equation 3 is presumed to be applicable since a flat bed is geometrically similar to every other flat bed.

Transport Functions of Unidirectional Flow

For formulation of input-sediment transport functions the experimental data from three sources were utilized:

(1) experimental results of R. A. Stein (22),

(2) experimental results of Rathbun and Guy (23),

(3) results obtained at Colorado State University as reported by Guy, Simons, and Richardson (24).

Stein's experiments (22) were conducted in a 4 ft wide flume having a length of 100 ft. The bed material was sand having a mean diameter, D_g, of 0.40 mm and a geometric standard deviation, σ_g, of 1.50. The sand depth in the flume was about 0.7 ft. The depth of flow varied from 0.30 ft to 1.20 ft. Stein's results are limited to the values of $N_s > 5.2$. Most of Stein's data were taken in the region of three-dimensional dunes and antidunes, that is, $N_s > 6.5$.

Rathbun and Guy (23) performed their experiments in an open-tilting flume 23.8 ft in length with a 0.65 ft by 0.65 ft cross section. The bed material used was well rounded quartz particles having a median diameter, D_g, of 0.30 mm and a geometric standard deviation, σ_g, of 1.26. The depth of flow varied from 0.21 ft to 0.17 ft. All of the data reported by Rathbun and Guy were taken at the values of sediment number less than 3.6, that is, in the region of two-dimensional dunes.

The experimental data of Colorado State University as reported by Guy, Simons and Richardson (24) are a compilation of 10 sets of conditions for a total of 339 equilibrium runs. Most of the data were collected in a recirculating flume 150 ft long, 8 ft wide, and 2 ft deep. Many data relative to the effect of temperature and fine sediment on sediment transport were collected in a 60 ft long, 2 ft wide, and 2.5 ft deep recirculating flume that has clear-plastic sidewalls. The properties of the ten different sediments used and the general character

of the experiments are given in Table 1. The experimental results of Colorado State University covered a large range of flow phenomena from a plane bed and no movement of sediment to antidunes.

Table 1. Properties of Bed Material Used in Colorado State University Studies

Mean Diameter D_g (mm)	Material	Geometric Standard Deviation, σ_g	Purpose of Study	Width of the flume used (ft)
0.19	Sand	1.30	General	8
0.27	Sand	1.56	do	8
0.28	Sand	1.67	do	8
0.45	Sand	1.60	do	8
0.93	Sand	1.54	do	8
0.32	Sand	1.57	Effect of Viscosity	2
0.33	Sand	1.25	Effect of Gradation	2
0.33	Sand	2.07	do	2
0.47	Sand	1.54	Effect of Viscosity	8
0.54	Sand	1.52	do	2

Using the independent flow variable that was used in expressing the rate of sediment pickup in Equation 3, as a model for correlation, the experimental data from the above three studies were analyzed. In computations the mean velocity of flow was used as the reference velocity, U. An angle of repose of 34° was assumed for all particles. The experimental results of Stein and of Rathbun and Guy are shown in Figure 1. The results of Colorado State University experiments are shown in Figure 2. The line approximating the results in Figure 1 is also shown in Figure 2. An examination of Figure 2 shows that the results obtained by

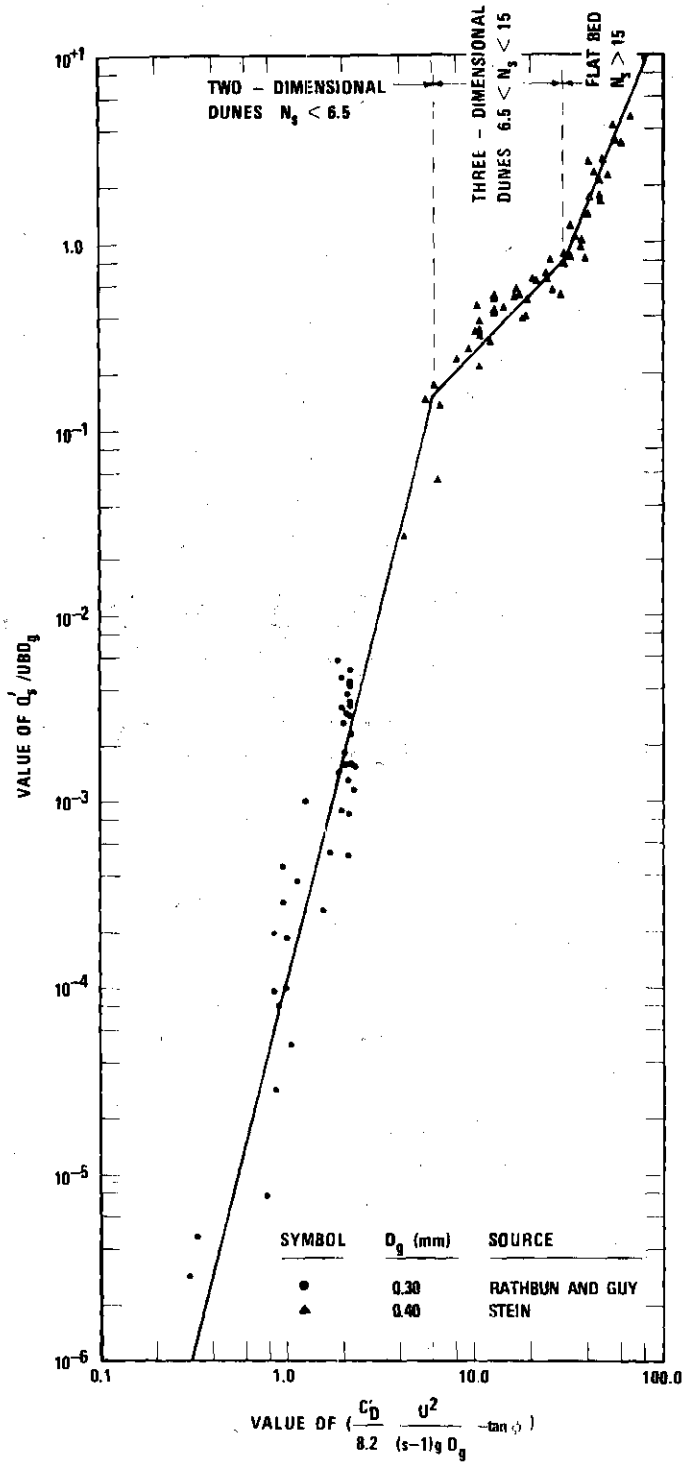

Figure 1. Sediment-Transport Rate

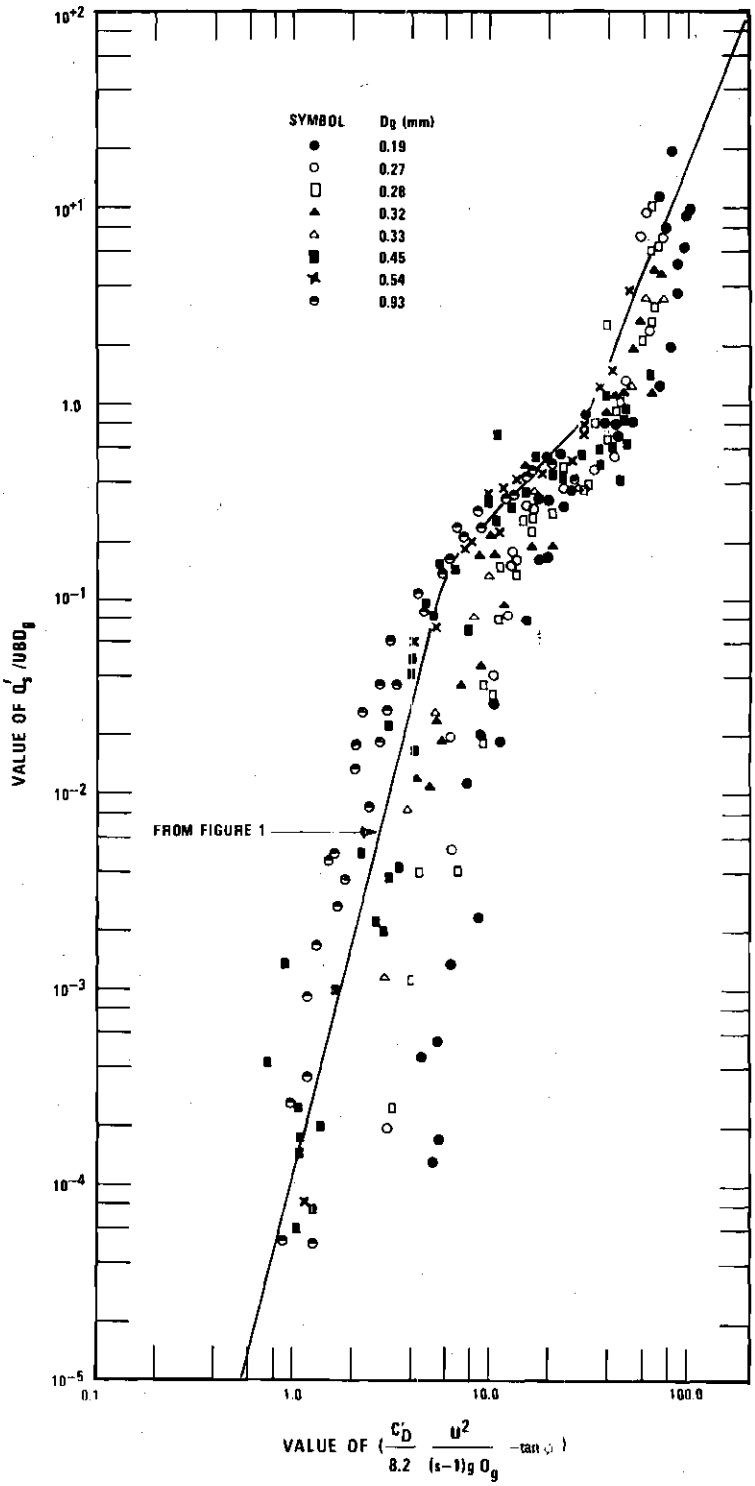

Figure 2. Sediment-Transport Data of Colorado State University

the correlation of data from three different sources are in good agreement. The scatter of experimental data at small values of N_s is quite expected inasmuch as the sediment-transport rate is extremely small.

In the range of two-dimensional dunes, the sediment-transport function shown by solid line in Figure 1 is approximately:

$$\frac{Q_s'}{UBD_g} \propto \left(\frac{C_D'}{8.2} N_s^2 - \tan\phi \right)^4 \qquad (6)$$

in which Q_s' is the volume rate of solids transport, B is the width of the bed, U is the mean velocity of the water.

In the region of the three-dimensional dunes, that is, $6.5 < N_s < 15$, the transport equation is as follows:

$$\frac{Q_s'}{UBD_g} \propto \left(\frac{C_D'}{8.2} N_s^2 - \tan\phi \right) \qquad (7)$$

In the flat-bed region, $N_s > 15$, the antidunes would appear when the value of Froude number is about unity. The transport function shown by solid line in Figure 1 can be approximated for N_s greater than 15 as follows:

$$\frac{Q_s'}{UBD_g} \propto \left(\frac{C_D'}{8.2} N_s^2 - \tan\phi \right)^{5/2} \qquad (8)$$

Equation 8 is similar in form to Equation 5 which expresses the rate of sediment pickup from a flat area at the bottom of the scour hole. Since a flat bed is geometrically similar to every other flat bed, similarity of Equations 5 and 8 is expected.

Transport Functions of Oscillatory Flow

The input sediment transport functions of oscillatory flow can now be written using analogous functions of unidirectional flow. The maximum velocity of oscillatory flow, U_m, is taken as the reference velocity instead of the mean velocity, U. The term B in Equations 6, 7, and 8 represents the width of the channel. For the case of localized scour around a vertical circular pile, the term B should be the top width of the scour hole through which the sediment is carried into the hole. Since the angle that the scour hole makes with the horizontal is equal to angle of repose, ϕ, the length B can be taken as $(D + 2S/\tan\phi)$.

Using above considerations, the input sediment transport functions of oscillatory flow can be written as follows:

For $a/D_g < a_c/D_g$,

$$Q_{si} = 0 \tag{9}$$

For $a_c/D_g < a/D_g < 775$,

$$Q_{si} = K_1 D_g D \left(1 + \frac{2S}{D\tan\phi} \right) U_m \left(\frac{C'_D}{8.2} N_s^2 - \tan\phi \right)^4 \tag{10}$$

For $775 < a/D_g < 1700$,

$$Q_{si} = K_2 D_g D \left(1 + \frac{2S}{D\tan\phi} \right) U_m \left(\frac{C'_D}{8.2} N_s^2 - \tan\phi \right) \tag{11}$$

For $a/D_g > 1700$,

$$Q_{si} = K_3 D_g D \left(1 + \frac{2S}{D\tan\phi} \right) U_m \left(\frac{C'_D}{8.2} N_s^2 - \tan\phi \right)^{5/2} \tag{12}$$

in which K_1, K_2, and K_3 are geometric variables to be determined experimentally. In a localized-scour situation around a vertical circular pile, the sediment movement will continue over the upstream and downstream slopes of the scour hole. The coefficients K_1, K_2, and K_3 of input sediment-transport equations are, therefore, expected to be the functions of scour-hole geometry. The most logical variable to express the scour-hole geometry, is the angle of repose, ϕ, of the cohesionless sediment which is an approximation to the angle that the wall slope of the scour hole makes with the horizontal.

Analysis of Scour Hole Development

The scour hole depth as a function of time is obtained by integration of the equation of continuity of sediment in the scour hole, Equation 2. This equation includes three separate terms, that is, the rate of sediment transport in, the rate of sediment transport out, and the rate of change of scour hole volume. A rational volume rate function for sediment being transported out of the hole is given by Equation 5. The volume rate functions for sediment transported into the hole are presented in Equations 9, 10, 11, and 12. These equations are presumed to be applicable not only for the localized-scour around a pile, but also the other localized scour-situations. However a mathematical expression to represent the time rate of change of scour-hole volume along with the constants of Equations of 5, 10, 11, and 12 will have to be determined experimentally for each localized-scour situation.

As in all sediment problems, a reduced scale model of a prototype situation is virtually impossible. While the flow obstruction (pile)

can be reduced in scale, a similar reduction of the bed material would result in a great reduction in settling velocity of the bed material. As a consequence, large quantities of the bed material would be picked up from the bed and would remain in suspension quite unlike the prototype situation in which the sand is scoured and is redeposited on the bed. For example, a 1/10 scale model of 0.3-mm sand would be 0.03-mm silt for which settling-velocity ratio would be of the order of 1/100, whereas the Froude criterion is indicative that the settling-velocity ratio should be 1/3.16.

A second difficulty that is associated with the model tests is the scale effect of the dunes. With a reduced-scale model, the dunes will be of the same order of magnitude in size as model. The flow pattern over the dunes will significantly influence the flow pattern around the reduced scale model but would be expected to be an insignificant influence on the flow pattern around the prototype provided that the pertinent length of the prototype object is greater than the dune wave length.

To overcome the difficulties of the scale effect and of the bed forms, model tests should be performed in accordance with Froude criterion and without dunes on the bed. To follow Froude criterion, the values of sediment number, N_s, of model tests should cover the same range as those of the prototype. This will, of course, result in outsize sediment diameters in the model. To minimize the effect of dunes, the model tests should be performed at the ranges of N_s where dunes are nonexistent, that is, (a) at lower values of the sediment number with a flat bed and no sediment movement, (b) at higher values of the

sediment number with flat bed.

The model tests in above ranges of the sediment number will provide the constants needed by Equations 5 and 12. The coefficients of the Equations 10 and 11 can, then, be obtained from the coefficient of the Equation 12.

CHAPTER III

EXPERIMENTAL APPARATUS

In order to study the development of the scour hole around a single vertical pile under wave action, the existing oscillating-flow water tunnel at Hydraulics Laboratory of the Georgia Institute of Technology was utilized. A single vertical circular cylinder was placed in the sand bed of the test section of the water tunnel. The water motion at a fixed point near to the bed is simple harmonic and is parallel to the bed approximating the flow at the sea bed beneath first-order Stokian waves.

Oscillating-Flow Water Tunnel

The description of the water tunnel is facilitated by referring to Figure 3. The water tunnel was constructed as a large U-tube in which the bottom horizontal leg is the test section. Forced oscillation of the water mass over a sand bed located in the test section is achieved by blowing air into one of the vertical legs as the water surface is falling and then exhausting the air as the water surface is rising in that leg.

The test section, B, is 1.0 ft (vertical) by 4.0 ft horizontal in cross section and is 10.0 ft long. The central section of the floor is depressed to form a bed-material container, D, which is 6.0 ft long, 4.0 ft wide and 4.0 in. deep. The side walls of the test section are made of transparent plastic permitting visual observation of the

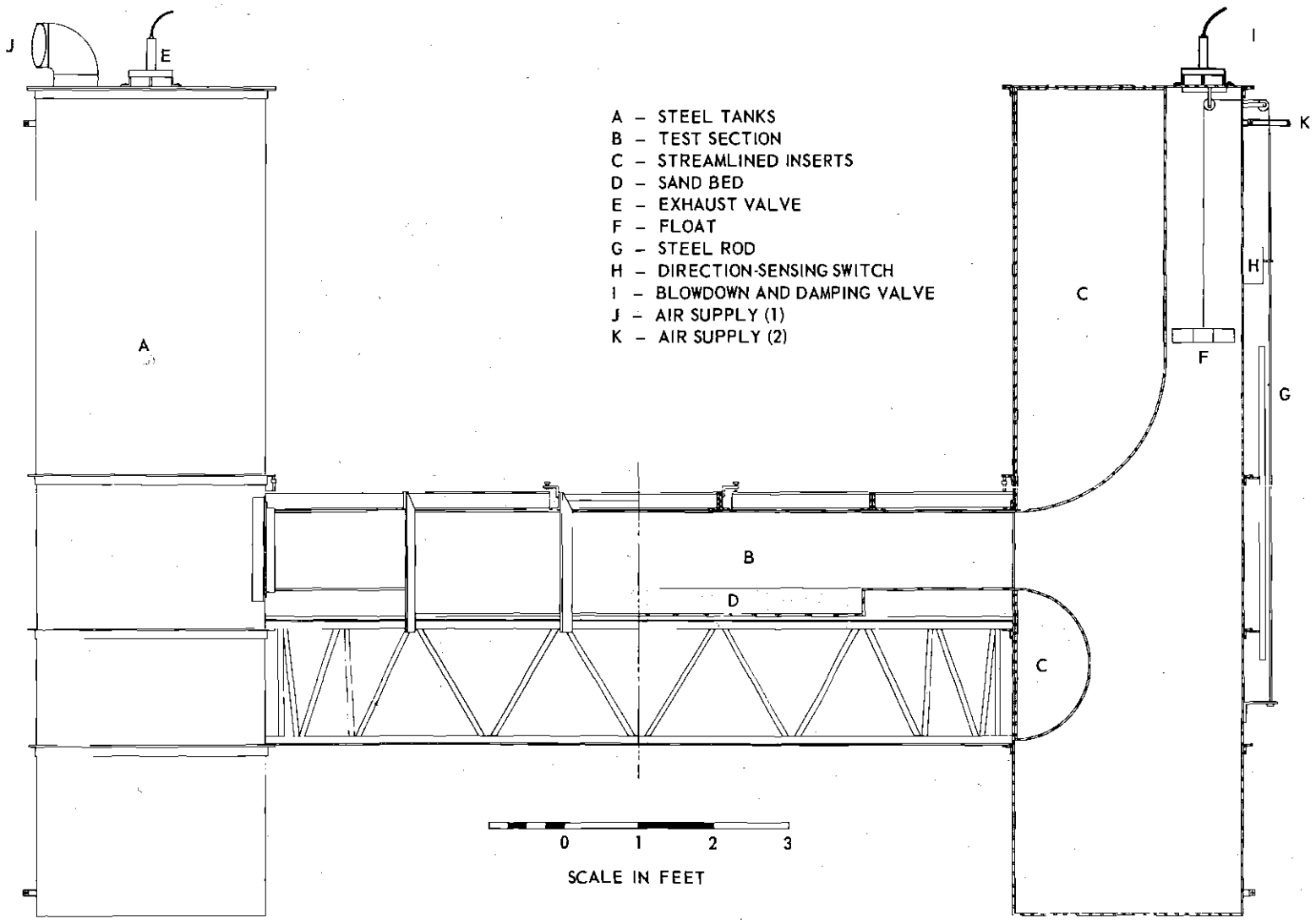

Figure 3. Oscillatory-Flow Water Tunnel

phenomena occurring within the test section.

The vertical legs of the U-tube are 1.0 ft by 4.0 ft in cross section and are joined to the horizontal legs so as to form a streamlined flow passage. The free surface of one leg, Figure 3, is utilized for the water-motion elevation measurements. The free surface of the other leg serves as a piston. Air is continuously forced into the air space above the water surface.

A feedback mechanism is used to operate the exhaust valves sequentially at the resonant frequency. Two 7-in. diameter, pneumatically powered, piston operated, exhaust valves, E, are used to quickly relieve the excess pressure in the air above the water surface. The exhaust valves are closed for approximately $\frac{1}{4}$ cycle during the time the water surface is falling in that leg. A float gage, F, in the other leg is joined to direction-sensing switch, H. Whenever the steel rod, G, is falling the switch, H, is closed and vice versa. The closing of the switch, H, actuates a single-cycle timer. This timer makes one revolution in 2 seconds and then stops. A second microswitch is contained within the timer unit. By means of an adjustable cam this second microswitch can be made to open or close at any time within the two-second interval. Solenoid valves which control the pneumatically operated pistons on the exhaust valves are in the circuit with the timer microswitch. The timer microswitch is set such that the exhaust valves close when the timer starts and remains closed for about one-quarter cycle. The feedback mechanism described above insures that the water is oscillated with simple harmonic motion at resonant frequency.

Total amplitude of the oscillation can be varied from 0 to 36 in.

by adjusting the magnitude of the air pressure at J. Air pressure at J is controlled by means of speed regulation of the blower.

Initial and final transients of the oscillatory motion are eliminated by means of a separate air system, K. Initially the water levels are unbalanced to the desired equilibrium amplitude. Upon release of the initial unbalance by opening the valve, I, the water oscillates at equilibrium. Final transients are eliminated by sealing the air space above the water by closure of the valve, I, over the exhaust port. A more complete description of the water tunnel is given elsewhere (32).

Cylindrical Piles

Six different cylindrical piles with a diameter range from 0.375 in. to 1.99 in. were tested. The pile to be tested was placed at midway (3.0 ft from each end) of the sand bed and 17 in. away from the nearest sidewall of the test section. Each pile was 16.0 in. long with the bottom four-inches being buried within the sand bed.

The two smallest piles (0.375 in. and 0.751 in. diameter) are made of steel and stand vertically over a base plate. The 0.875 in. diameter pile and the larger (1.244 in., 1.732 in., and 1.00 in.) sizes are fabricated of transparent plastic tubing with an interior fluorescent-lamp for target illumination. In order to allow positioning of the electric point gage close to the pile after a run, all piles are fabricated so that the top nine inches can be detached.

The pile to be tested is placed vertically in the sand bed by fastening the base plate of the pile to the floor of the test section.

Instrumentation

The object of the model tests was to observe and record the development of the scour around a single vertical pile. This required instrumentation for the following measurements:

(1) determination of the amplitude of the water motion,

(2) recording the development of scour depth,

(3) time measurements of water motion and scour depth, and

(4) determination of the geometry of scour hole.

Water motion amplitude is determined from the water-surface level in the East leg of the water tunnel. The float-elevation sensor system consists of an endless, stainless-steel cable which passes over pulleys at the top and bottom of the East leg. The spring-tensioned endless cable is fastened to the wooden float, F. A three-turn potentiometer, which is connected to the axle of the upper pulley, is one leg of a Wheatstone bridge. Bridge unbalance is sensed and recorded by means of a direct-writing oscillograph. In addition to the continuous measurements of float-level, the maximum and minimum levels can be directly read from the float scale, G.

Scour depth is determined and recorded by means of a cathetometer. The bottom of the scour hole is observed through the transparent sidewall of the test section. The telescope of the cathetometer is attached to a traversing mechanism so that an observer can raise or lower the telescope by turning a crank. The telescope is attached to a differential transformer which serves as a transducer for the recording of the elevation of the telescope by means of a direct-writing oscillograph. The

cathetometer is set vertically at the side of the water tunnel at a higher level than the sand bed. The telescope of the cathetometer is inclined at about 35 degrees from horizontal. In case of transparent plastic piles with an interior fluorescent-lamp for illumination, the junction of the pile and the sand was a very satisfactory target upon which the cross-hairs of the cathetometer are focused. In case of steel piles without an interior light, the pile was painted black to obtain contrast with the surrounding light-colored sand. Exterior lights were used for target illumination.

A dual system of time measurement is provided. A timing marker in the two-channel Sanborn direct-writing oscillograph produces pips at one-second intervals on the strip chart record in addition to the records of transient float elevation and scour depth. An electrically operated digital counter placed in circuit with the direction-sensing switch, H, provides a separate time measurement. The readout of the counter is the integer number of cycles since the beginning of a run.

A pair of precision instrument rails have been mounted over the test section so that an instrument carriage on which an electric point gage is mounted can be accurately positioned anywhere over the 3 ft square access opening located in the center of the roof of the test section. Using this instrument, a topographic map of the scour hole can be prepared.

Bed Material

Two different sands were used in this study. The finer, 0.19-mm median diameter sand, (Banding sand) was obtained from the Ottawa Silica

Company and the coarser, 0.30-mm median diameter sand, (Glass beads), was obtained from the Minnesota Mining and Manufacturing Company. Size and gradation of the sands were determined by sieve analysis following the procedures recommended by Vanoni, Brooks, and Kennedy (26). The results were analyzed following the practice described in a committee publication of the American Society of Civil Engineers (27). Standard techniques are used to determine the specific-weight ratio, γ_s/γ or s. The Banding sand is well rounded for which a shape factor of 0.7 is applicable (28). The glass beads are almost spherical with a shape factor of nearly unity. Physical properties of sediment are listed in Table 2.

Table 2. Properties of Sediment

Property	Ottawa Sand (Banding)	Glass Beads
Geometric mean diameter, Dg, (mm)	0.19	0.30
Geometric standard deviation, σ_g	1.35	1.06
Specific gravity, s	2.66	2.47
Angle of repose, ϕ, (degrees)	34.0	24.7

CHAPTER IV

EXPERIMENTAL PROCEDURE

Model tests were performed without dunes on the bed. Model tests were performed with low velocities with a flat bed and with high velocities with a flat bed. The purpose of this procedure was to avoid dunes which are a dominant factor in the flow patterns past the model in contrast to the prototype. The principal features of the dune geometry and the range of water-motion amplitudes in which the dunes disappear have been investigated in a previous study (29).

Regular Run

The following description of the operating procedure during a run is in chronological order.

Prior to each run, the pile to be tested was placed in the test section. Next water was added to submerge the sand bed. After mixing the sand to remove the air, which tends to stick to the sand particles in tiny bubbles, the submerged sand bed was leveled by means of a wooden screed which is long enough to bridge the bed material container, D, in Figure 3. The portion of the bed in the vicinity of the pile was flattened with a straight-edged steel plate. After the bed was leveled, the roof hatch was fastened.

Prior to filling the water tunnel the float-elevation sensor system was calibrated. Calibration consisted of clamping the float at various levels as noted on the scale which is parallel to the steel rod, G, in

Figure 3, and making a short record on the oscillograph recorder at each level.

During the time that the water tunnel was being filled, the telescope of the cathetometer system was calibrated. The calibration consisted of making short records on the oscillograph recorder at several elevations of telescope between initial bed level and the bottom of the scour hole. The relative elevation of the telescope at these various levels was read on the scale of the cathetometer and was recorded directly on the strip chart beside the corresponding trace.

The water level within the tunnel was carefully adjusted to a reference level as determined by pointer on the rod, G, which moved parallel to a scale as indicated in Figure 3. By having the mass of water in the tunnel constant during each run, the period of oscillation was maintained at a nearly constant value of 3.5 seconds.

Immediately prior to a run, the water temperature was read from a thermometer which is taped on the inside of the transparent sidewall at the end of the test section.

Next the blower was started. The master switch for designating the operating conditions was placed in the "stop" position. In the "stop" position both of the exhaust valves, E, in Figure 3, are open and the damping valve, I, is closed. With the valves in this position, the blower can be operated without oscillating the water in the tunnel. The blower speed was then adjusted so that work input would be that required to maintain the desired amplitude of oscillation. The requisite speed setting was determined through measurement of the stagnation pressure in the blower outlet. A calibration curve of this stagnation pressure

as a function of water-motion amplitude and the range of water-motion amplitude in which dunes disappear were established in a previous study by Carstens, Neilson, and Altinbilek (29). Reference was made to that study for the selection of desired water-motion amplitude and corresponding stagnation pressure in blower outlet.

With the blower-speed adjusted, the next step was to turn the master switch to "blowdown". In the "blowdown" position both of the exhaust valves, E, in Figure 3, are open, the damping valve, I, is closed, and the solenoid valve in the high-pressure air supply line, K, is open. Air is forced into the now-closed chamber above the water surface thereby forcing a difference in the water levels in the two vertical legs of the U-tube. When the unbalance reaches the desired amplitude, the master switch is turned to "run" which shuts off the air supply through K, opens the valve, I, and switches control of the exhaust valves, E, to the float-actuated feedback system. The purpose of the above described "blowdown" sequence is to eliminate the initial transients of the oscillatory motion and to have a flat-bed initial condition with an amplitude which is nearly at equilibrium as shown in the upper trace of Figure 4.

During a run, two operators are needed. One of the operators is responsible for the "blowdown" operation to start the oscillatory motion. This operator reads the maximum and minimum elevations of the float position several times during a run and records them on the strip chart of the recorder. He observes the scouring phenomena around the vertical pile and also checks for the development of scour holes and dunes at the ends of the sand bed during high amplitude runs. The final duty of

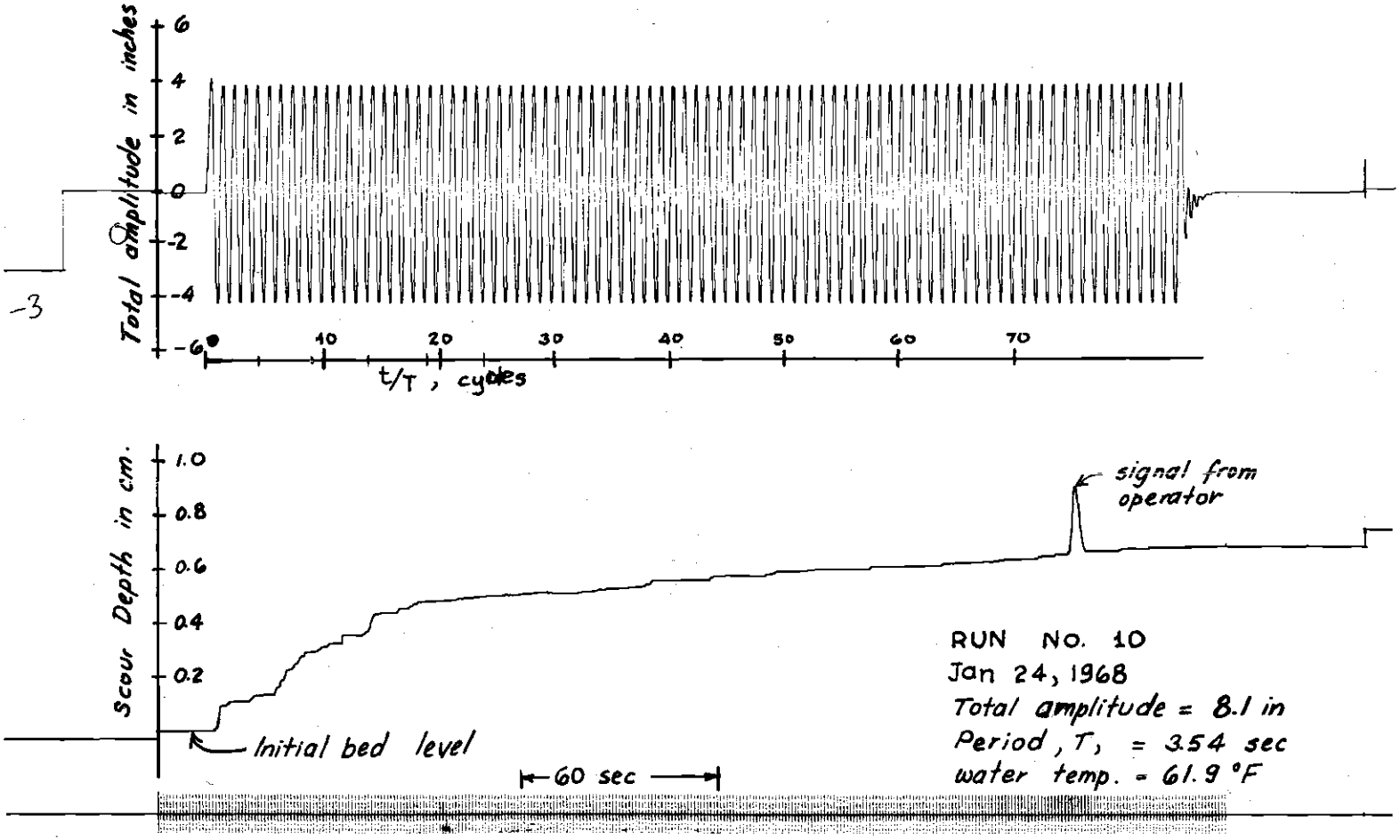

Figure 4. Recorded Data of Water Motion, Scour Depth, and Time

the first operator is to stop the oscillatory motion at the end of the run.

The second operator's only duty is to collect scour data during a run. He is seated at the side of the water tunnel in a way to observe the bottom of the scour hole through the telescope of the cathetometer. The horizontal cross-hair of the inclined cathetometer telescope is initially set at the junction of the pile and the sand bed. With the start of the oscillatory motion, the operator maintains the horizontal cross-hair of the telescope on the bottom of the scour hole as the scour progresses. During high velocity runs, sometimes, the operator encountered some difficulty in maintaining the telescope on the bottom of the scour hole because of very rapid scour rate during initial cycles. However after a few cycles (four or five cycles), he could follow the scour rate satisfactorily.

A run was terminated either when scour depth appeared to cease increasing or when the scouring was influenced by a dune system. The water motion is stopped by turning the master switch to "stop". In the "stop" position both exhaust valves, E, in Figure 3, are open and the damping valve, I, is closed. By switching from "run" to "stop" position, the motion is rapidly but gently damped as shown in the upper trace of the Figure 4, to a condition of equal water levels in both vertical legs.

After the oscillatory motion is stopped, the blower is turned off, the water temperature is read and recorded. While the water level is being lowered in the vertical legs of the water tunnel, the cathetometer system is calibrated. Next the float-elevation sensor system is calibrated. The calibration procedures remain the same as before the run.

Scour Hole Geometry

After a high amplitude run, scour-hole geometry was determined either by preparing a topographic map or by preparing a scour hole profile for the longitudinal and transverse center lines of the vertical cylinder. For mapping purposes, instrument rails have been mounted above the test section so that an instrument carriage can be accurately positioned in the axial direction over the 3-ft square hatch opening in the roof of the test section. An electrical point gage is mounted on the instrument carriage so that the point gage can be accurately positioned in the transverse direction. The electrical point gage gives excellent response upon the contact with the moist-sand bed. Because of the careful fabrication of the instrument carriage and the careful leveling of the instrument rails (from water surface), the belief is that all elevations could be determined within ± 0.5 mm of the true value. Following a run, the water was slowly drained from the water tunnel in order to avoid any change in the scour hole geometry. The roof hatch was removed from the test section. The remaining water in the depressed sand bed container, D, in Figure 3, was then pumped out very slowly through the filter until the water in the scour hole is completely drained. Next, the upper part of the vertical cylinder was detached in order to be able to move the point gage close to the pile.

For the preparation of the topographic map after a high-amplitude run, the elevations of the scour hole and the elevations of the surrounding unscoured region were determined at the grid points of a horizontal rectangular grid. The grid lines were spaced at 1.00-in. intervals across the test section and at 0.050-ft intervals along the test section.

In order to measure the side slope of the scour hole, bed profiles were measured along the longitudinal and transverse centerlines of the pile at intervals of 0.05 ft and 1.00 in. respectively.

Mean bed elevation in the above cases was measured by a point gage survey of the unscoured region around the pile and was taken as the average of the point gage readings.

After a low amplitude run, the scour hole geometry could not be determined by mapping or profiling because of the small size of the scour hole. In this case, the general features of the hole was sketched visually and overall dimensions were measured and recorded.

Auxiliary Tests

Auxiliary tests were determinations of the angle of repose of the sand. Tests were made by pouring dry sand through a funnel into a pile and measuring its natural slope which is defined as the angle of repose. An additional test was performed by preparing a large hole by sucking sand with a vacuum from the flat sand bed under water. The elevation measurements with point gage indicated that the sideslope of the hole was a good approximation to the angle of repose for the bed material.

Scope of the Experiments

A total of 24 regular runs were performed. When the results of a run were in doubt because of the appearance of the dunes or because of the large variations in water-motion amplitude, an additional run was performed with the same physical conditions. A listing of all regular runs and the physical conditions is contained in Table 3.

Table 3. Scope of the Experiments

Run No.	D (in)	D_g (mm)	Water Temperature (°F)	Total Amplitude (in)	Period, T (sec)
1	0.751	0.19	75.0	10.4	3.54
2	0.875	0.19	66.1	4.8	3.56
3	0.875	0.19	77.5	27.5	3.54
4	1.732	0.19	66.1	28.4	3.54
5	0.375	0.19	67.8	28.7	3.53
7	0.375	0.19	62.3	8.2	3.55
8	0.375	0.19	63.8	8.5	3.55
9	0.375	0.19	57.3	8.4	3.55
10	0.375	0.19	61.9	8.1	3.54
11	1.244	0.19	64.5	23.4	3.53
12	1.244	0.19	60.8	28.4	3.53
13	0.375	0.30	66.0	31.8	3.53
14	0.375	0.30	66.5	8.4	3.54
15	0.375	0.30	66.3	8.4	3.54
16	0.375	0.30	69.1	8.7	3.54
17	0.875	0.30	68.0	32.2	3.53
18	0.875	0.30	70.0	9.1	3.41
19	1.990	0.30	71.8	32.0	3.52
20	1.732	0.30	73.5	32.2	3.53
21	1.244	0.30	75.0	36.8	3.55
22	0.875	0.30	75.0	31.9	3.53
23	0.375	0.30	74.7	8.6	3.54
24	0.375	0.30	74.0	8.6	3.55
25	1.244	0.30	77.5	31.7	3.54

The typical recorded data for a regular run (Run 10) is shown in Figure 4. The upper trace is that of the water motion amplitude. The

middle trace is that of the scour depth, S, which is measured from the initial bed level to the bottom of the scour hole. The bottom trace is a timing mark with a pip being produced at every second.

CHAPTER V

ANALYSIS OF EXPERIMENTAL RESULTS

Description of Scour

A description of the development of the scour hole is helpful in understanding the scour phenomenon. In the laboratory experiments the surface of the bed initially was level. With the start of the oscillatory water motion, the scour hole starts forming at a rapid rate. As the scour hole becomes deeper, the rate of change in depth of the scour hole decreases gradually. The vortices that form at the base of the cylinder twice every cycle appeared to be the active agent of scour. The location of the most active scour was the immediate vicinity of the pile. The sediment particles that were being picked up by vortices from the bottom of the hole during the first-half cycle of the water oscillation, were lifted to some distance above the scour hole before being carried away from the pile during the next half cycle of the water oscillation. Some scoured particles were deposited on the slopes of the scour hole while the others were carried far enough to be deposited on the surrounding bed.

During the earlier stages of the low-amplitude runs, $\frac{a}{D_g} < 550$, the bed movement was observed only adjacent to the pile within the scour hole. Later, the scoured particles that were deposited on the bed on each side of the scour hole, formed a band of oscillating particles. The low-amplitude runs were terminated upon the appearance of such a

band of moving grains which would eventually become the crests of the two dimensional dunes.

During the high-amplitude runs, $\frac{a}{D_g} > 1500$, the scour phenomenon was a very lively one. The inside of the scour hole was clouded by the large amount of sediment that was picked up from the bottom of the scour hole. The entire surface of the bed was in motion resembling a second fluid under the water. This general oscillatory movement of sediment (bed load transport) was also continuous over the slopes of the scour hole.

Geometry of Scour Hole

With a vertical cylindrical pile, the scour hole is in the shape of an inverted frustum of right circular cone. The lower diameter of the frustum is approximately equal to the diameter of the pile, D. The angle that the scour hole makes with the horizontal is equal to the angle of repose, ϕ, of the bed material. The topographic maps in Figures 5,6,7, and 8 show the shape of the scour hole developed during Runs 3,4,5, and 12 (Table 3). The volume, V, of the scour hole can be closely approximated as follows:

$$V = \frac{\pi S^2}{6} \cot \phi \, (3D + 2S \cot \phi) \qquad (13)$$

The change of the scour-hole volume, dV, is as follows:

$$dV = \pi S \cot \phi \, (D + S \cot \phi) \, dS \qquad (14)$$

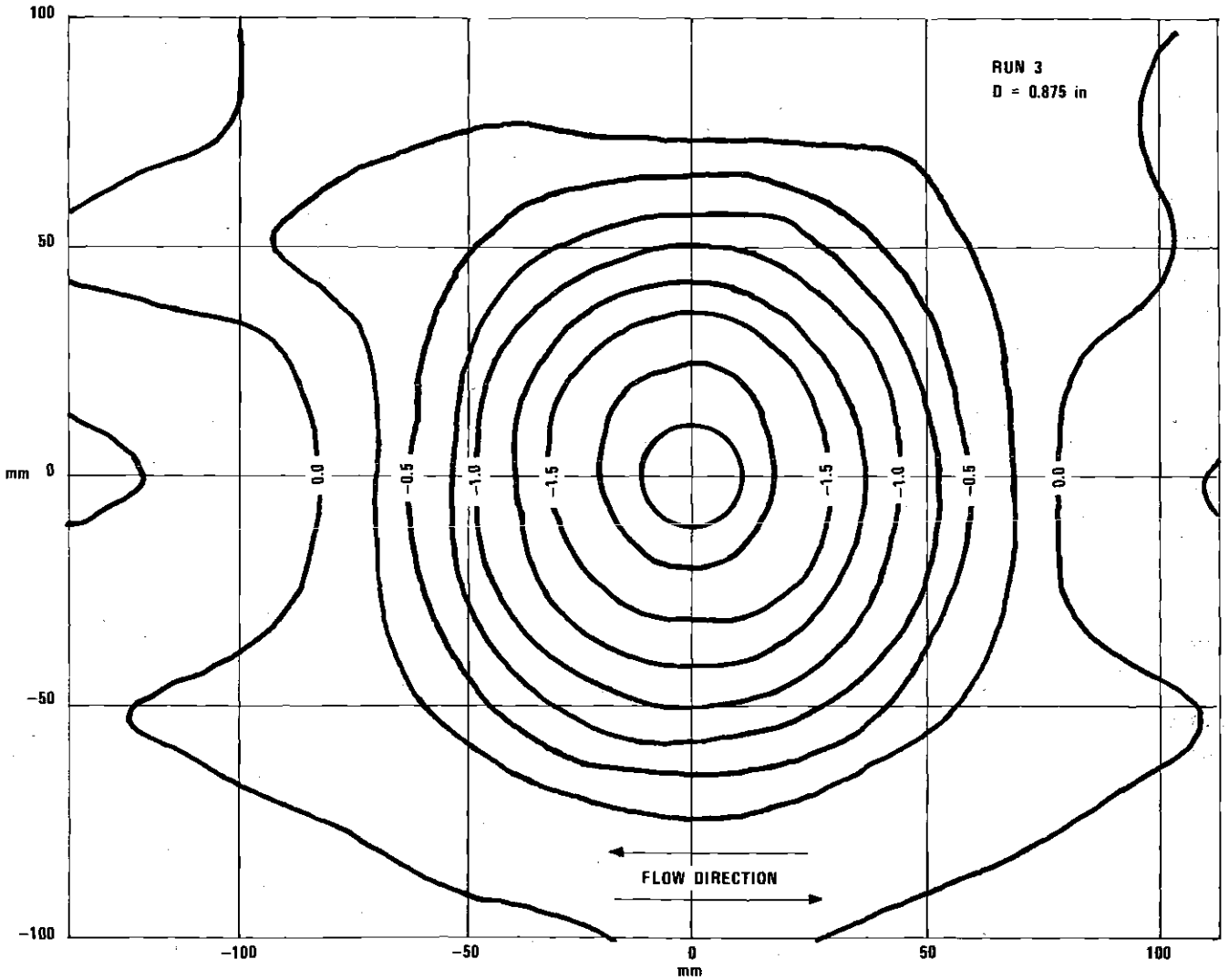

Figure 5. Topographic Map (Contours in D-Units)

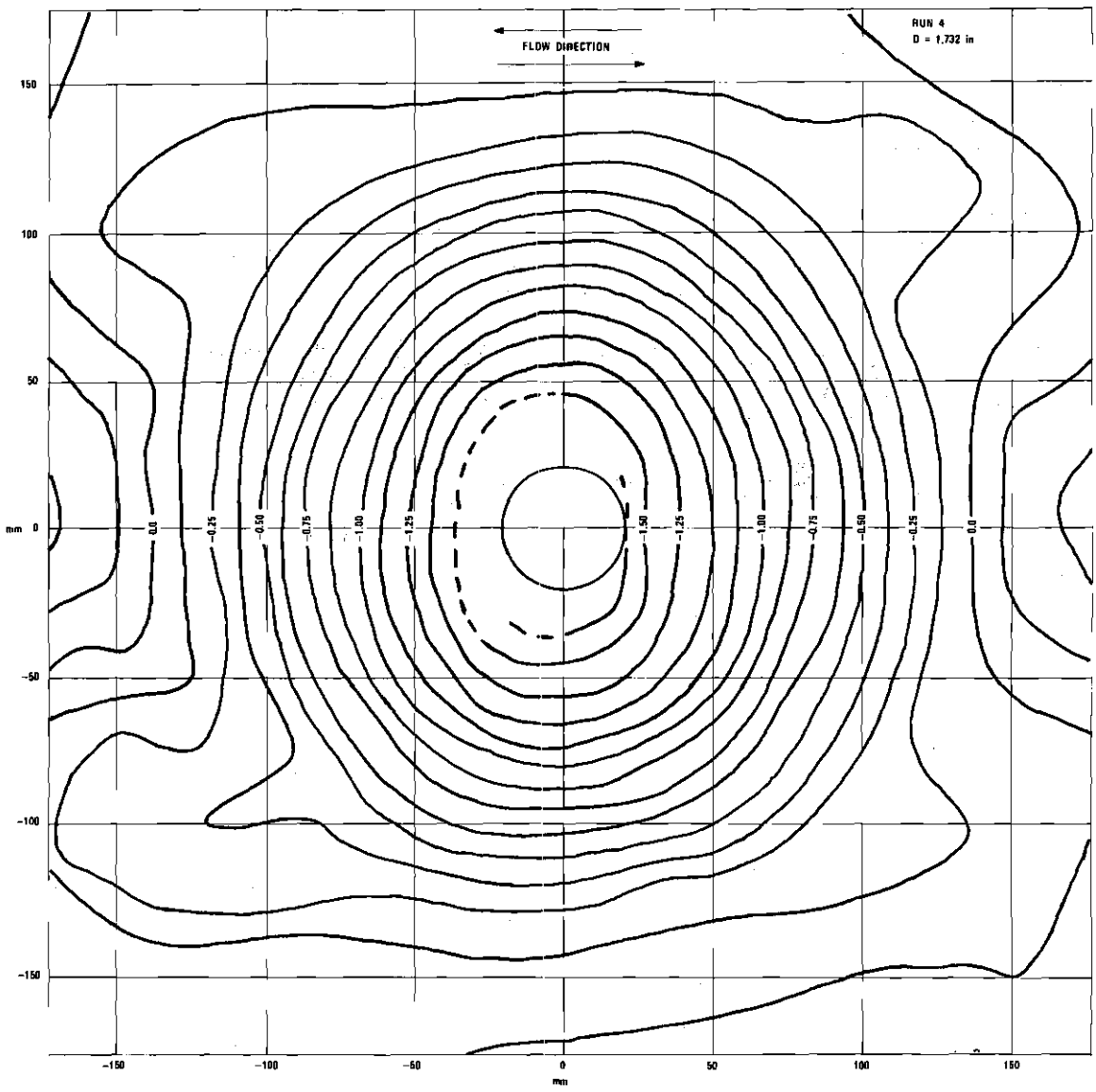

Figure 6. Topographic Map (Contours in D-Units)

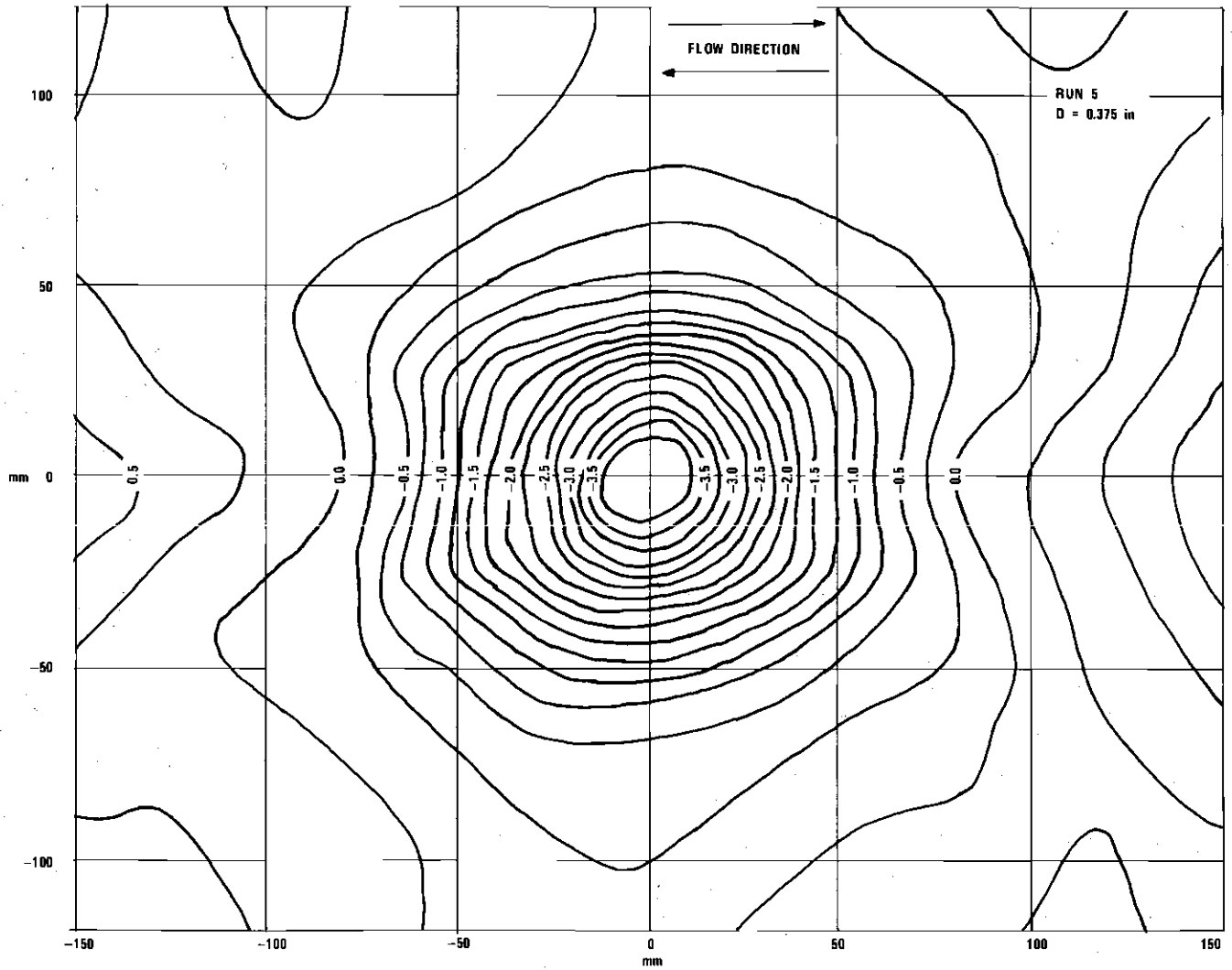

Figure 7. Topographic Map (Contours in D-Units)

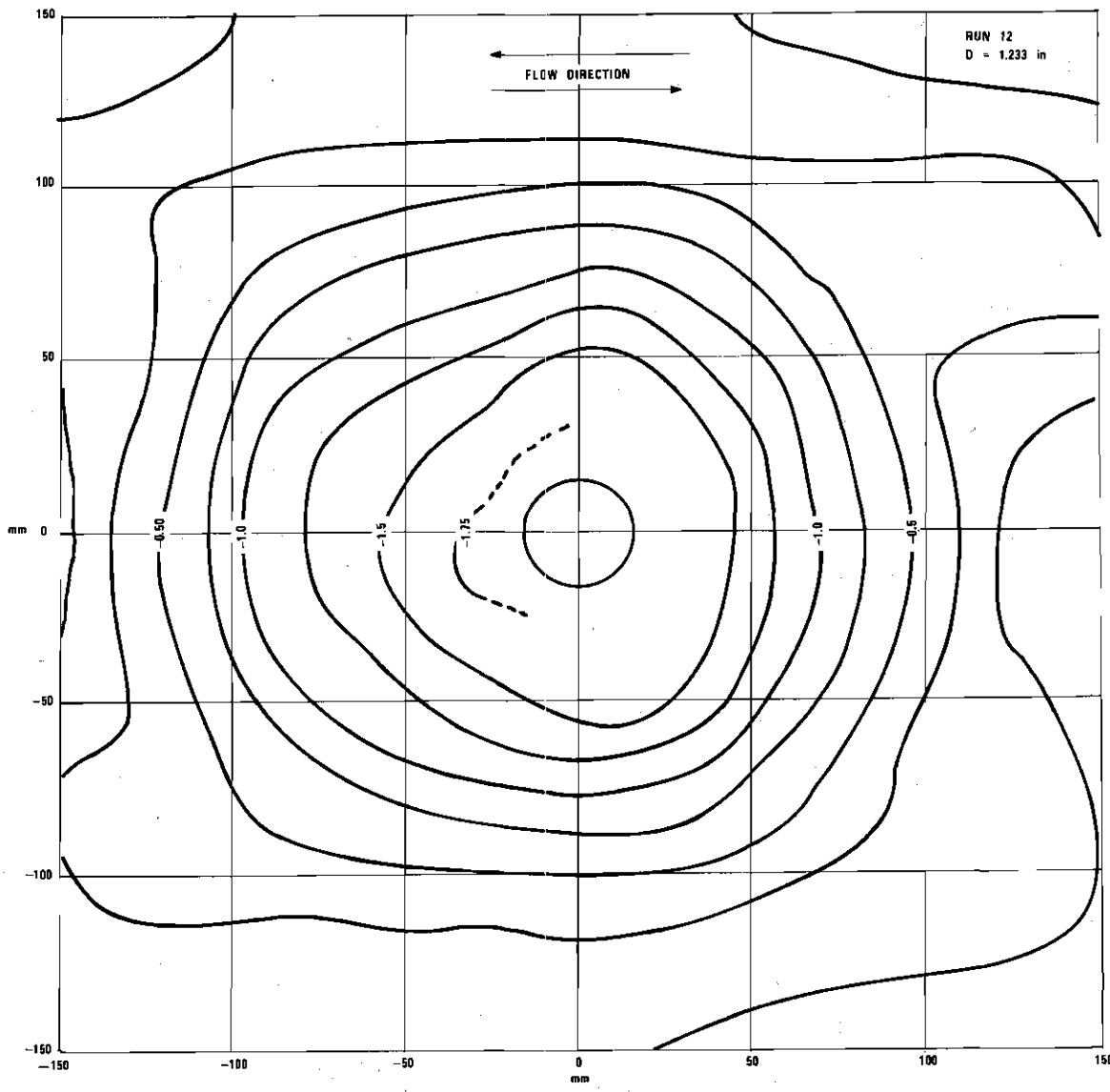

Figure 8. Topographic Map (Contours in D-Units)

Determination of the Coefficients of Sediment-Transport Functions

The output sediment-transport function expressing the rate of pickup of the sediment out of the scour hole, Q_{so}, is given by Equation 5. The input sediment-transport functions expressing the rate of supply of the sediment into the scour hole, Q_{si}, are given by Equations 9,10,11, and 12. In order to formulate a scour function, the functional coefficients K_0, K_1, K_2, and K_3 in the above transport equations are to be evaluated using the experimental results.

For the low-amplitude runs in which a/D_g was less than 550, the sediment transport into the scour hole, Q_{si}, was zero. Therefore the net rate of sediment transport can be expressed by Equation 5. Re-arranging Equation 5, the net rate of transport of sediment for low-amplitude runs is written in nondimensional form as follows:

$$K_0 = \frac{Q_{so}}{U_m D D_g \left(\frac{C_D'}{8.2} N_S^2 - \tan \phi \right)^{5/2}} \qquad (15)$$

During the high-amplitude runs in which a/D_g was greater than 1500, the dunes on the bed did not influence the flow pattern around the cylinder. The sediment was transported into the scour hole due to the general movement of a flat bed. The net rate of sediment transport for high-amplitude runs can be expressed by linearly combining the expressions of the rate of transport out, Equation 5, and of the rate of transport into the scour hole, Equation 12. Combining and re-arranging Equations 5 and 12, the net rate of sediment transport for high-amplitude

runs is written as:

$$K_0 - K_3\left(1 + \frac{2S}{D \tan \phi}\right) = \frac{Q_{so} - Q_{si}}{U_m D D_g \left(\frac{C'_D}{8.2} N_s^2 - \tan \phi\right)^{5/2}} \quad (16)$$

The net rate of transport from a scour hole is alternately expressed in Equation 1 as the rate of change of the scour-hole volume, V. Accordingly the sediment transport rates on the right hand sides of Equations 15 and 16 can be calculated experimentally using Equations 1 and 13, and the experimental results of scour depth, S, as a function of time, t, of low and high amplitude runs.

The calculated values of the net rate of sediment transport for Runs 5,10,13, and 23 are shown in Figures 9 and 10. Runs 10 and 23 in Figure 9 were performed at low water-motion amplitudes while Runs 5 and 13 in Figure 10 were high-amplitude runs. In all four runs, 0.375-in.-diameter pile was utilized.

Coefficients of Input Sediment Transport Functions

For a given sand and pile size, the functional coefficients K_0, K_1, K_2, and K_3 of sediment-transport functions should be the same from one scouring situation to another. Thus the difference between the net sediment-transport rates given by Equations 15 and 16 should yield the value of functional coefficient K_3 of input sediment-transport function. Subtracting Equation 16 from Equation 15,

$$K_3\left(1 + \frac{2S}{D \tan \phi}\right) = \frac{Q_{so}}{U_m D D_g \left(\frac{C'_D}{8.2} N_s^2 - \tan \phi\right)^{5/2}} -$$

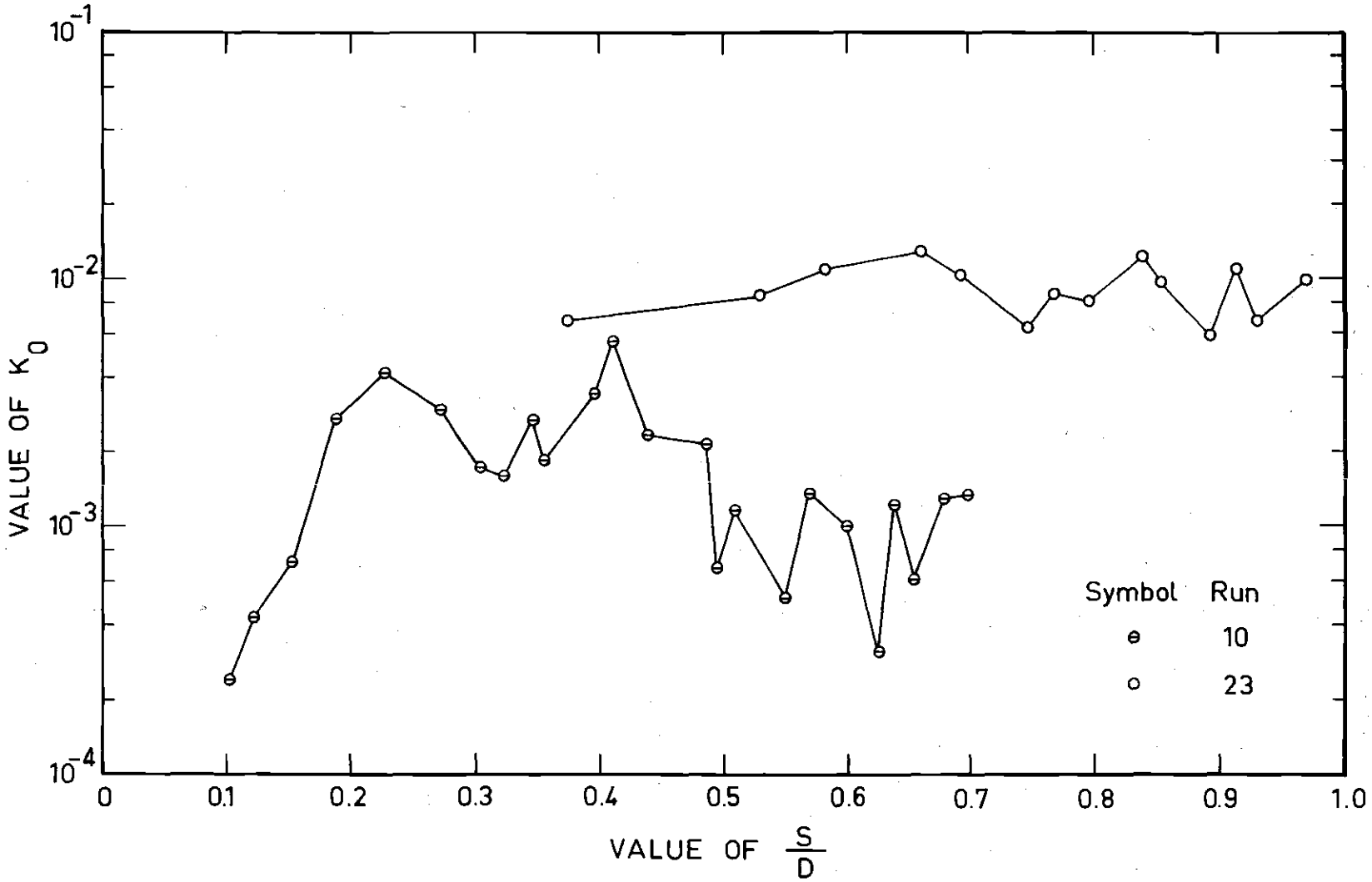

Figure 9. Sediment-Transport Rate (D = 0.375 in.)

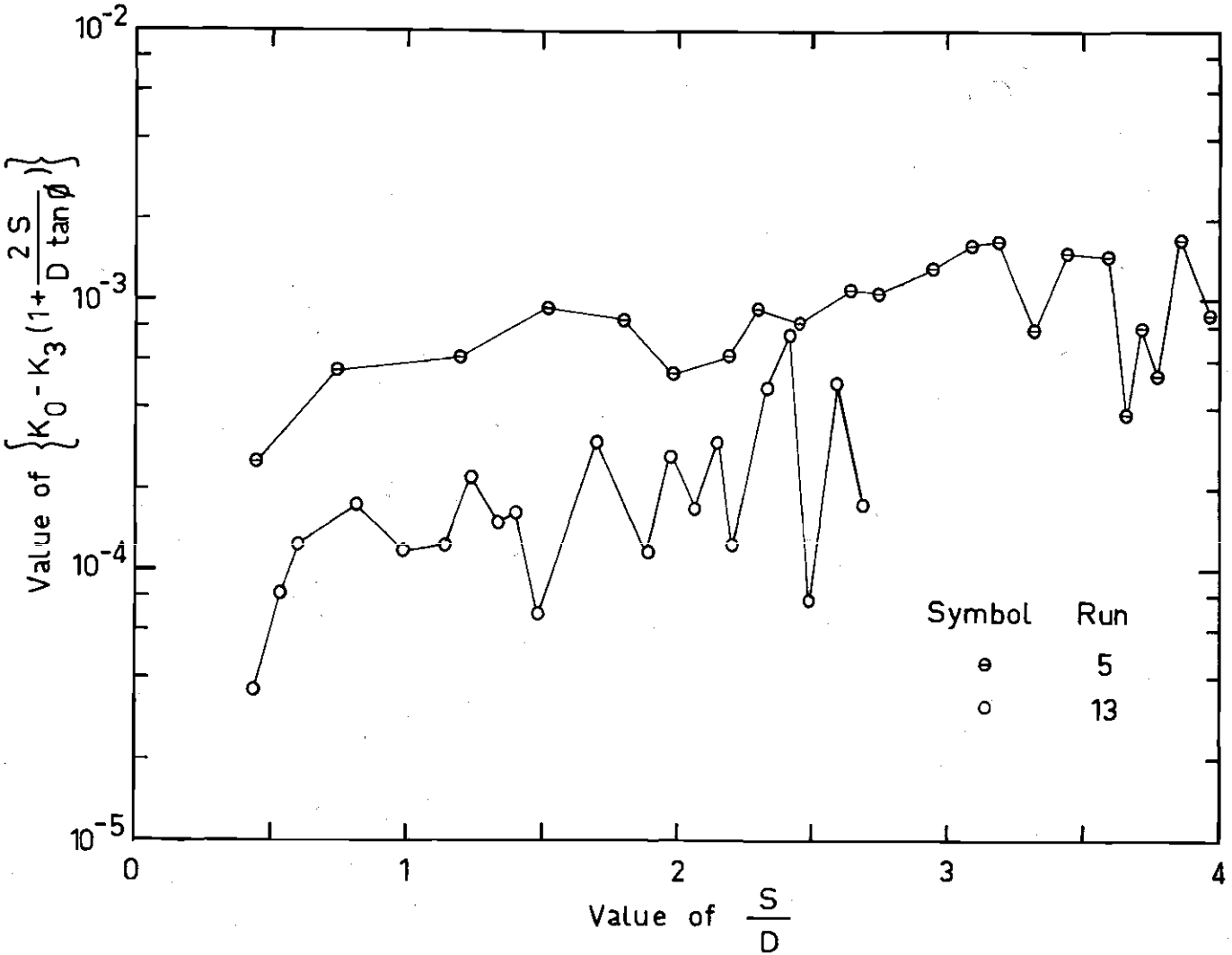

Figure 10. Sediment-Transport Rate (D = 0.375 in.)

$$\frac{Q_{so} - Q_{si}}{U_m D D_g \left(\frac{C'_D}{8.2} N_s^2 - \tan \phi \right)^{5/2}} \qquad (17)$$

The constant K_3 is determined by evaluating the right-hand side of Equation 17 experimentally for both sands using the values of net sediment transport rates shown in Figures 9 and 10 at a given value of scour depth, S/D. If $K_3 = f(\phi)$ is simply assumed to be proportional to a power of tan ϕ, then, the coefficient K_3 of input sediment-transport function is as follows:

$$K_3 = 1.5 \ (10^{-4}) / \tan^4 \phi \qquad (18)$$

The K_3 is given for the range of a/D_g greater than 1700. After the value of the K_3 is determined, the values of the K_1 and K_2 of Equations 10 and 11 can be computed for a given bed material. The computed values of K_1 and K_2 for 0.30-mm-diameter glass beads are given in Equations 19 and 20. The water temperature was taken as being 60 degrees Fahrenheit.

For $a_c/D_g < a/D_g < 775$,

$$K_1 = 6.0 \ (10^{-5}) / \tan^4 \phi \qquad (19)$$

for $775 < a/D_g < 1700$,

$$K_2 = 2.26 \ (10^{-2}) / \tan^4 \phi \qquad (20)$$

Coefficient of Output Sediment-Transport Function

The value of the coefficient K_0, $K_0 = f\ (S/D,\ D_g/D,\ \phi)$, in the output sediment-transport function, Equation 5, is calculated by using the experimental results. For low-amplitude runs, the coefficient K_0 is computed by Equation 15 as a function of S/D. The values of K_0 for Runs 10 and 23 are shown in Figure 9. For high-amplitude runs, the coefficient K_0 is evaluated from Equation 16 using the experimentally determined value of K_3. The calculated values of K_0 for high-amplitude runs are shown in Figures 11 and 12. The straight lines in Figures 11 and 12 show the values of dimensionless coefficient K_3 $(1+2S/\ (D\ \tan\phi))$ of input sediment-transport function. An inspection of Figures 9, 11, and 12 discloses that the value of K_0 at the start of a high-amplitude runs is approximately equal to the value of input sediment transport coefficient K_3 $(1 + 2S/\ (D\ \tan\phi))$. With the increase in the scour depth, S/D, the value of K_0 increases especially at the initial stages of the scour. The increase of the output sediment-transport rate from an initial value close to input sediment-transport rate is also observed from the experimentally evaluated net sediment-transport rates (rate of output minus rate of input) shown in Figure 10. It is also observed that at given values of S/D and water-motion amplitude, the larger the pile diameter, the larger the value of K_0.

In order to determine the functional coefficient of output sediment transport function, the mass transport equation, Equation 2, and the experimental results of scour depth, S, as a function of time, t, of model tests were used. The function K_0 was evaluated by assuming

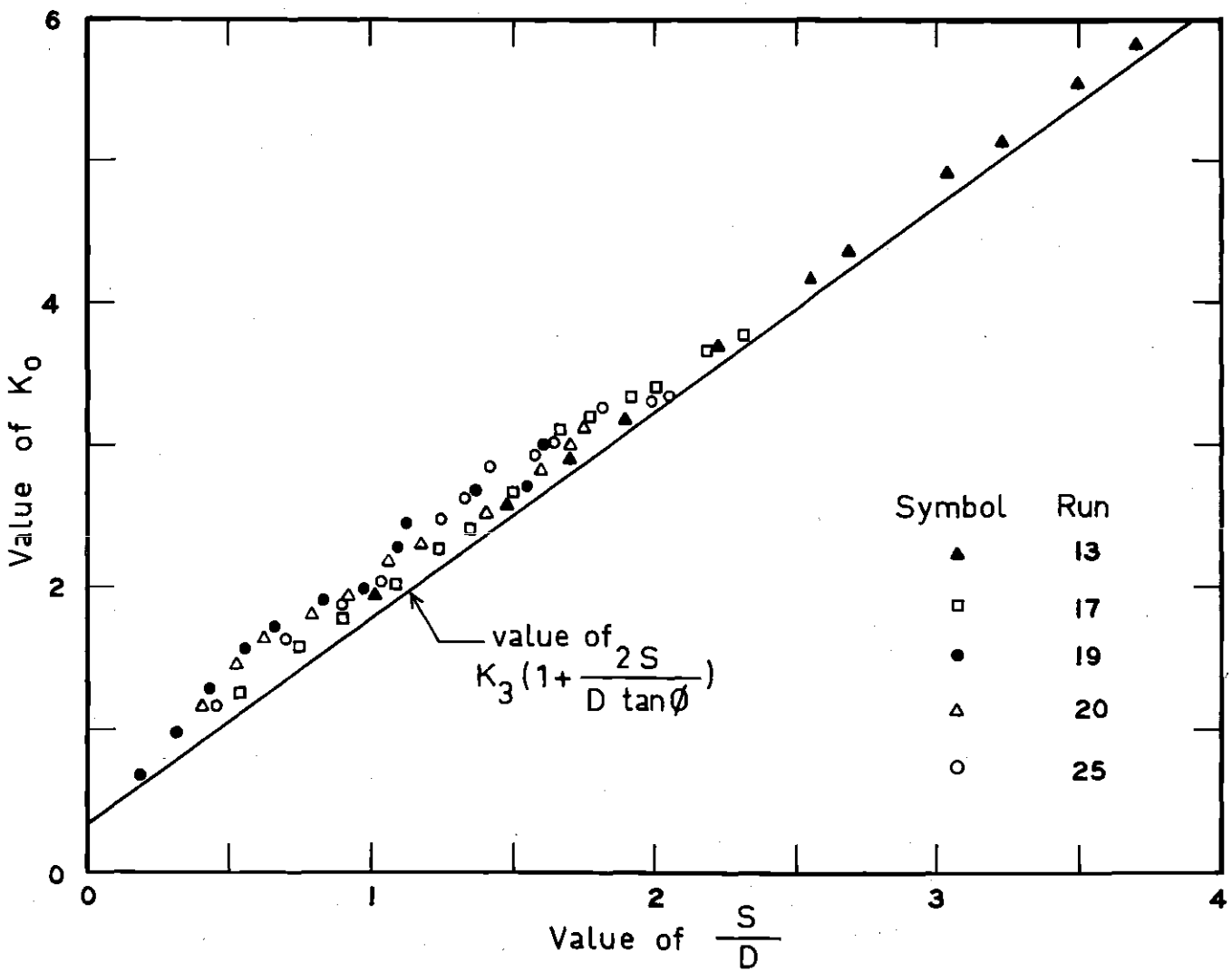

Figure 11. Sediment-Transport Rate (D_g = 0.30 mm)

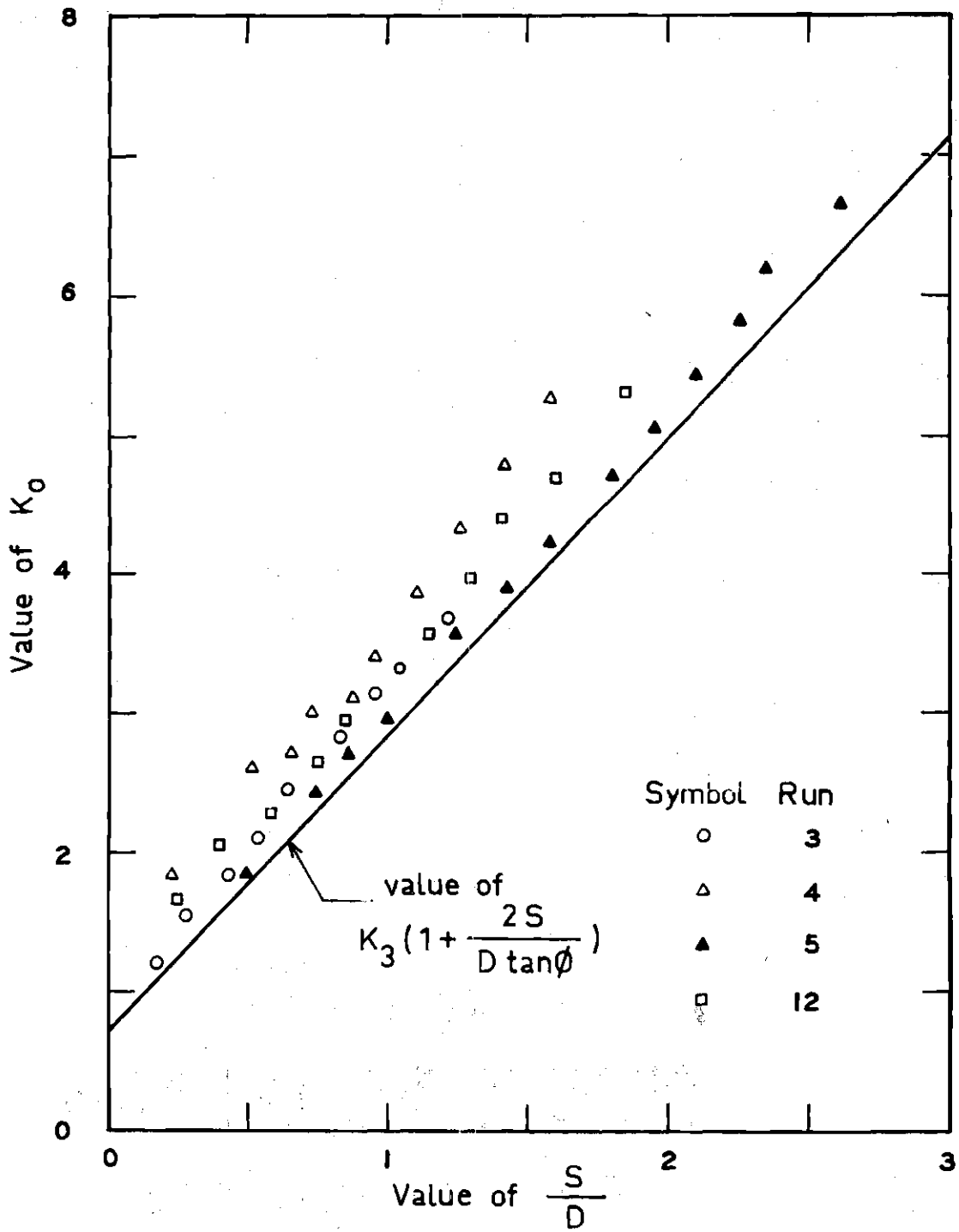

Figure 12. Sediment-Transport Rate (D_g = 0.19 mm)

a general function for K_0 conforming the above mentioned observations from Figures 9,11, and 12, then by substituting Equations 5,12, and 14 into Equation 2 and integrating. The integral of Equation 2 is a scour-depth-versus-time function. The function K_0 was varied systematically until the integral of Equation 2 matched experimentally determined scour-depth-versus-time data of model tests. This method of determination of K_0 was found advantageous over fitting a function of K_0 to experimental data shown in Figures 9,11, and 12. Relatively large scatter of experimental data in Figures 9,11, and 12 did not allow a satisfactory direct formulation of coefficient K_0. The scour-depth-versus-time curves resulting from the integral of Equation 2 was considerably more sensitive to variations in function K_0.

A total of nine model tests out of eleven that were performed at the values of a/D_g greater than 1500, were acceptable for the analysis. The other two tests were rejected because of excessive variations in water-motion amplitude throughout the tests. The scour-depth-versus-time data for the tests that were performed with the Ottawa sand as bed material, Runs 3,4,5, and 12 are given in Figure 13. The scour-depth data for the tests that were performed with glass beads as the bed material, Runs 13,17,19, 20 and 25 are given in Figure 14.

A total of ten runs were performed at the value of a/D_g less than 550. Of the ten runs, Runs 8,10,23 and 24 are analyzed. In all these runs, the variation of water motion amplitude was less than one-half inch or the variation in N_s is no more than $\pm$ 0.2 from the mean value. Runs 8 and 10 were performed with the 0.19-mm sand, while Runs 23 and 24 were performed with the 0.30-mm glass beads as the bed material. In

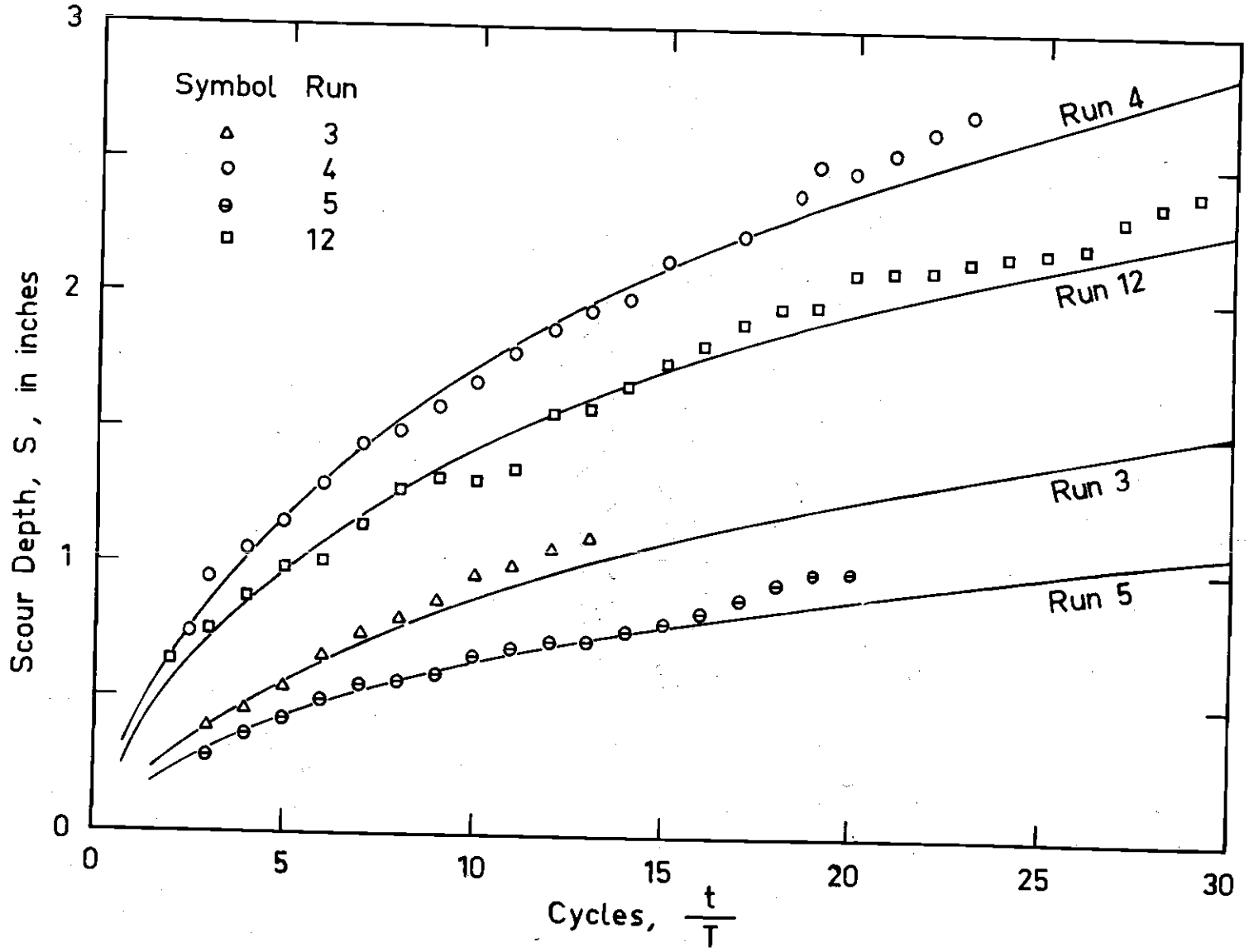

Figure 13. Scour Depth versus Time (D_g = 0.19 mm)

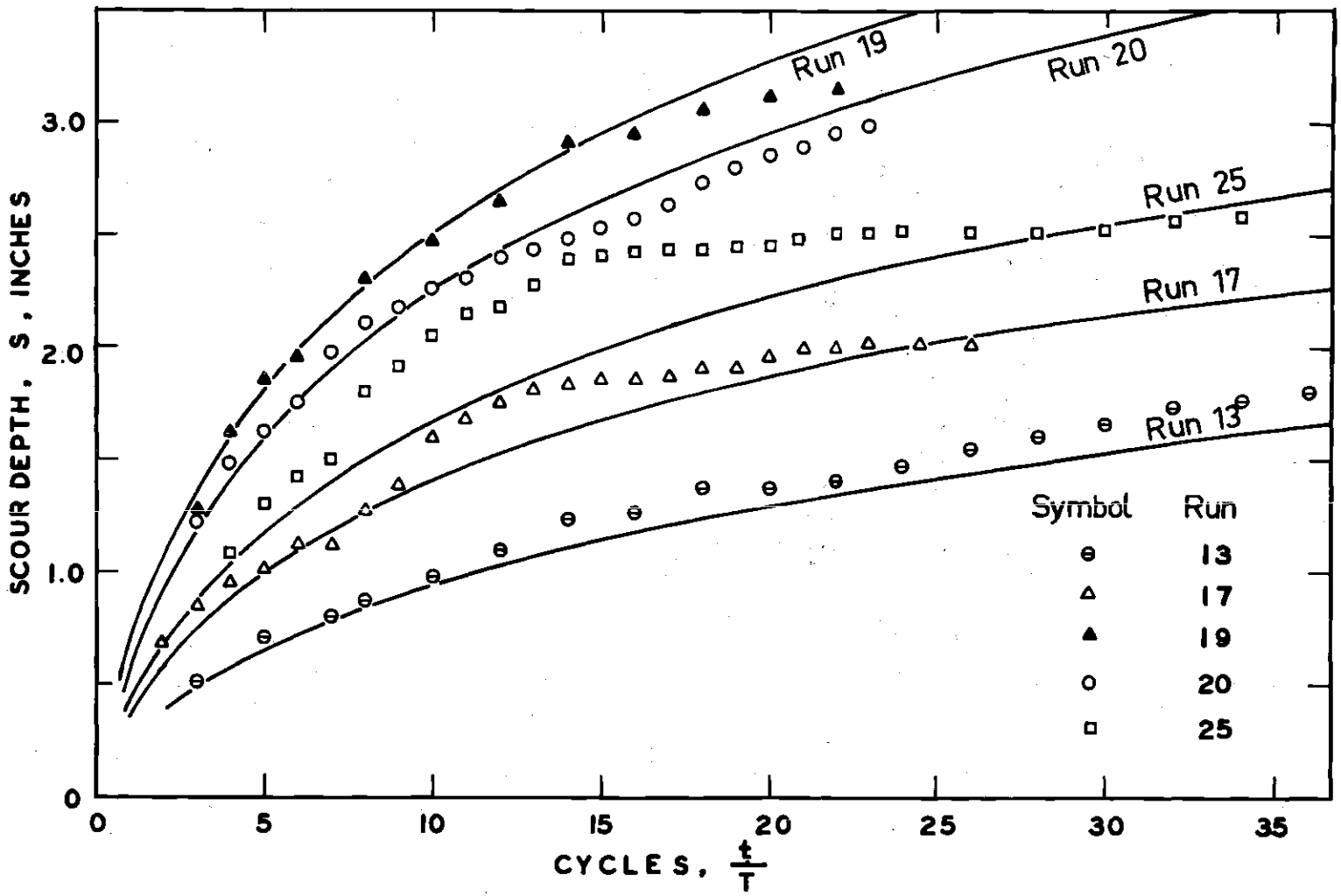

Figure 14. Scour Depth versus Time (D_g = 0.30 mm)

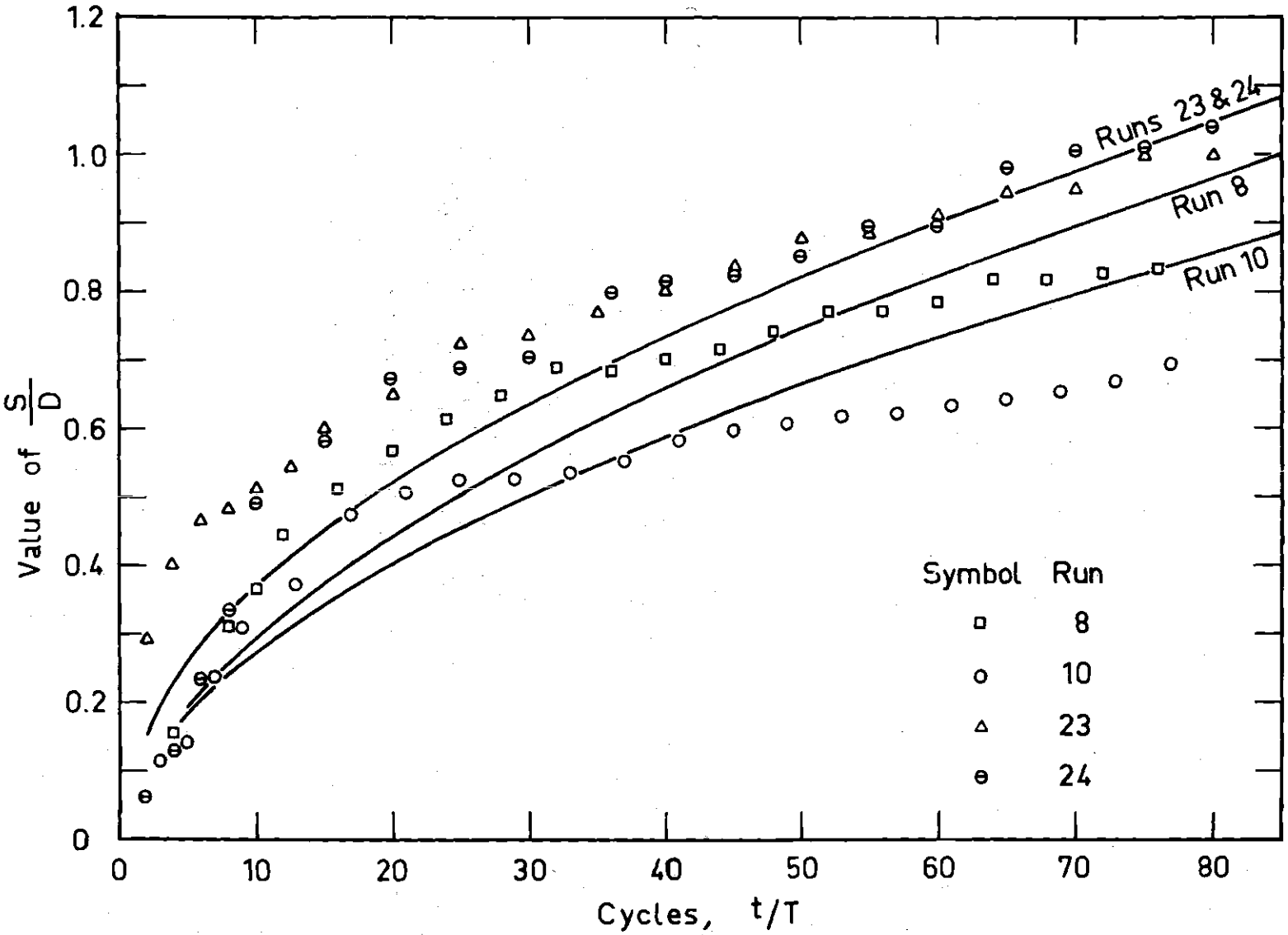

Figure 15. Scour Depth versus Time (D = 0.375 inches)

all runs, 0.375-in.-diameter pile was utilized. The scour-depth-versus-time data of Runs 8,10,23 and 24 are shown in Figure 15.

The continuous curves shown on Figures 13,14 and 15 were obtained by using

$$K_0 = \frac{1.5(10^{-4})}{\tan^4\phi} + \frac{\left[7.2(10^{-4}) + 46.5\left(\frac{D_g}{D}\right)^2\right]\frac{S}{D}}{\tan^5\phi\left[1.5(10^5)\left(\frac{D_g}{D}\right)^2 + \frac{S}{D}\right]} \qquad (21)$$

in integration of Equation 2. Since the integral of Equation 2 is not an elementary integral, a numerical scheme had to be used to evaluate the integral at various values of scour depth, S. The continuous curves shown in Figures 13,14, and 15 were deemed to be satisfactory fits to the measured scour depth data. The systematic variation of various forms of K_0 had not resulted a noticeable overall improvement in prediction curves shown in Figures 13,14 and 15 within the range of the data. To compare several general forms of function K_0, also, a multivariate curve-fitting technique was utilized. Using a numerical non-linear least square method, the function K_0 in Equation 21 was fitted to experimental data shown in Figures 11 and 12. The resulting multiple correlation coefficient was 0.965. Error residual to fitting was also found to be at a minimum indicating the strongest correlation among the tried forms. For a review of the applications of multivariate analysis, the reader is referred to Snyder (31). Thus, the output sediment-transport function to be utilized in formulation of the scour-depth function is as follows:

$$\frac{Q_{so}}{U_m D D_g} = \left\{ \frac{1.5(10^{-4})}{\tan^4\phi} + \frac{7.2(10^{-4}) + 46.5 \left(\frac{D_g}{D}\right)^2}{\tan^5\phi \left[1.5(10^5) \left(\frac{D_g}{D}\right)^2 + \frac{S}{D}\right]} \frac{S}{D} \right\}$$

$$\left\{ \frac{C_D'}{8.2} N_s^2 - \tan\phi \right\}^{5/2} \qquad (22)$$

Formulation of Scour-Depth Function

The scour around a vertical pile induced by oscillatory flow is given by the integral of the sediment continuity equation, Equation 2. For steady cyclic water motion, the volume of scour hole, V, the rate of pickup of sediment, Q_{so}, and the rate of fill of sediment into the scour hole, Q_{si}, have been presumed to be functions of the scour-hole depth, and of the time-invariant flow, fluid and sediment variables. The scour-depth-versus-time function is obtained by substituting the right hand side of Equation 14 for dV, by substituting the right-hand side of Equation 22 for Q_{so}, and by substituting the right-hand side of either Equations 9, 10, 11 or 12 for Q_{si}. The coefficients K_1, K_2, and K_3 of Equations 10, 11, and 12 are given by Equations 19, 20, and 18 respectively. Comparison of experimental scour-depth-versus-time data with those obtained by integration of Equation 2 are shown in Figures 13, 14, and 15.

The general scour-depth-versus-time functions can be determined by repeated numerical integration of the dimensionless form of Equation 2. The dimensionless form used is as follows:

$$\frac{t\, D_g \sqrt{(s-1)g\, D_g}}{D^2} = \int_0^{\frac{S}{D}} \frac{d\left(\frac{V}{D^3}\right)}{\frac{Q_{so}}{DD_g\sqrt{(s-1)g\, D_g}} - \frac{Q_{si}}{DD_g\sqrt{(s-1)g\, D_g}}} \qquad (23)$$

The expression under the integral sign is a function of the dimensionless variables of the geometric variable, S/D; sediment number, N_s; the coefficient of drag, C_D'; the angle of repose, ϕ; and sediment-grain variable, D_g/D. Scour-depth-versus-time curves have to be prepared separately for each sediment size.

The dimensionless scour-depth-versus-time curves for the tests performed with 0.30-mm bed material (glass beads) are shown in Figures 16 and 17. In each figure, the scour depth, S/D, is shown as a function of a/D_g and $tD_g\left[(s-1)g\, D_g\right]^{1/2}/D^2$. Figure 16 shows the scour-hole development in the presence of sediment transport into the scour hole. The scour-hole development in the absence of sediment transport into the scour hole is shown in Figure 17. The value of a_c/D_g at incipient motion for glass beads was taken as 600 as reported in a previous study (29). In laboratory experiments, the period of oscillations was a constant 3.55 seconds. The water temperature was taken as being 60 degrees Fahrenheit. The value of pile-diameter-to-grain-size ratio was taken as 1000. Similar figures can be prepared for other sediment sizes, wave periods and pile-diameter-to-grain-size ratios. The scour hole development for varying values of N_s and C_D' is shown in Figures 18, 19, 20, and 21. The varying values of C_D' shown in Figures 18

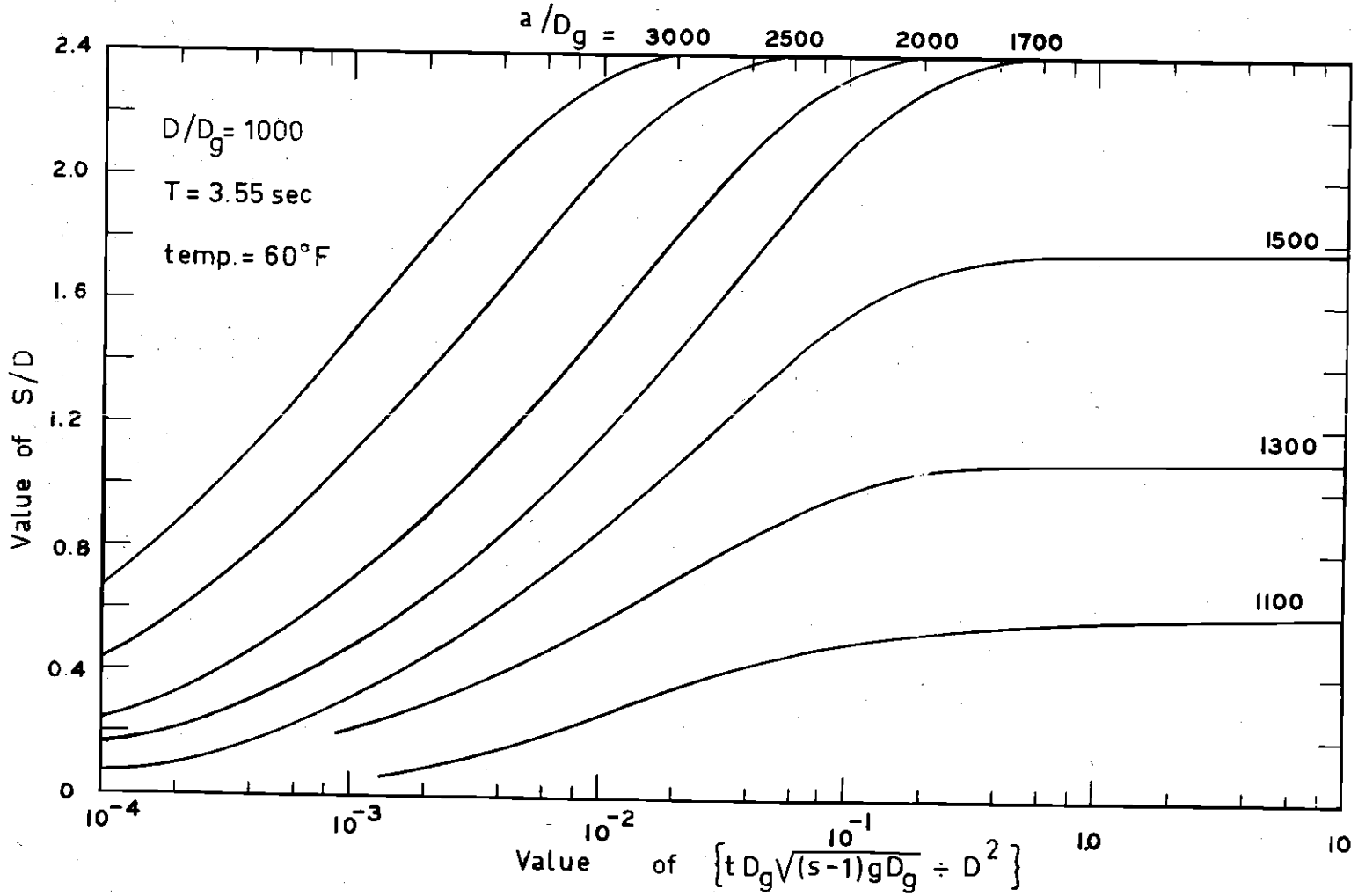

Figure 16. Scour Depth versus Time (Glass Beads)

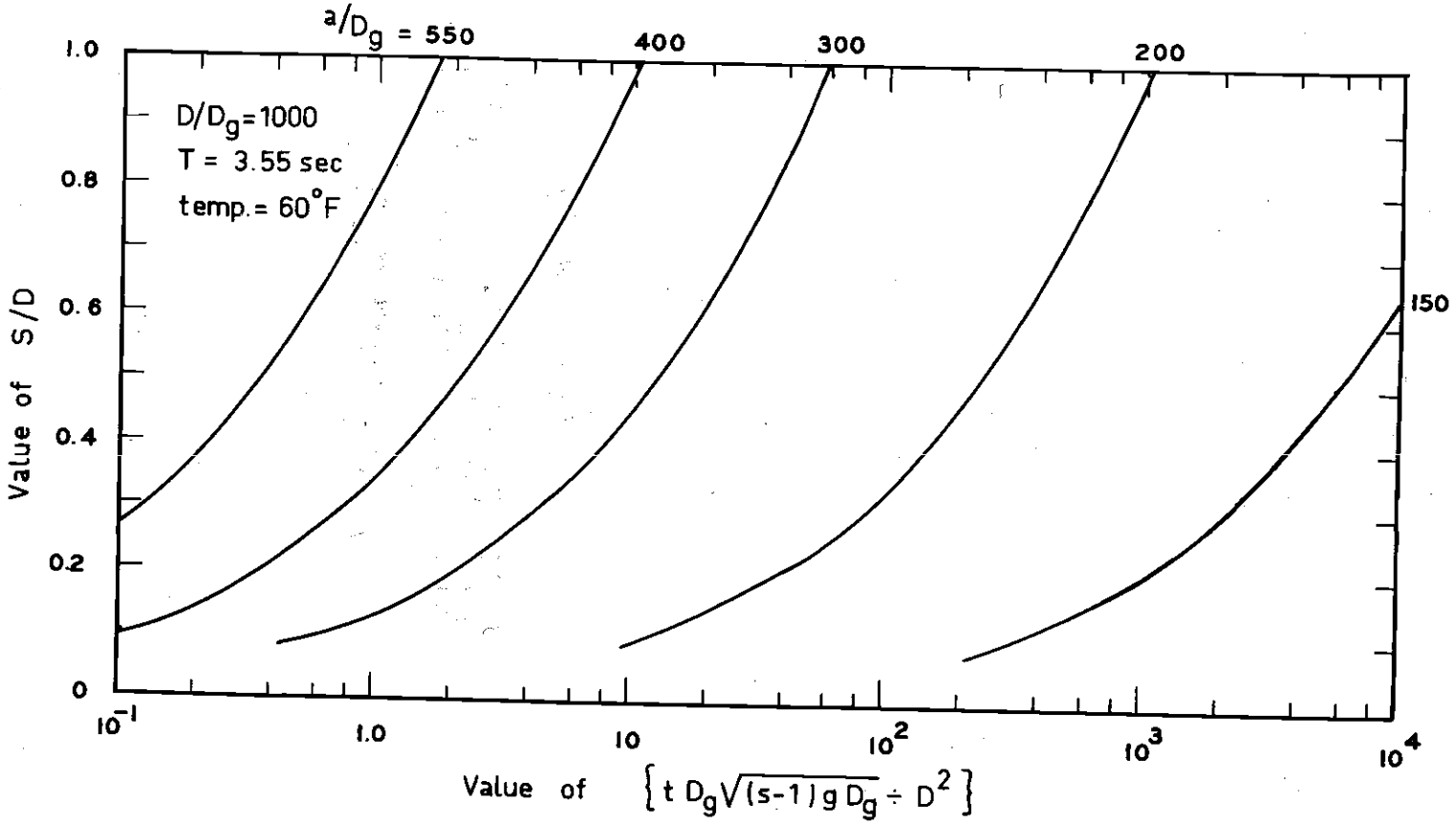

Figure 17. Scour Depth versus Time (Glass Beads)

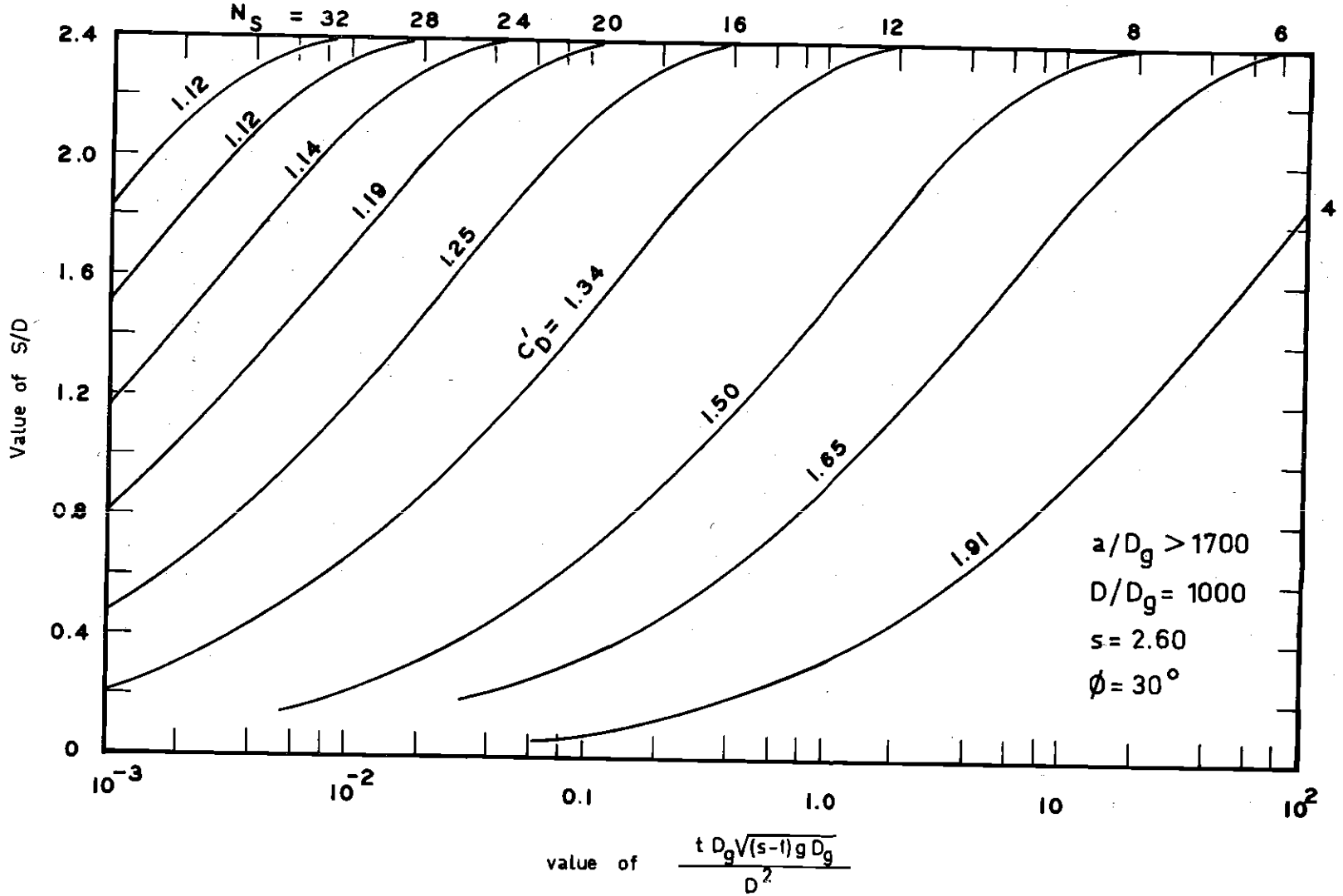

Figure 18. Scour Depth versus Time

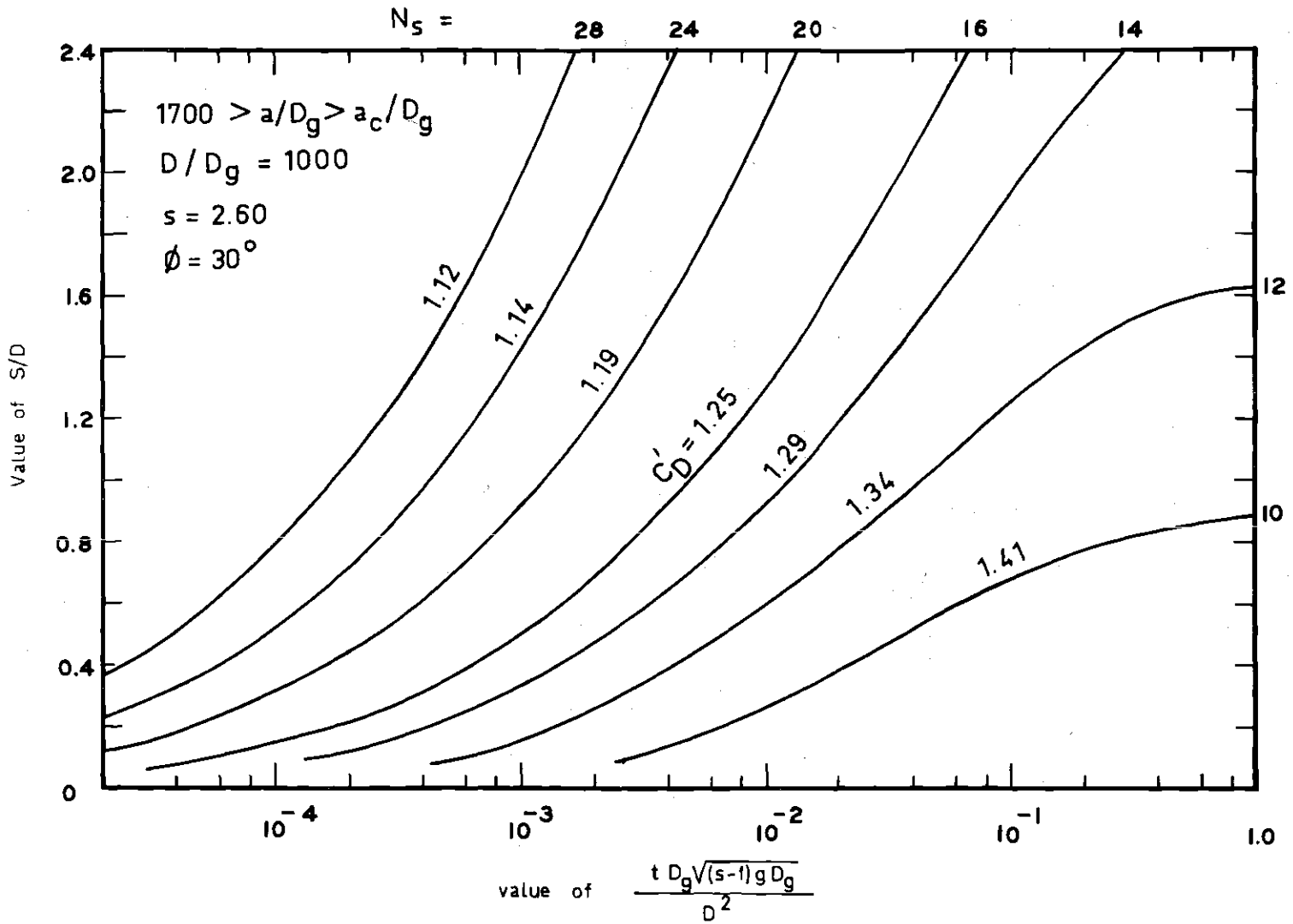

Figure 19. Scour Depth versus Time

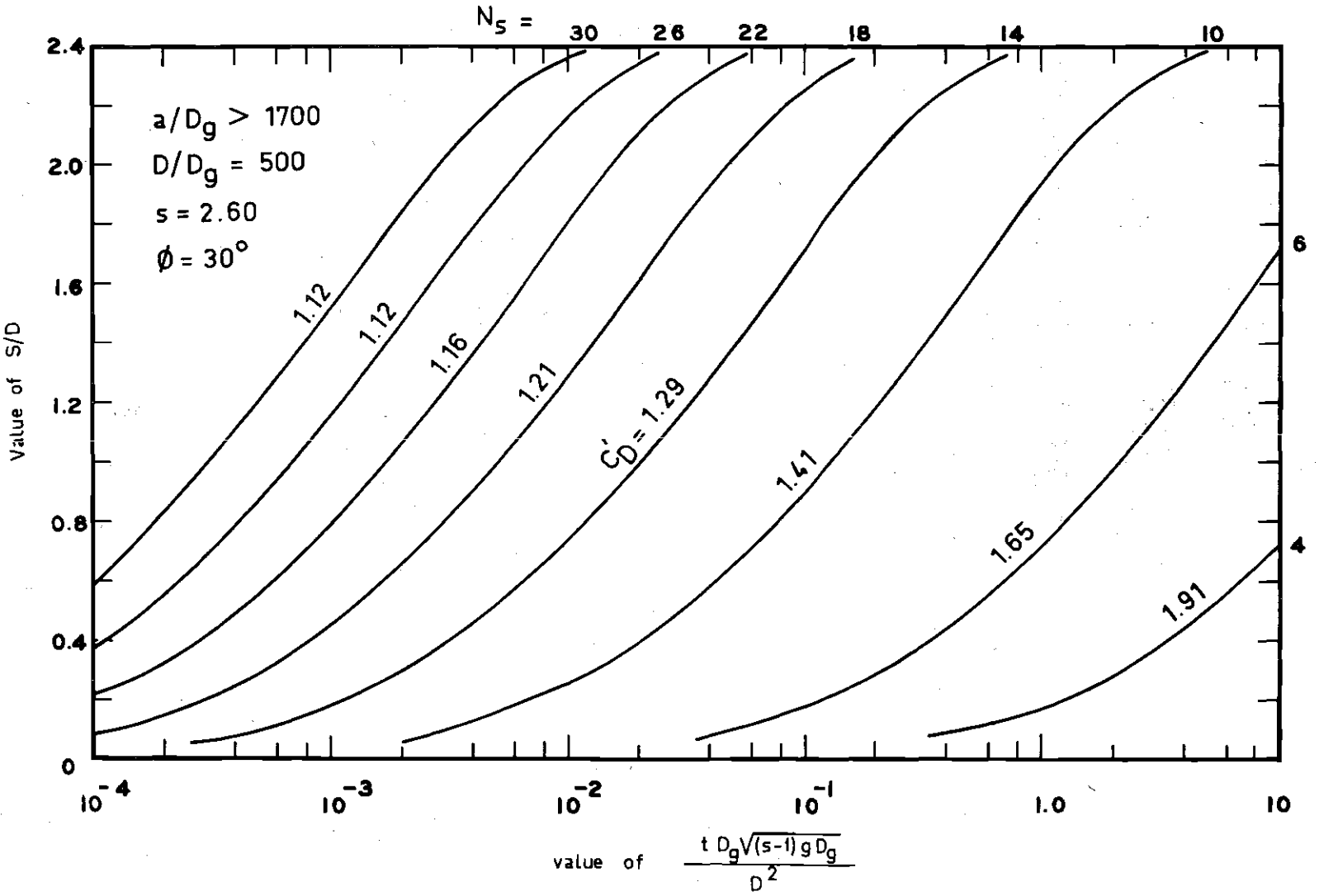

Figure 20. Scour Depth versus Time

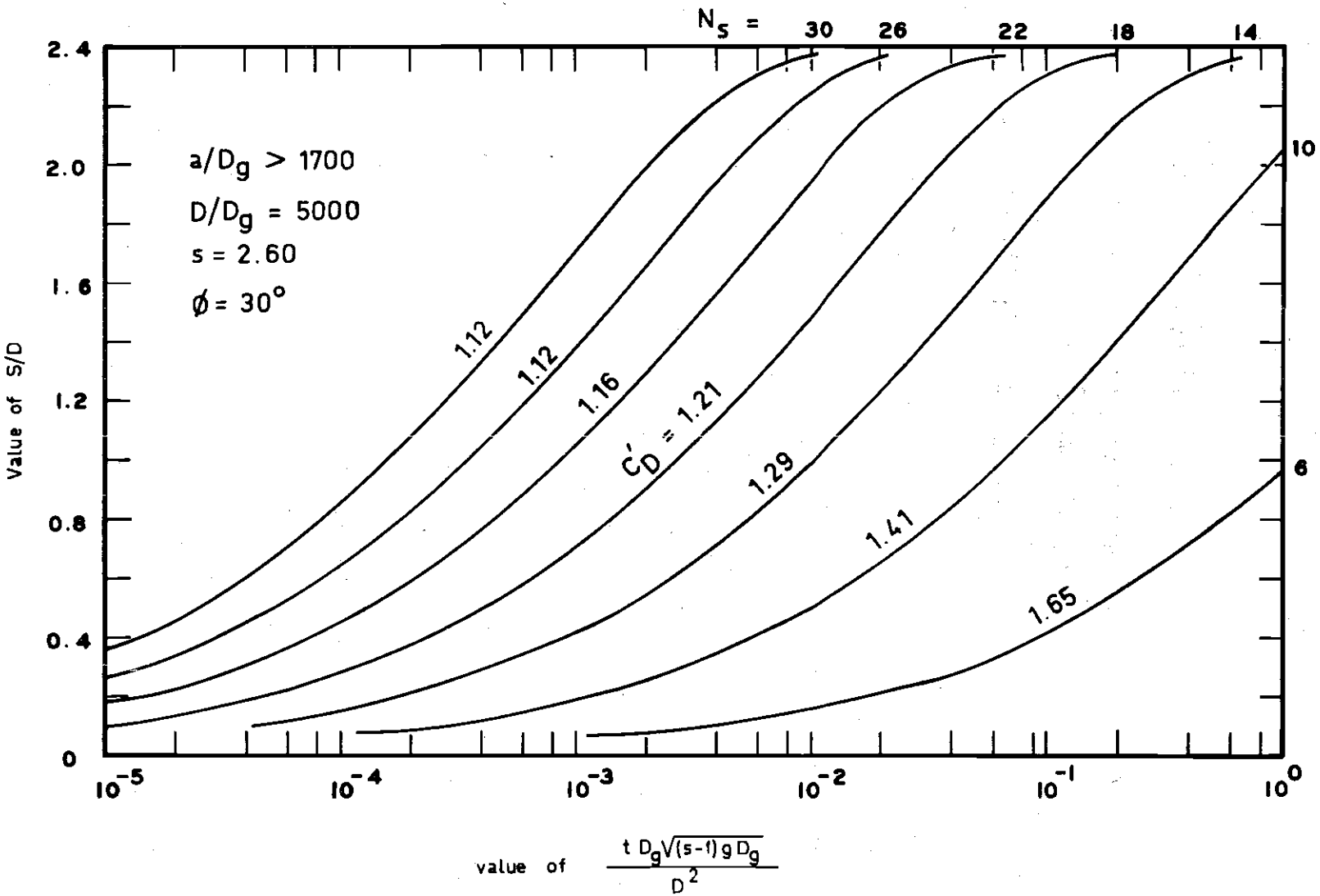

Figure 21. Scour Depth versus Time

thru 21 were computed for a sediment size 0.30 mm and for water temperature 60 degrees Fahrenheit. Inasmuch as C_D' is a dimensionless coefficient, Figures 18 thru 21 would not be limited to 0.30 mm sand. The scour hole development for a constant value of C_D' is shown in Figures 22, 23 and 24 for values of R greater than 500. The value of the coefficient of drag, C_D', for natural sand particles is a constant 1.12 for values of R greater than 500. The curves shown in Figures 22 thru 24 are applicable for all sediment sizes. An inspection of Figures 22, 23, 24 shows that the effect of the variable D/D_g upon the time variation of scour is minor. Therefore the values of dimensionless time parameter could be interpolated satisfactorily for other ranges of D/D_g in between those values that Figures 22, 23 and 24 were prepared. In preparation of Figures 18 thru 24, inclusive, the specific gravity of sediment was assumed to be 2.60 as of quartz sand in sea water. The angle of repose of bed material was taken as 30 degrees as for well-rounded sands.

Terminal Scour Depth

When the rate of sediment transport into the scour hole equals the rate of sediment out of the scour hole, a terminal depth, S_T, is attained. Terminal depth is approached asymptotically with increasing time. The theoretical limit, S_T, is attained when the denominator of integral, Equation 23, is zero.

In the presence of flat-bed sediment transport over the bed surrounding the scour hole, the terminal scour depth is found to be independent of flow velocity. Terminal depth is found to be at least 2.4 times the diameter of the pile when a/D_g is greater than 1700. The

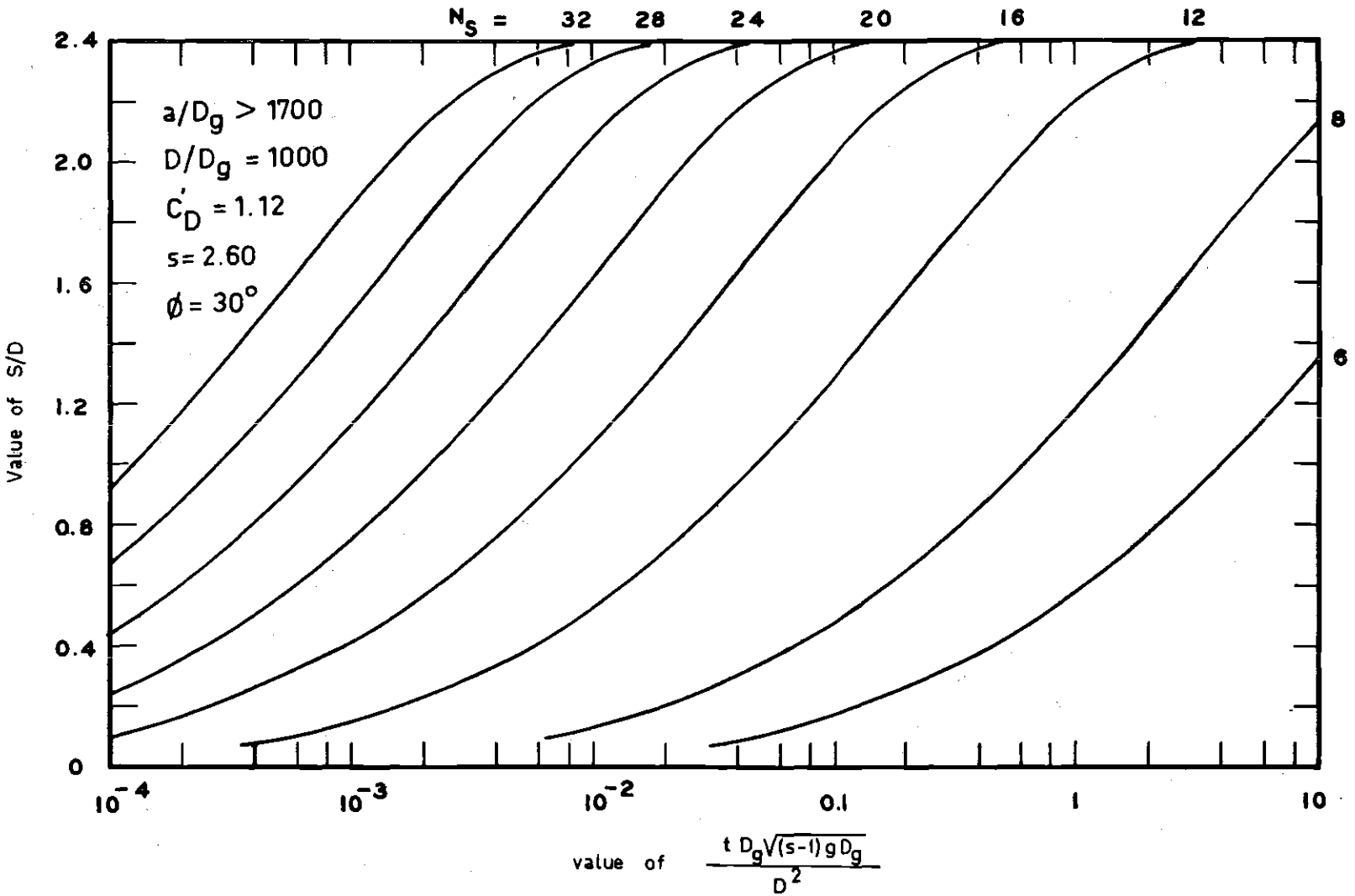

Figure 22. Scour Depth versus Time

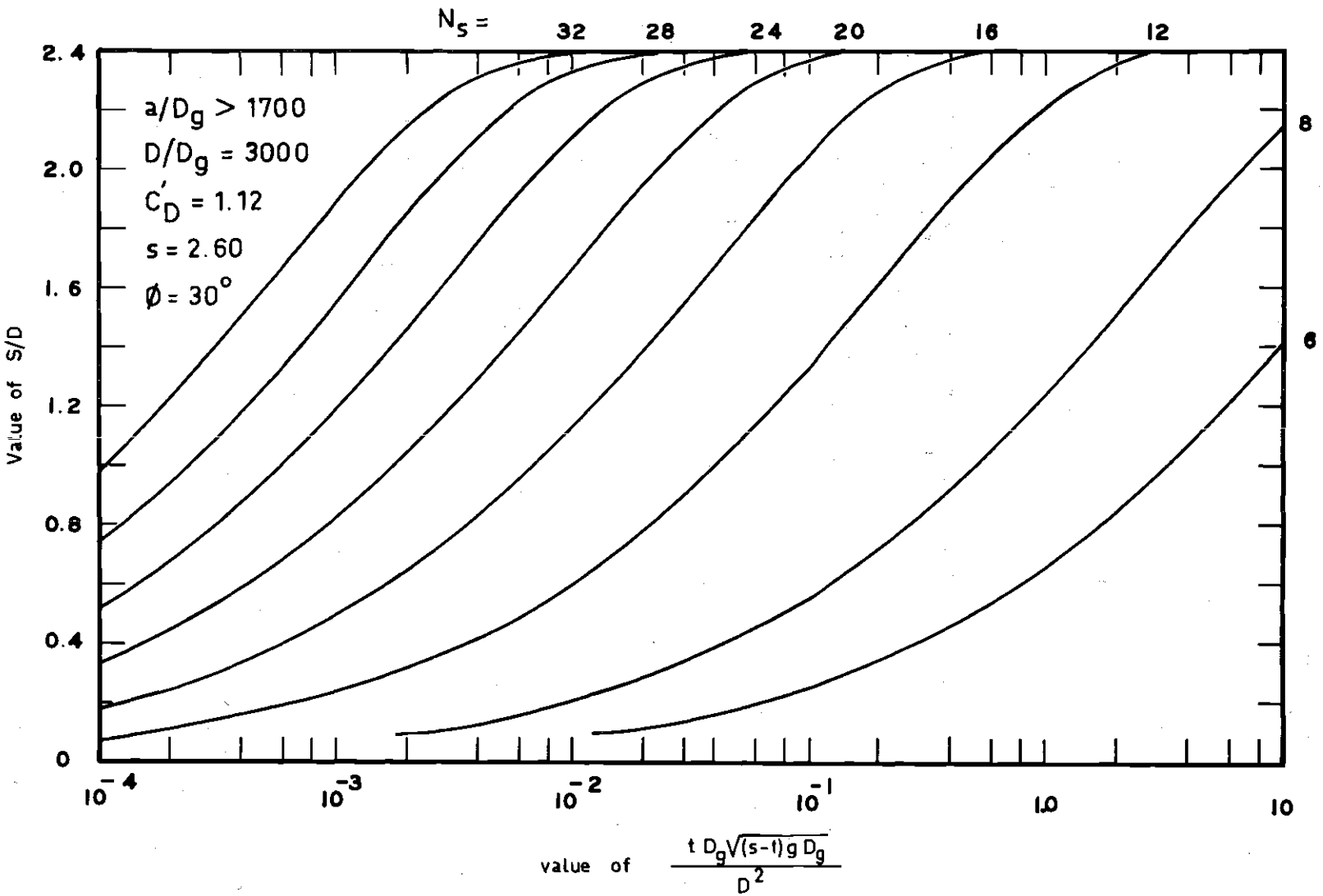

Figure 23. Scour Depth versus Time

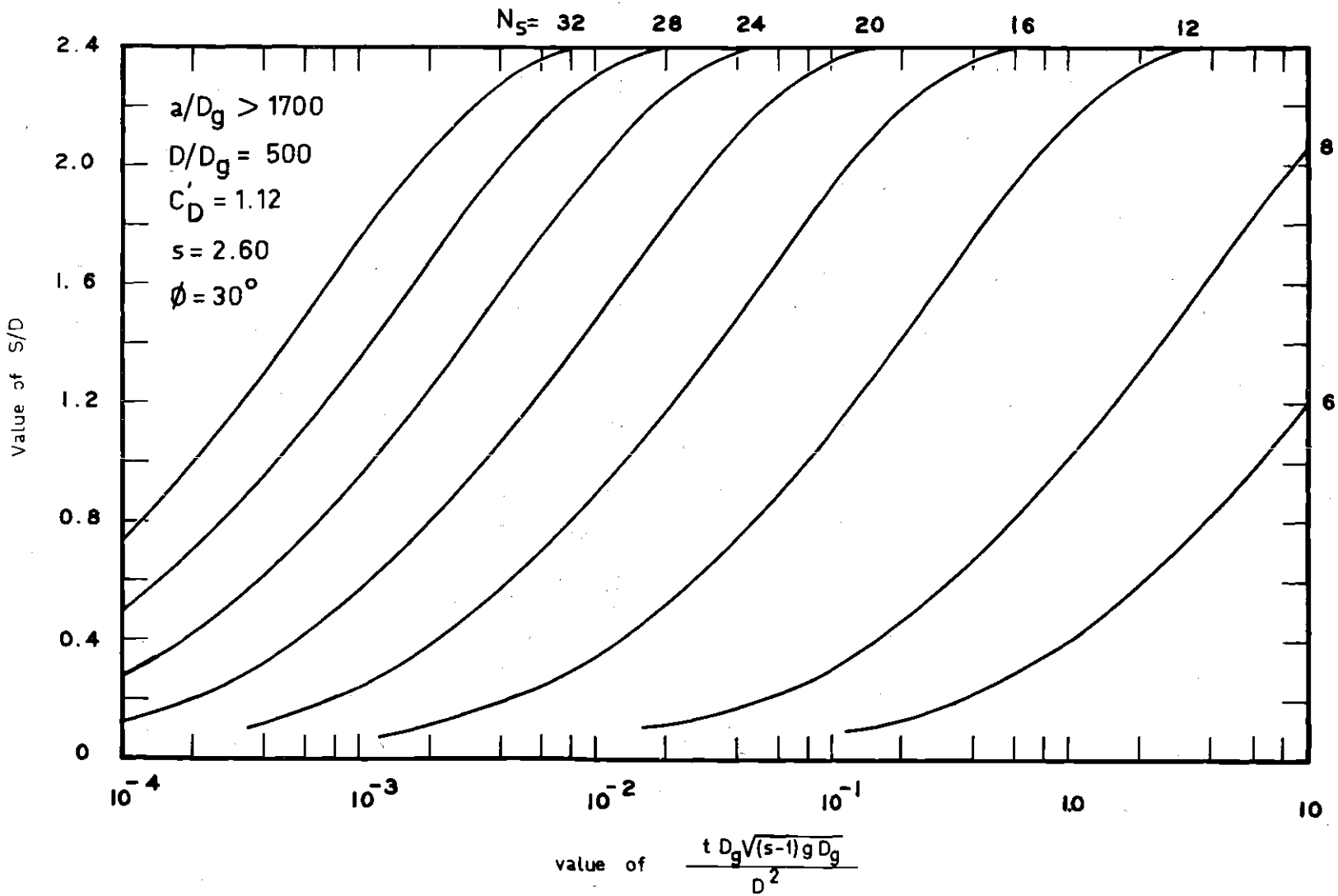

Figure 24. Scour Depth versus Time

computed values of terminal scour depth, S_T/D, are shown in Figure 25 as a function of D_g/D. In the presence of three-dimensional dunes on the surrounding bed, the terminal scour depth decreases. With further decrease in a/D_g, the scour hole is expected to join the dune system. Assuming that the scour hole will form the trough of the dune system, the terminal scour depth should approximately equal to the half of the dune amplitude. In the absence of sediment transport into the scour-hole, no terminal depth is predicted. For the range of a/D_g less than a_c/D_g, the scour-depth-versus-time curves of Equation 23 should yield satisfactory predictions for the time variation of scour depth within the range of experimental data, that is, S/D less than unity.

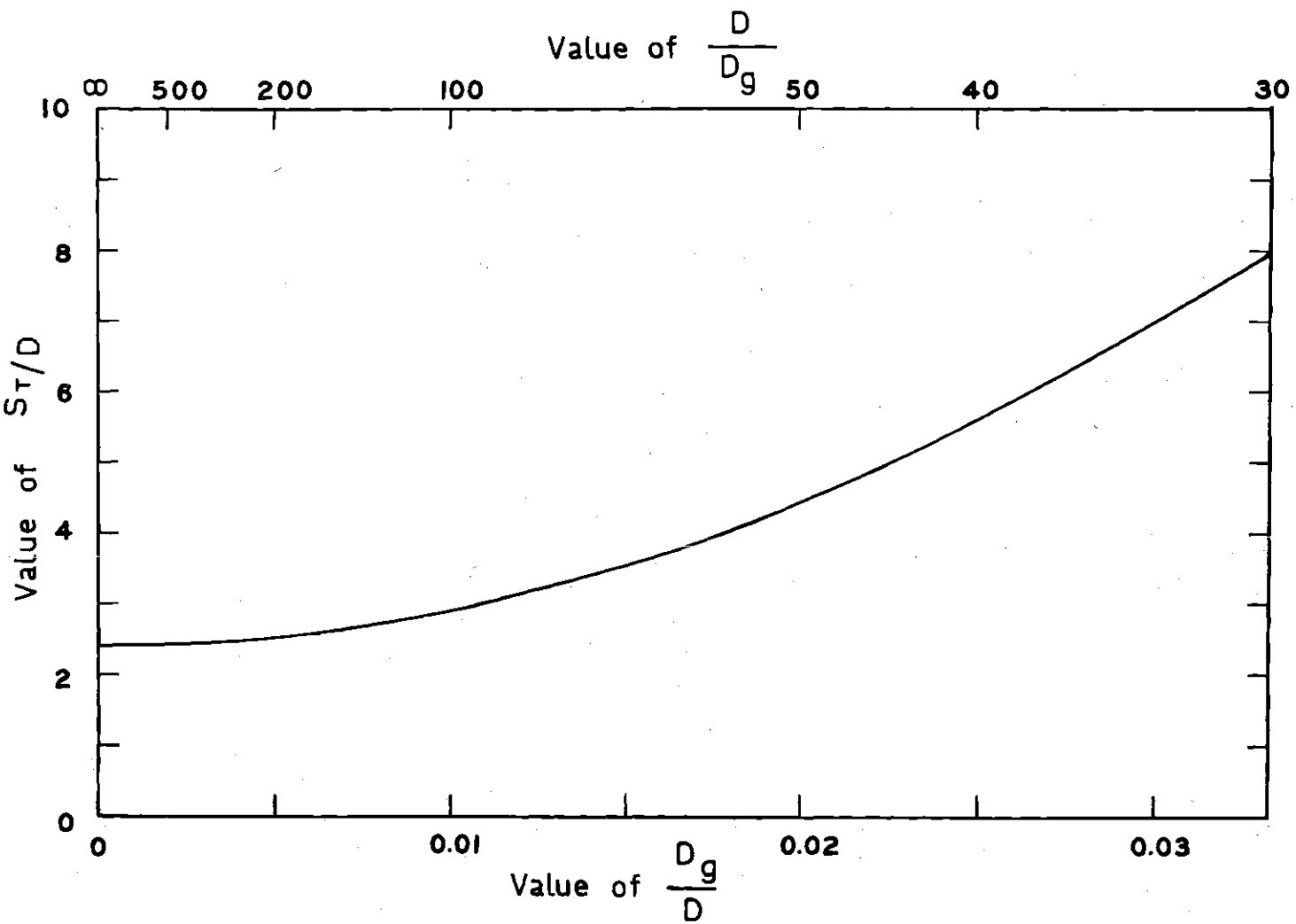

Figure 25. Terminal Scour Depth ($a/D_g > 1700$)

CHAPTER VI

DISCUSSION OF RESULTS

A method has been presented for analyzing the localized scour which develops around a single vertical circular cylinder in a cohesionless bed under the action of first-order Stokian water waves. The analysis of the experimental results is based on the assumption that the sediment transport in and out of the scour hole are independent processes which can be linearly combined into the equation of continuity of sediment. It is also assumed that the velocity and velocity distribution in the areas of active local scour are free of boundary layer effects, that is, the boundary layer is of negligible thickness.

A terminal scour depth is predicted when sediment is being transported into the scour hole from surrounding flat bed. The term "terminal depth" does not imply that the transport out of scour hole approaches zero. "Terminal" refers to the condition of balance wherein the amount of sediment being picked up from the scour hole is equalled by the amount of material filled by the bed-load transport of approaching flow.

With sediment transport into the hole from surrounding flat bed; that is, when a/D_g is greater than 1700, the terminal depth of scour is independent of magnitudes of approach velocity and sediment size. This conclusion is in agreement with the conclusions of the studies in unidirectional flow of Carstens (16), Laursen and Toch (9), and Tarapore (12). With flat-bed sediment transport on the bed, the terminal scour

depth is 2.4 times the diameter of pile if the ratio of pile-diameter-to-sediment-size is large. The lack of effect of the flow velocity and the sediment size on the terminal scour depth can be rationalized on the basis of the necessary balance between the pickup capacity of the vortex and the transport capacity of approaching flow. For given flow velocity and sediment size, the angular velocity of the vortex would be proportional to the velocity of the flow that generates the vortex. At equilibrium scour conditions, any change in the maximum flow velocity would alter the velocity at the grain level both in the scour hole and in the surrounding bed in the same proportion. Therefore the absolute rates of the sediment movement into and out of the scour hole would change, but the balance between pickup and fill would still be maintained. Similarly, if the sediment size changed, the absolute rates of transport into and out of the scour hole would change but equilibrium would still remain.

Analysis of experimental results (Figure 16) indicates that localized scour around a vertical cylinder is influenced by the dunes which form on the bed if a/D_g is less than 1700. The analysis of model tests performed without dunes on the bed indicates that the rate of input sediment transport is close in magnitude to the rate of output sediment transport. For high-amplitude runs, it is computed that the net sediment transport rate (pickup minus fill) is only a small fraction of the rate of pickup. When the function of input sediment transport is extended into the range of dunes by rational analysis, the rate of transport by dunes into the scour hole is found to be in excess of the rate of pickup. Scour-depth-versus-time curves of Figure 16 shows that

for 0.30-mm bed material in the range of $600 < a/D_g < 1000$, no scour hole is predicted. To verify the conclusion that in the region of the dunes the scour hole will join the dune system, two model tests, Runs 26 and 27, were performed. In both runs, the bed material was 0.30-mm glass beads. The procedure during Runs 26 and 27 was the same as that of the regular runs described in Chapter IV, except that no continuous record of the scour hole development was taken. The variation of the scour depth was observed visually. The scour depth at the end of each run was measured and recorded using the electrical point gage.

During Run 26, 1.99-in.-diameter plastic pile which was also used during Run 19, was utilized. The total water-motion amplitude, 2a, was maintained at 18.6 inches. Since the ratio of a/D_g was 780, at the equilibrium conditions the scour hole was expected to join the dune system. With the start of the oscillatory motion, a scour hole formed rapidly on the flat bed around the pile. After formation of the dunes on the bed, however, the scour depth was observed to decrease due to the deposition from surrounding bed. After approximately 200 cycles of oscillations, the scour hole was a part of the dune system. When the run was terminated after 400 cycles of oscillations, the scour hole around the pile was completely transformed into a trough of the dunes around the pile. The topographic map in Figure 26 shows the final geometry of the dunes on the bed around the pile at the end of Run 26.

Run 27 was performed to confirm the reliability of the scour depth relation, Equation 23, in near prototype situations. An 8.6-in.-diameter steel pile was placed vertically in the sand bed of the test

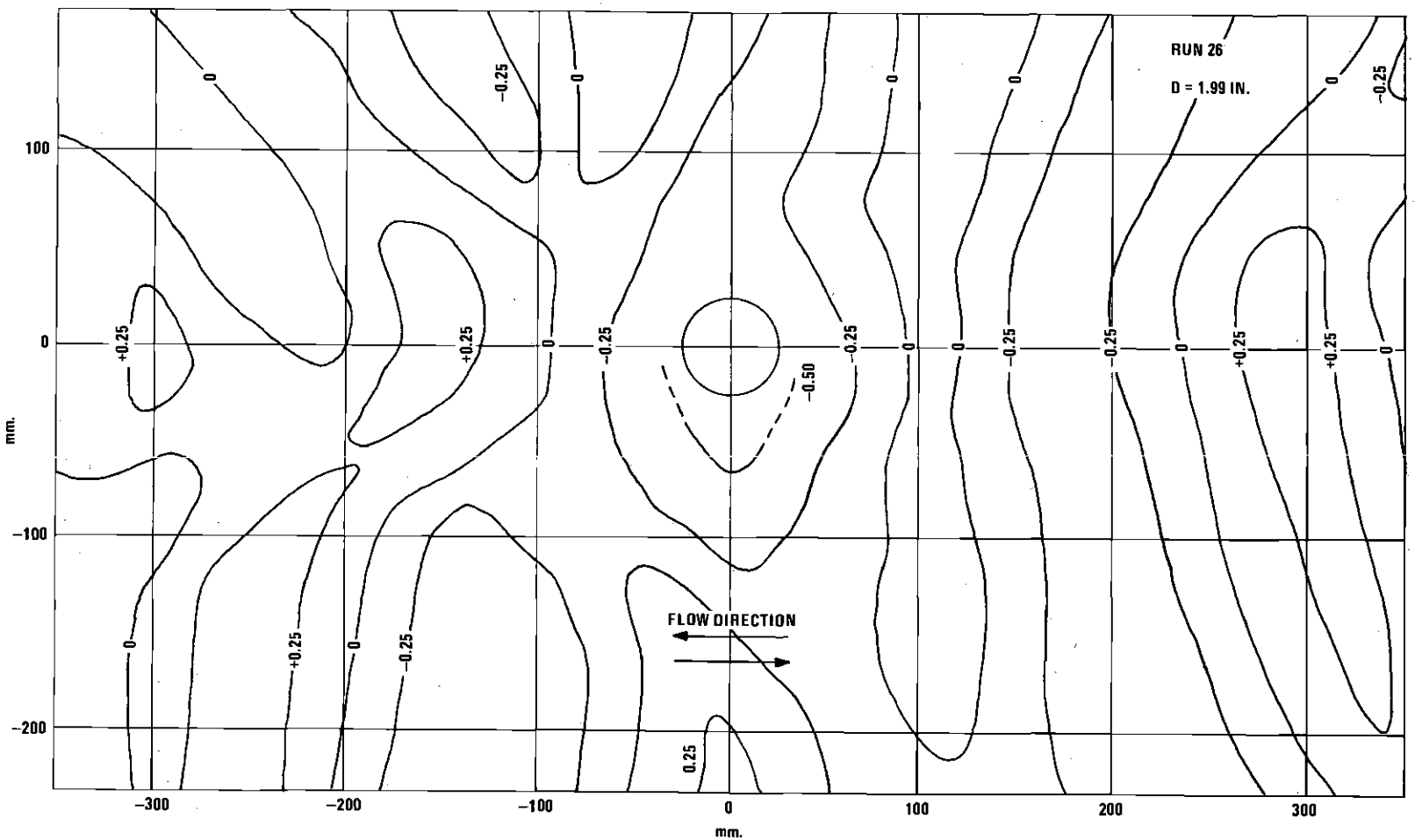

Figure 26. Topographic Map

section of the water tunnel. The ratio of a/D_g was maintained at 740. During Run 27 the scour depth was also observed to decrease from an initially higher value similar to Run 26 described above. With the formation of the dunes on the bed the scour hole was filled rapidly and joined the dune system. The run was terminated after 688 cycles of oscillations. The maximum scour depth at the end of the run was measured at the sides of the pile as S/D equal to 0.12. The final depth of scour was in the same order of magnitude as the amplitude of dunes on the bed. The photograph in Figure 27 shows the duned bed around the 8.6-inches pile at the end of Run 27.

Scour phenomena observed during Runs 26 and 27 have confirmed the reliability of the results given by Equation 23 in the region of dunes.

The conclusion that the localized scour around the vertical pile is influenced by the dunes, is in contradiction with the original expectation that the dunes would exert a negligible influence if the cylinder diameter was greater than the dune wave length. For cylinders used in this study, however, the analysis of model tests that were performed without dunes on the bed, indicated an interference from the dunes due to high rates of bed load transport.

The conclusion that the localized scour around the vertical cylinder in oscillatory flow is influenced by the dunes, is also contrary to the conclusion of Carstens' study (17) on localized scour around a horizontal cylinder. During the model tests with the horizontal cylinder under the oscillatory flow, Carstens reported that the cylinder joined the dune system with the axis of cylinder coinciding with a

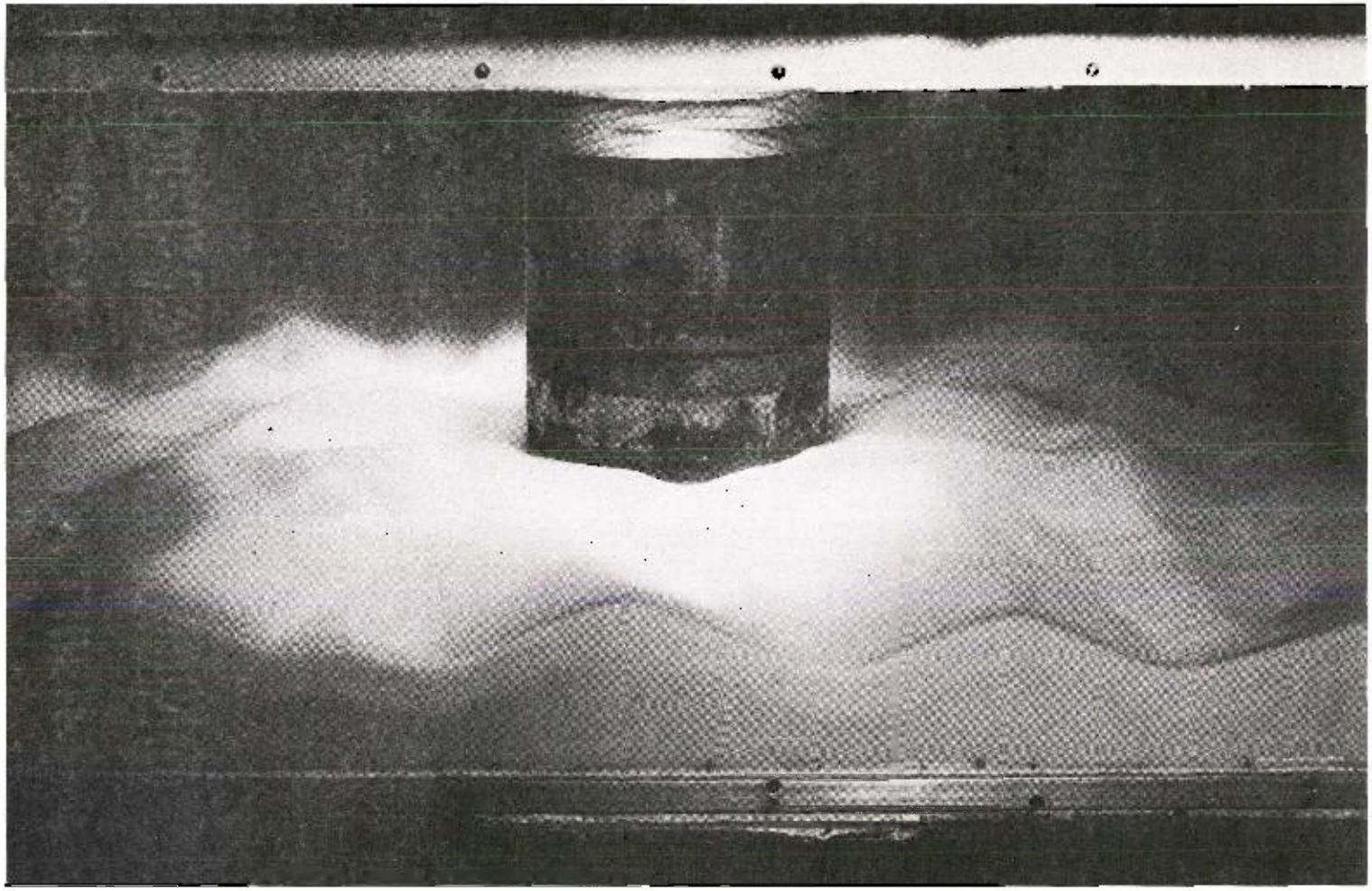

Figure 27. Model Incorporated into Dune System (Run 27)

ripple crest. When the cylinder acted as a pseudo dune, scour holes did not develop at the ends of the cylinder and settlement appeared to cease. However Carstens (17) has predicted a terminal settlement depth by assuming that prototype horizontal cylinder and scour hole will be large enough that the dunes will be negligible in respect to the flow pattern around the cylinder in the bottom of scour hole. The result of the present study, however, shows that the scour hole will be a part of the dune system not because of the altered flow pattern but due to high rate of sediment transport into the hole. The localized scour around a horizontal cylinder was influenced by the dunes for the cylinders used in Carstens' experiments. Thus, experiments around a horizontal cylinder also confirm the influence of dunes on the scour depth.

It is also appropriate to point out the differences between the settlement of a horizontal cylinder laying on the surface of the sand bed and the scour around a vertical cylinder which is partly buried within the sand bed. The settlement of the horizontal cylinder is an irreversible process. Once the horizontal cylinder has settled, the settlement depth cannot decrease but either continues to increase or stops as in the case of terminal depth. In localized scour around a vertical cylinder, on the contrary, the scour depth can decrease due to the sediment transport into the scour hole from a moving dune crest. The oscillating scour depth resulting from a dune passage in unidirectional flow has been reported by many researchers (9, 13, 14, 30).

In the absence of sediment transport into the scour hole, no terminal scour depth is predicted. This conclusion is in agreement with Carstens (16), Laursen and Toch (9). The scour depth is found to

increase at a progressively slower rate with time. Inasmuch as the absolute measured scour is small, the terminal condition is very difficult to identify. Terminal condition during a low-amplitude run would be reached when the sediment pickup from the scour area stopped. It is shown in Figures 9 and 10 that the rate of sediment pickup during the low-amplitude Runs 5 and 23, did not become zero. Insofar as these experiments could determine, no terminal condition does exist without sediment transport into the hole.

Illustrative Examples

The use of the similarity criterion is best demonstrated by means of numerical examples. To illustrate the application of the scour-depth-versus-time curves to realistic situations six sample problems are presented. These examples should also serve to demonstrate the effects of the associated parameters on the development of the localized scour.

Problem 1

Consider a cylindrical pile driven into a sand bed under the sea under following conditions:

diameter of pile = D = 1.0 ft;

mean diameter of sand = D_g = 0.3 mm or $9.84(10^{-4})$ ft;

s = 2.60 (quartz sand in sea water);

ϕ = 30 degrees (well-rounded sand);

wave period = T = 10 sec;

wave amplitude (trough to crest) = H = 10 ft;

still-water depth = h = 50 ft; and

water temperature = 60 degrees Fahrenheit.

Assuming the sand bed is initially flat, what is the expected terminal scour depth? What is the time to reach 95% of the terminal scour depth?

Assuming first-order Stokian water waves, the maximum horizontal bottom velocity is given (33) as follows:

$$U_m = \frac{g\ H\ T}{2L\ \cosh\ (\frac{2\pi h}{L})} \tag{24}$$

in which L is the wave length. The wave length, L, may be expressed as a function of water depth, h, and wave period, T, as follows:

$$L = \frac{g\ T^2}{2\ \pi}\ \tanh\ (\frac{2\pi h}{L}) \tag{25}$$

If the water depth and wave period are known, the wave length, L, can be determined from Equation 25 by a trial and error procedure. The amplitude of horizontal displacement of water particles at the bottom is given as follows:

$$a = \frac{H}{2\ \sinh\ (\frac{2\pi h}{L})} \tag{26}$$

Note that the maximum horizontal bottom velocity, U_m, can be related to the amplitude of horizontal displacement of water particles, a, at the bottom as follows:

$$U_m = \frac{2\ \pi\ a}{T} \tag{27}$$

Using Equations 24 and 25, the maximum bottom velocity, U_m, for problem 1 is calculated to be 3.18 fps. The amplitude of horizontal displacement of water at the bottom is computed as 5.06 ft from Equation 26. The dimensionless parameters are, then, computed as follows:

$$D/D_g = 1.0/9.84(10^{-4}) = 1015$$

$$a/D_g = 5.06/9.84(10^{-4}) = 5150$$

$$N_s = \frac{U_m}{\sqrt{(s-1)g\ D_g}} = \frac{3.18}{\sqrt{(2.6-1)\ (32.17)\ (9.84)\ (10^{-4})}} = 14$$

From Figure 25, the terminal scour depth is

$$\frac{S_T}{D} = 2.4$$

or

$$S_T = 2.4 \text{ ft.}$$

The time parameter corresponding to 95% of the terminal scour depth is obtained from Figure 18, at S/D = 2.28 as follows:

$$\frac{t\ D_g\ \sqrt{(s-1)g\ D_g}}{D^2} = 0.6$$

solving for t

$$t = \frac{0.6\ (1.0)^2}{9.84\ (10^{-4})\ \sqrt{(2.6-1)\ (32.17)\ (9.84)\ (10^{-4})}} = 2710 \text{ sec}$$

or

$t = 45$ minutes

Problem 2

The conditions of Problem 2 are the same as those of Problem 1 except that the still-water depth is:

(a) 100 ft;

(b) 20 ft.

For the case (a) the amplitude of horizontal motion at the bottom is calculated to be 2.66 ft. The maximum bottom velocity, U_m, is 1.67 fps. The dimensionless parameters become as follows:

$a/D_g = 2700$;

$D/D_g = 1015$;

$N_s = 7.4$.

The terminal scour depth is obtained from Figure 25 as

$$S_T = 2.4 \text{ ft.}$$

From Figure 18, at $S/D = 2.28$ the time parameter is as follows

$$\frac{t\, D_g \sqrt{(s-1)g\, D_g}}{D^2} = 14$$

or

$t = 63300$ sec $= 17.6$ hours

In case of (b), it was similarly found that $U_m = 5.83$ fps and

$S_T = 2.4$ ft

$t = 1$ minute

Problem 2 indicates that any decrease in the still-water depth will increase the bottom velocity, hence, accelerate the localized scour greatly. The bottom velocity, U_m, in Problem 2 has changed only 3.5 times while the time to reach 95% of the terminal scour depth has changed more than 60000 times.

Problem 3

The conditions of Problem 3 are the same as those of Problem 1 except that the wave amplitude (trough to crest) is

(a) 20 ft

(b) 5 ft

With the change in wave amplitude, H, the horizontal displacement of water at the bottom and the maximum bottom velocity are changed in direct proportion. Referring to Problem 1, for a wave amplitude 20 ft

$a/D_g = (\frac{20}{10})\ 5150 = 10300$

$N_s = (\frac{20}{10})\ 14.1 = 28.2$

$D/D_g = 1015$

From Figure 25 the terminal scour depth is

$S_T = 2.4$ ft.

From Figure 18, as $S/D = 2.28$, the time parameter is as follows

$$\frac{t\ D_g \sqrt{(s-1)g\ D_g}}{D^2} = 0.0082$$

or

$t = 37$ sec

For the case (b) it is similarly determined that the maximum terminal

scour depth is 2.4 ft. Time required to reach 95% of the scour depth is 22 hours.

Problem 3 demonstrates that any change in the wave amplitude will change the maximum bottom velocity in direct proportion, hence, accelerate or retard the scour process greatly as in Problem 2.

Problem 4

The conditions of Problem 4 are the same as those of Problem 1 except the wave period, T, is

(a) 15 sec

(b) 5 sec

For the case (a), the amplitude of horizontal displacement at the bottom is calculated 8.66 ft. The maximum bottom velocity is 3.63 fps. The dimensionless parameters are as follows

$a/D_g = 8800$

$D/D_g = 1015$

$N_s = 21.6$

From Figure 25 the terminal scour depth is

$S_T = 2.4$ ft

From Figure 18, at S/D = 2.28, the time parameter is as follows

$$\frac{t\, D_g \sqrt{(s-1)g\, D_g}}{D^2} = 0.18$$

solving for t

t = 814 sec = 13.5 minutes

For the case (b), the amplitude of horizontal displacement at the

bottom is calculated 0.81 ft. The maximum bottom velocity is 1.03 fps. The dimensionless parameters are as follows

$a/D_g = 884$

$N_s = 4.6$

Since the ratio of a/D_g is less than 1700, the Figure 25 is not applicable. Figure 19, shows that in this case scour hole will act as a part of the dune system. No localized scour around the pile is predicted.

Problem 4 dramatically demonstrates the role of bed configuration upon the localized scour around the pile. The changes in the maximum bottom velocity, U_m, and in the amplitude of horizontal displacement of water particles, a, at the bottom can be accompanied with a change in the bed configuration. In existence of dunes on the bed, the scour hole is expected to join the dune system.

Problem 5

The conditions of Problem 5 are the same as those of Problem 1 except that the diameter of pile D, is

(a) 5.0 ft

(b) 0.5 ft

The independent dimensionless parameters of Problem 5 are the same as in Problem 1 except for the ratio of D/D_g. For the case (a), the ratio D/D_g is about 5000.

From Figure 25, the terminal depth of scour is

$$\frac{S_T}{D} = 2.4$$

or

$$S_T = 12.0 \text{ ft.}$$

The time parameter to reach 95% of the terminal scour depth is obtained from Figure 21 as

$$\frac{t\, D_g \sqrt{(s-1)g\, D_g}}{D^2} = 0.35$$

solving for t

t = 36100 sec = 10 hours

For the case (b), the ratio D/D_g is about 500. It is similarly determined that

S_T = 1.2 ft.

t = 500 sec = 8.3 minutes. (Figure 20)

Problem 5 demonstrates that the change in pile diameter creates a change in terminal scour depth in direct proportion in presence of flat mobile bed. The larger the pile diameter, the longer it takes to reach the 95% of the terminal scour depth. On the other hand, for a larger pile it would take less time to reach to a given scour depth than a smaller pile. For the 5-ft pile in case (a), for example, it would take only 31 seconds to scour 1.2 ft while 0.5-ft-diameter pile in case (b) would scour to the same depth in 8.3 minutes.

Problem 6

The conditions of Problem 6 are the same as those of Problem 1 except the mean diameter of the bed material, D_g, is 0.6 mm.

The maximum bottom velocity, U_m, and the amplitude of horizontal

displacement at the bottom for Problem 6 are the same as of Problem 1. Since a/D_g is 2550, Figure 25 is applicable. The terminal scour depth is

$$\frac{S_T}{D} = 2.4 \quad \text{or} \quad S_T = 2.4 \text{ ft}$$

Referring to Problem 1, the Reynold's number, R, is calculated as follows

$$R = \frac{U_m D_g}{\nu} = \frac{(3.18)\ (1.97)\ (10^{-4})}{1.21\ (10^{-5})} = 518$$

For values of R greater than 500, the value of C_D' is constant 1.12. Since D/D_g is about 500, using Figure 24, the time parameter to reach 95% of the terminal scour depth is

$$\frac{t\ D_g \sqrt{(s-1)g\ D_g}}{D^2} = 0.66$$

or

$$t = 1050 \quad \text{sec} = 17.5 \text{ minutes}$$

Comparing the results of Problem 6 with Problem 1, it is found that the larger the sediment size, the less it takes to reach to a given depth of scour.

In Problems 1-5, inclusive, Figures 18, 19, 20, and 21 were used to determine the time for scour development. The value of C_D' of each curve on these figures represents the value of C_D' for 0.3 mm sand for

the stated values of N_s at a temperature of 60° F. Thus, strictly speaking, Figures 18, 19, 20, and 21 are special curves for the 0.3 mm sand. For sediment sizes other than 0.3 mm, Figures 22, 23, and 24 are given for Reynolds numbers greater than 500 irrespective of sediment size. In a strict sense Figures 22, 23, and 24 are applicable to Problem 2b, 3a, and 6. However, for the range of R less than 500, Figures 22 thru 24 would still yield answers in the same order of magnitude. Inasmuch as, changes in flow variables will result in time changes of several order of magnitudes as demonstrated in Problem 2, the small errors involved in using a constant C_D' of 1.12 will be negligible in a practical sense. Therefore, it is recommended that Figures 22, 23 and 24 be used to estimate the time of scour for a/D_g greater than 1700. It is further recommended that localized scour be ignored when a/D_g is less than 1700.

CHAPTER VII

CONCLUSIONS

A method has been proposed for computing the terminal depth of local scour and for determining the time variation of the scour depth around a single vertical circular pile in a cohesionless bed under the action of first-order Stokian water waves. The conclusions of this study are limited to a homogeneous level bed consisting of cohesionless sand of reasonably uniform size. From this investigation the following conclusions are considered pertinent:

1. With sediment transport into the scour hole from surrounding mobile flat bed, the terminal depth of scour is independent of magnitudes of approach velocity and sediment size. The terminal scour depth is 2.4 times the diameter of the cylinder when the ratio of the diameter of pile to the diameter of sand is reasonably large (Figure 25).

2. Localized scour around a vertical cylinder is influenced by the dunes. The terminal scour depth is found to be decreasing with the decreasing values of a/D_g in the region of three dimensional dunes. When the dune system is two dimensional, the scour hole will join the dune system with scour hole acting as a part of the dune system.

3. No terminal scour depth is predicted in absence of the sediment transport into the scour hole. For the case of an immobile flat bed around the pile, the similarity relationship should be used within the range of the experimental data, that is, S/D less than unity.

4. The localized scour around a pile is not expected to be critical in the design of pilings of relatively small diameter. The generalized scour, that is, the lowering of the bed level by bed-load transport due to increased velocities during the storms would be of a greater magnitude than the localized scour due to the pile alone. In the design of hydraulic structures of significant width such as cofferdams, however, knowledge concerning the magnitude of maximum depth of the localized scour and how this depth is related to different flow conditions is essential.

REFERENCES CITED

1. Karaki, S. S., and R. M. Haynie, "Mechanics of Local Scour, Part II, Bibliography," Report No. CER63SSK46, Contract No. 11-8022, U.S. Department of Commerce, Bureau of Public Roads, Division of Hydraulic Research, also Civil Engineering Section, Colorado State University, Fort Collins, Colorado, November 1967, 51 pp.

2. Schneible, D. E., "Some Field Examples of Scour at Bridge Piers and Abutments," Better Roads, Vol. 24, No. 8, August 1954.

3. Borhek, R., "Scouring of Foundations as a Cause of Bridge Failures," Roads and Bridges, August 1943, p. 33

4. Hubbard, P. G., "Field Measurement of Bridge-Pier Scour," Proceedings, Highway Research Board, Washington, D.C., 1955, pp. 184-188.

5. Anderson, A. G., "The Hydraulic Design of Bridges for River Crossings - A Case History," 45th Annual Meeting of the Highway Research Board of the National Academy of Sciences - National Research Council, Washington, D.C., January 17-21, 1966. Abstracted in Highway Research Abstracts, Vol. 35, No. 12, December 1965, p. 37.

6. Peck, R. B., W. E. Hanson, and T. H. Thornburn, "Piles in Sand," Foundation Engineering, John Wiley and Sons, Inc., New York, 1953, pp. 238-242.

7. Engels, H., "Experiments Pertaining to the Protection of Bridge Piers Against Undermining," Hydraulic Laboratory Practice, Chapter V, Edited by John R. Freeman, American Society of Mechanical Engineers, New York, 1929.

8. Laursen, E. M., "Scour at Bridge Crossings," Transactions, American Society of Civil Engineers, Vol. 127, Part 1, 1962, pp. 166-179.

9. Laursen, E. M., and A. Toch, "Scour Around Bridge Piers and Abutments," Iowa Highway Research Board, Bulletin No. 4, prepared by Iowa Institute of Hydraulics Research in cooperation with the Iowa State Highway Commission and Bureau of Public Roads, May 1956, 60 pp.

10. Chitale, S. V., "Discussion of Scour at Bridge Crossings," Transactions, American Society of Civil Engineers, Vol. 127, Part 1, 1962, pp. 191-196.

11. Marin, J. N., "An Investigation of Local Scour Around Bridge Piers," M. Tech. Thesis, University of South Wales, Water Resources Laboratory, Manley Vale, N.S.W., Australia, 1962.

12. Tarapore, Z. S., "A Theoretical and Experimental Determination of the Erosion Pattern Around Obstructions Placed in an Alluvial Channel with Particular Reference to Vertical Cylinders and Piers," PhD. Dissertation, University of Minnesota, 1962.

13. Chabert, J., and P. Engeldinger, "Etude des Affouillements Autour des Piles de Ponts," Report, National Hydraulics Laboratory, Chatou, France, Series A, October 1956.

14. Shen, H. W., V. R. Schneider, and S. S. Karaki, "Mechanics of Local Scour," Report No. CER66HWS22, Contract No. CPR 11-8022, Engineering Research Center, Colorado State University, Fort Collins, Colorado, prepared for U.S. Department of Commerce, Bureau of Public Roads, Office of Research and Development, June 1966, 56 pp.

15. Laursen, E. M., "Observations on the Nature of Scour," Proceedings of 5th Hydraulics Conference, State University of Iowa, Iowa City, Iowa, Bulletin 34, June 9-11, 1952, pp. 179-197.

16. Carstens, M. R., "Similarity Laws for Localized Scour," Journal of Hydraulics Division, American Society of Civil Engineers, Vol. 92, No. HY3, Proc. Paper 4818, May 1966, pp. 13-36.

17. Carstens, M. R., "Part - II, - Localized Scour Around a Horizontal Cylinder," Final Report, Contract No. N600(24)-59885, U.S. Navy, Mine Defense Laboratory, Panama City, Florida, prepared by Engineering Experiment Station, Georgia Institute of Technology, Atlanta, Georgia, June 1967, 96 pp.

18. Tsuchiya, Y. and Y. Iwagaki, "On the Mechanism of the Local Scour from Flows Downstream of an Outlet," Proceedings, 12th Congress on the International Association for Hydraulics Research, Sept. 11-14, 1967, Vol. 3, pp. 55-64.

19. Tarapore, Z. S., "Scour Below a Submerged Sluice Gate," Thesis presented to the University of Minnesota, at Minneapolis, Minn. in 1956, in partial fulfillment of the requirements for the degree of Master of Science.

20. LeFeuvre, A. R., "Sediment Transport Functions with Special Emphasis on Localized Scour," Thesis presented to the Georgia Institute of Technology, Atlanta, Georgia, in 1965, in partial fulfillment of the requirements for the degree of Doctor of Philosophy, 93 pp.

21. Manohar, M., "Mechanics of Bottom Sediment Movement Due to Wave Action," Technical Memorandum No. 75, Beach Erosion Board, Corps of Engineers, Department of the Army, June 1955, 121 pp.

22. Stein, Richard A., "Laboratory Studies of Total Load and Apparent Bed Loads," Journal of Geophysical Research, Vol. 70, No. 8, April 15, 1965, pp. 1831-1842.

23. Rathbun, R. E., and H. P. Guy, "Measurement of Hydraulic and Sediment Transport Variables in a Small Recirculating Flume," Water Resources Research, Vol. 3, No. 1, 1967, pp. 107-122.

24. Guy, H. P., D. B. Simons, E. V. Richardson, "Summary of All Alluvial Channel Data From Flume Experiments, 1956-61," Professional Paper 462-I, U.S. Geological Survey, United States Government Printing Office, Washington, 1966, p. 96.

25. "Nomenclature for Bed Forms in Alluvial Channels," Proc. ASCE, Journal of the Hydraulics Division, Vol. 92, No. HY3, May 1962, pp. 51-64.

26. Vanoni, V. A., Norman H. Brooks, and John F. Kennedy, Lecture Notes on Sediment Transportation and Channel Stability, Report No. KH-R-1, California Institute of Technology, Pasadena, California, January 1961, Appendix 3A, pp. 3-20.

27. "Sediment Transportation Mechanics: Introduction and Properties of Sediment, Proc. ASCE, Journal of the Hydraulics Division, Vol. 88, No. HY4, July 1962, p. 98.

28. Kennedy, J. F., and Robert C. Y. Koh, "The Relation Between the Frequency Distributions of Sieve Diameters and Fall Velocities of Sediment Particles," Journal of Geophysical Research, Vol. 66, No. 12, December 1961, pp. 4233-4246.

29. Carstens, M. R., F. M. Neilson, and H. D. Altinbilek, "An Analytical and Experimental Study of Bed Forms Under Water Waves," Final Report, Contract No. DA-49-005-CIVENG-65-1, Dept. of Army, Coastal Eng. Research Center, September 1967, 120 pp.

30. Gradowczyk, M. H., O. J. Maggiola, and H. C. Folguera, "Localized Scour in Erodible-Bed Channels," Journal of Hydraulic Research, International Association for Hydraulic Research, Vol. 6, 1968, No. 4, pp. 289-326.

31. Snyder, W. M., "Some Possibilities for Multivariate Analysis in Hydrologic Studies," Journal of Geophysical Research, Vol. 67, No. 2, February 1962, pp. 721-729.

32. Carstens, M. R., Part I, "The Effect of Dunes upon Localized Scour," Final Report, Project A770, Engineering Experiment Station of the Georgia Institute of Technology, Atlanta, Georgia, December 31, 1965, 111 pp.

33. Ippen, A. T., "Estuary and Coastline Hydrodynamics," McGraw-Hill Book Company, 1966, 744 pp.

APPENDIX

A SEDIMENT-PICKUP FUNCTION

By A. R. LeFeuvre,[1] M. ASCE, H. D. Altinbilek,[2] and M. R. Carstens,[3] M. ASCE

Introduction

Understanding of sediment transport and localized scour depends upon an understanding of pickup and deposition of particles from the surface of the bed. Even the simple case of equilibrium transport resulting from uniform flow over a flat bed involves both pickup and deposition--the equilibrium condition results from the equality of the rate of pickup and the rate of deposition. Localized scour is unsteady because the rate of pickup exceeds the rate of deposition whereas localized fill is unsteady because the rate of deposition exceeds the rate of pickup.

Even though steady flow over a duned bed may be analyzed as uniform in a gross sense, the existence of dunes depends upon alternating regions of localized scour and fill. In the trough of a dune, the rates of pick-up and deposition are zero. The upstream face of a dune is a region of

---

[1]Chief, Planning and Reports Unit, Southeast Comprehensive Planning and Programs Division, Federal Water Pollution Control Administration, U.S. Department of Interior, Atlanta, Georgia.

[2]Graduate Student, School of Civil Engineering, Georgia Institute of Technology, Atlanta, Georgia.

[3]Professor of Civil Engineering, Georgia Institute of Technology, Atlanta, Georgia.

localized scour with the maximum scour occurring where dune slope is steepest. Near the crest, the dune slope tends to be horizontal indicating an equality of the rates of pickup and deposition. To the lee of the crest is a region of localized fill where the pickup rate is zero. The region of localized scour on the upstream face is a region where more particles are removed from the surface than are replaced in a unit time. Of course, because of this localized scour, the upstream face of the dune recedes, that is, moves downstream. Conversely localized fill occurs on the lee of the crest causing that surface to advance, that is, moves downstream. The shape and size of a dune is self adjusting so that the dune will move downstream at a uniform rate with an unchanging form. The configuration of the bed is the predominant influence on the boundary-drag force opposing the motion of the stream which, in turn, is reflected in the stage-discharge characteristics of the stream. In the writers' opinion, the key process in this closed system is the localized scour and fill which occurs at the interface of the fluid and the bed of particles.

With the exception of the incipient-motion condition, surprisingly little attention has been given to study of the process of particle removal from the surface of the bed by the overlying flowing fluid. The majority of incipient-motion studies have been made in laboratory flumes with steady uniform flow and with a carefully (but artificially) flattened bed. With these simplified boundary conditions (particularly the flat bed), the mean value of the boundary-shear stress, τ_o, is a convenient variable to use in analysis of the incipient-motion condition. As a result, incipient-motion results are almost universally presented

in terms of the value of the Shields' parameter, $\tau_o/(s-1)\gamma D_g$, in which s is the specific-weight ratio of sediment to fluid, γ is specific weight of the fluid, and D_g is the geometric mean diameter of the bed particles. Undoubtedly because of this precedent, the tractive-force method is most used in stable-channel design.

In regions of nonuniform flow or in unsteady flow situations, the choice of boundary-shear stress as the key variable for definition of incipient motion or for evaluating a local sediment-pickup rate is unsuitable. The principal drawback of boundary-shear stress as an independent variable is that values of boundary-shear stress must be determined indirectly either as a residual in the linear momentum equation(s) or by use of the Preston tube.

A better choice of variable for use in analyzing incipient motion and localized scour is velocity. First, the hydrodynamic surface forces, lift and drag, are conventionally expressed in terms of fluid velocity; second, velocity measurements and velocity profile measurements are standardized procedures for which a variety of instruments are available; and third, velocity distribution can be closely approximated by irrotational-flow analysis in regions of converging flow where boundary-layer development is negligible.

An incipient-motion criterion and a sediment-pickup function are analyzed in the following using a force analysis on a typical surface particle. Since movement of the surface particles results from the hydrodynamic surface forces, velocity is the key variable.

Force Analysis

Incipient Motion

Incipient motion of the protruding surface particles occurs when the hydrodynamic forces on the protruding particles are sufficient to roll these surface particles over the bed. This analysis is based upon the hydrodynamic surface forces of drag, F_D, and lift, F_L, and the submerged weight, W, on a typical protruding particle. Additional forces arising from inertial reaction of the particles and of the fluid around the particles are not included. In other words, the lift and drag force on a typical protruding particle are considered to be quasi-steady in the following analysis.

The simplest case of incipient motion is illustrated in Figure 1 in which submerged weight is the only force other than adjacent particle reactions. If the bed is inclined at the angle of repose, Φ, some of the protruding surface particles will be at the incipient-motion condition. As shown in Figure 1, the stability limit is:

$$\tan\Phi = F_T/F_N \qquad (1)$$

in which F_T and F_N are the summation of the external forces on the particle which are tangential and normal to the bed, respectively. The angle of repose, Φ, is a function of particle shape, angularity, and porosity. Typical values of Φ are given by Simons and Albertson (1)[4] showing the relationship between Φ, particle size, and angularity for an unspecified porosity.

---

[4]Numerals in parentheses refer to corresponding items in References.

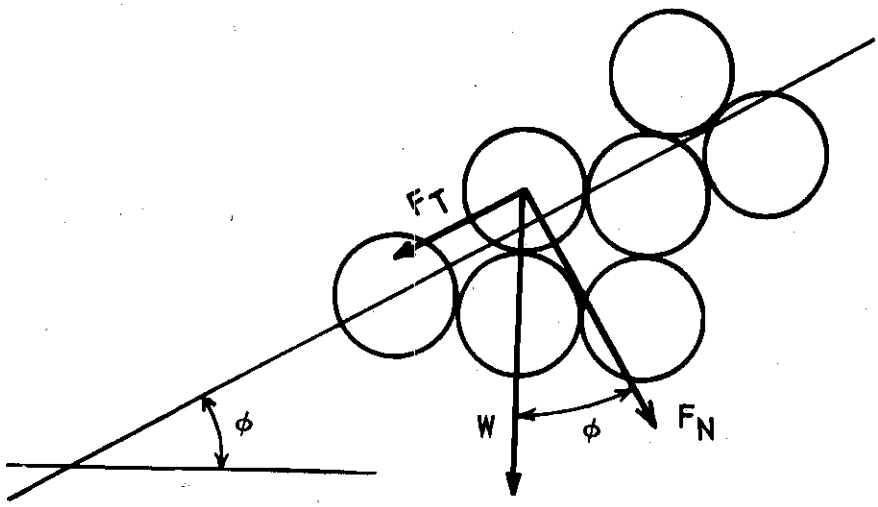

Figure 1. Gravity Forces on Bed Particles.

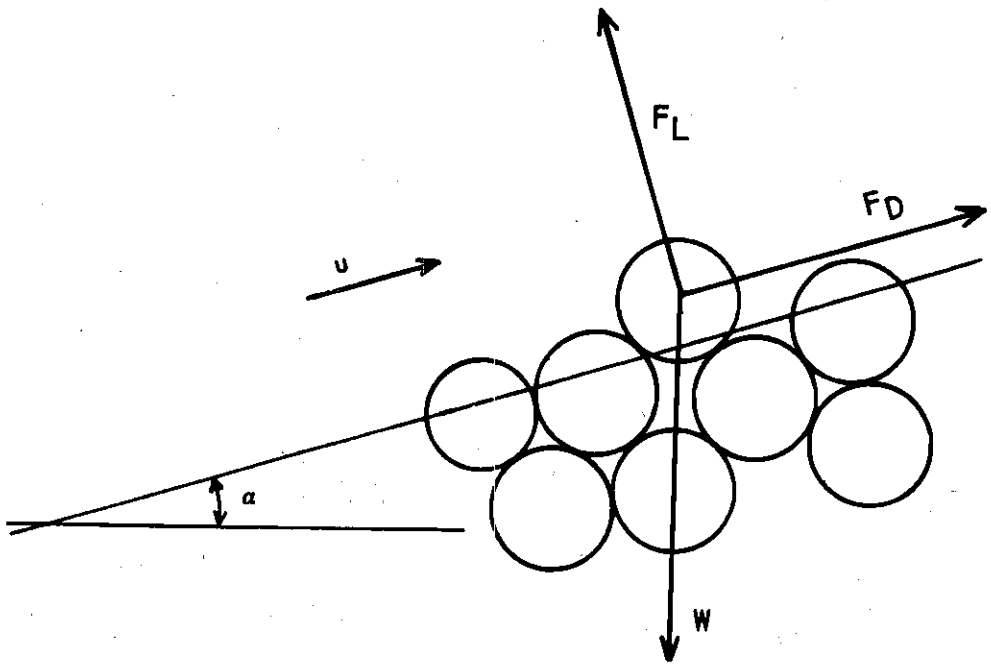

Figure 2. Forces on a Bed Particle.

A more complex force system is illustrated in Figure 2 in which F_D and F_L are hydrodynamic drag and lift forces, respectively, W is the submerged weight, and α is the inclination of the bed from horizontal. Substituting the forces shown in Figure 2 into Equation 1,

$$\tan\Phi = \frac{F_D - W \sin \alpha}{W \cos \alpha - F_L} \tag{2}$$

The drag and lift forces can be written in the conventional form

$$F_D = C_D k_1 D_g^2 \frac{\rho u^2}{2} \tag{3}$$

and

$$F_L = C_L k_2 D_g^2 \frac{\rho u^2}{2} \tag{4}$$

in which C_D and C_L are coefficients of drag and lift, respectively, k_1 and k_2 are particle-shape coefficients, D_g is mean size of particle, ρ is fluid density, and u is fluid velocity at the level of the protruding particle. The submerged weight, W, can be written as:

$$W = k_3 (\gamma_s - \gamma) D_g^3 \tag{5}$$

in which γ_s and γ are the specific weights of the bed particles and the fluid, respectively, and k_3 is another particle-shape coefficient. Substituting Equations 3, 4, and 5 into Equation 2, and rearranging,

$$\frac{u_c^2}{(s-1)g D_g} = \frac{2k_3 (\tan \Phi \cos \alpha + \sin \alpha)}{k_1 + k_2 (C_L/C_D) \tan \Phi} \left(\frac{1}{C_D} \right) \tag{6}$$

in which s is the specific-weight ratio, γ_s/γ, and u_c is the initial-motion value of the bottom velocity. Chepil (2) measured the lift and drag on a hemisphere placed on a plane boundary. He found that C_L was about 0.8 C_D. Since the protruding particles under consideration probably protrude further from the bed than the hemisphere and since the pressure condition under a protruding particle is unknown and variable depending upon the configuration of the flow passages under the particle, a value of unity for the ratio, C_L/C_D, is taken as a reasonable average value. In addition, the assumption is made that the particle-shape coefficients, k_1 and k_2, are equal. Also the assumption is made that the value of C_D for the protruding particle is proportional to C_D' for the freely falling particle at the same particle Reynold number, that is:

$$C_D = k_4 C_D' \tag{7}$$

Substituting the above simplifications into Equation 6

$$\frac{u_c^2}{(s-1)g\,D_g} = \left(\frac{\tan\Phi\cos\alpha + \sin\alpha}{1 + \tan\Phi}\right)\frac{K}{C_D'} \tag{8}$$

in which K is equal to $2k_3/k_1k_4$. Since the constant, K, involves only particle-shape coefficients and a proportionality factor relating C_D and C_D', the constant, K, is independent of the orientation of the gravity force with respect to the other forces.

As discussed elsewhere (3), the value of K was found to be 8.2 from an experiment in which the cessation of motion of sand grains was observed on dune crests under oscillatory flow. In the same studies, in-

cipient motion on a flat bed under oscillatory flow with a laminar boundary layer was also observed. Using Equation 8 with K = 8.2, using the theoretical solution for velocity distribution, and using the observed flat-bed incipient-motion conditions, the height y above the bed at which u_c should be evaluated was calculated to be at $y = 0.6\ D_g$.

The above criterion was validated (3) by using Equation 8 to compute the value of the Shields' parameter $\tau_o/(s-1)\gamma\ D_g$, for two-dimensional, uniform, steady, turbulent flow. This flow was chosen because (a) numerous experiments have been performed to evaluate the incipient-motion condition on a flat bed in rectangular flumes, and (b) widely-used and well-substantiated functions for velocity distribution exist for this type of flow. Equations were derived for Shields' parameter for flow over a hydraulically smooth boundary and over a hydraulically rough boundary. Good agreement between the derived functions and the experimental results of others was interpreted as being a confirmation of Equation 8 and of the constants, K = 8.2 and $y = 0.6\ D_g$ inasmuch as the constants were obtained from oscillatory-flow data yet the same constants were applicable to unidirectional, two-dimensional flow.

Rate of Sediment Pickup

Knowledge about the dynamics of particle pickup and transport is too rudimentary for the formulation of a complete theory. The best hope is to employ theoretical considerations in the formulation of a rational hypothesis of the general form of the pickup function and then to utilize experimental results for completion of the analysis.

In the same manner as for incipient motion, a reasonable hypothesis

is that sediment-pickup rate is proportional to the ratio of motivating forces to resisting forces, that is, to F_T/F_N. A refinement of this hypothesis is that the sediment pickup rate is proportional to the difference between the force ratio F_T/F_N and tan Φ. Referring to Equation 1, tan Φ is seen to be the value of the force ratio F_T/F_N at the incipient-motion condition.

Since the particles being transported will be rolling over their neighbors and will not be in sheltered recesses, the expectation is that the lift force, F_L, shown in Figure 2 will be diminished enough to be neglected. Substituting the remaining forces into the force ratio,

$$\frac{F_T}{F_N} = \frac{F_D - W \sin \alpha}{W \cos \alpha} \tag{9}$$

Substituting from Equations 3, 4, 5, and 7

$$\frac{F_T}{F_N} = \frac{C_D'}{K \cos \alpha} \frac{u^2}{(s-1)g D_g} - \tan \alpha \tag{10}$$

in which $K = 2 k_3/k_1 k_4$ as before. As a first approximation, the value of K can be assumed to be 8.2 and the value of y can be taken as $0.6 D_g$ for the evaluation of u.

The rate of sediment pickup from the bed can be conveniently expressed as a velocity, u_e, of the bed normal to itself. The pickup velocity, u_e, is a transport velocity which is the volume rate of bed removal per unit area of bed per unit time. Since u_e is the total volume rate, voids as well as particles are removed. The pickup velocity, u_e, is assumed to be independent of the deposit velocity, u_d, so that

the net transport velocity, u_t, is

$$u_t = u_d - u_e \tag{11}$$

If the deposit velocity, u_d, exceeds the pickup velocity, u_e, localized fill occurs. Conversely if the pickup velocity, u_e, exceeds the deposit velocity, u_d, localized scour occurs. In the following, only the pickup velocity, u_e, is considered.

Combining the above concepts, the expectation is that the functional form of the pickup velocity can be expressed as follows:

$$\frac{u_e}{u} = f\left\{ \frac{C_D'}{8.2 \cos \alpha} \frac{u^2}{(s-1)g D_g} - \tan \alpha - \tan \Phi \right\} \tag{12}$$

The dependent variable, u_e/u, in Equation 12 is a function of a single independent variable -- the expression within parentheses on the right side of Equation 12. Experiments are required to establish the functional relationship.

Experiments

In order to experimentally determine the pickup-velocity function, Equation 12, equipment was constructed whereby sediment was forced upward at a constant velocity through an opening in the wall of a rigid conduit into a clear water stream flowing across the opening. The velocity of the flowing water was adjusted so that a slight mounding (almost flat bed) of the sediment occurred at the opening. Pickup velocities were varied about one hundred fold with each of six uniform sediments ranging in density from nickel to Lucite.

Experimental Apparatus

A schematic drawing of the apparatus is shown in Figure 3. Water is supplied to the test section through a 6-in. diameter pipe from a constant head tank. The flow section of the 3-in. diameter, transparent, plastic pipe of the horizontal test section is joined to the 6-in. pipe by means of an annular contraction which is machined to an elliptical shape as shown in Figure 4. The water flows horizontally over the open end of the sediment supply tube through the 3-in. pipe and then down into the weir tank where the water discharge can be measured by means of a calibrated, 90-degree, triangular weir. The weir tank serves as a sediment trap in addition to being a stilling basin. Water discharge (velocity) through the test section is controlled by means of a pinch valve through which the sediment can pass without clogging.

The sediment is pushed upward through a 1-in. diameter copper water tube (Type "L") by a piston as shown in Figure 4. The speed of the vertical movement of the piston could be set at 32 different values by means of the mechanical drive system which originated at an 1800-rpm synchronous motor. The maximum piston velocity is 4.51 (10^{-3}) fps and the minimum is 3.57 (10^{-5}) fps.

Sediment

The pertinent properties of the six different sediments are listed in Table 1.

Experimental Procedure

At the beginning of a run, the gear train on the sediment-feed system was set in motion so as to achieve a predetermined piston velocity. The water discharge was then adjusted by means of the pinch valve (Figure

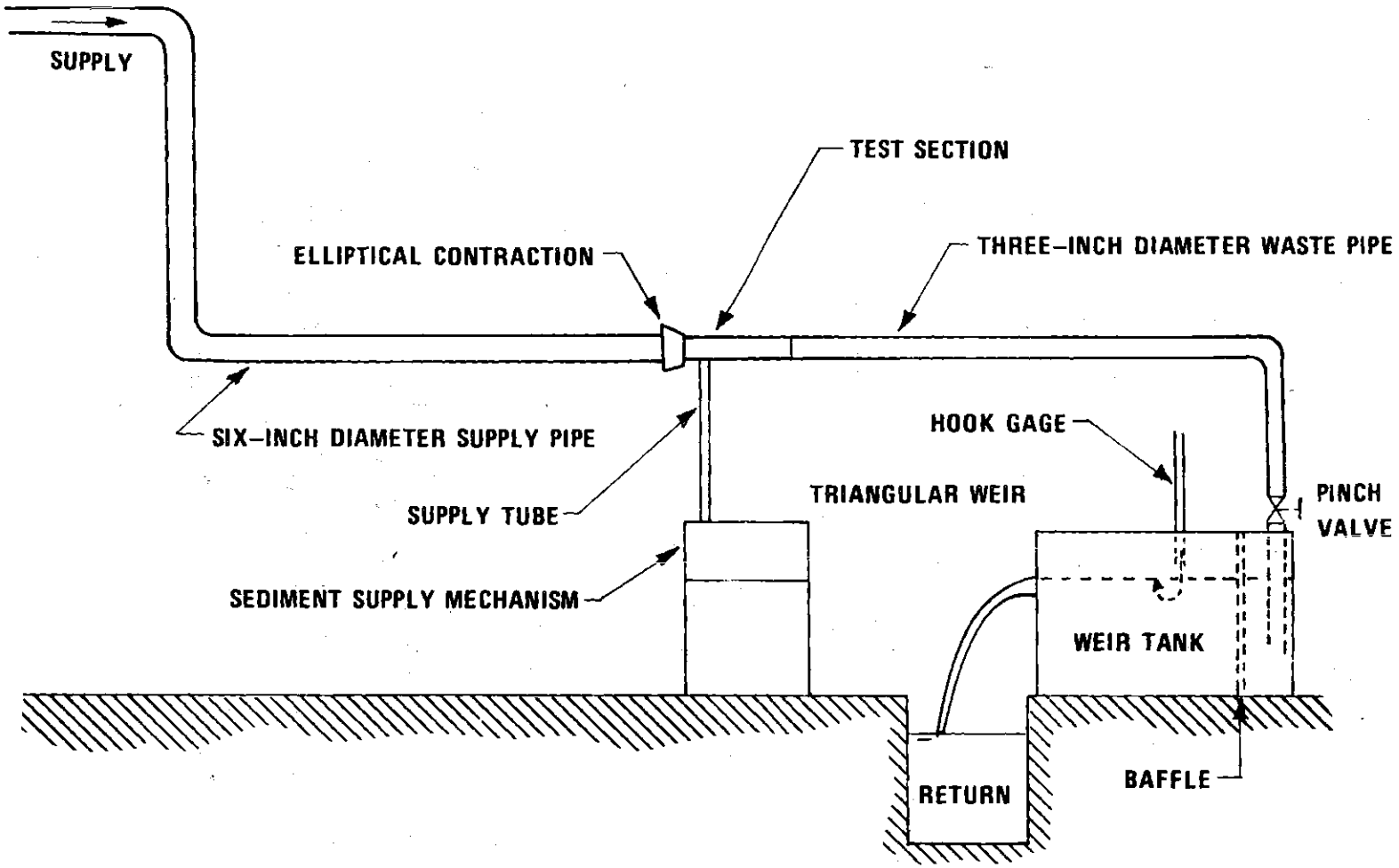

Figure 3. Schematic of Experimental Apparatus

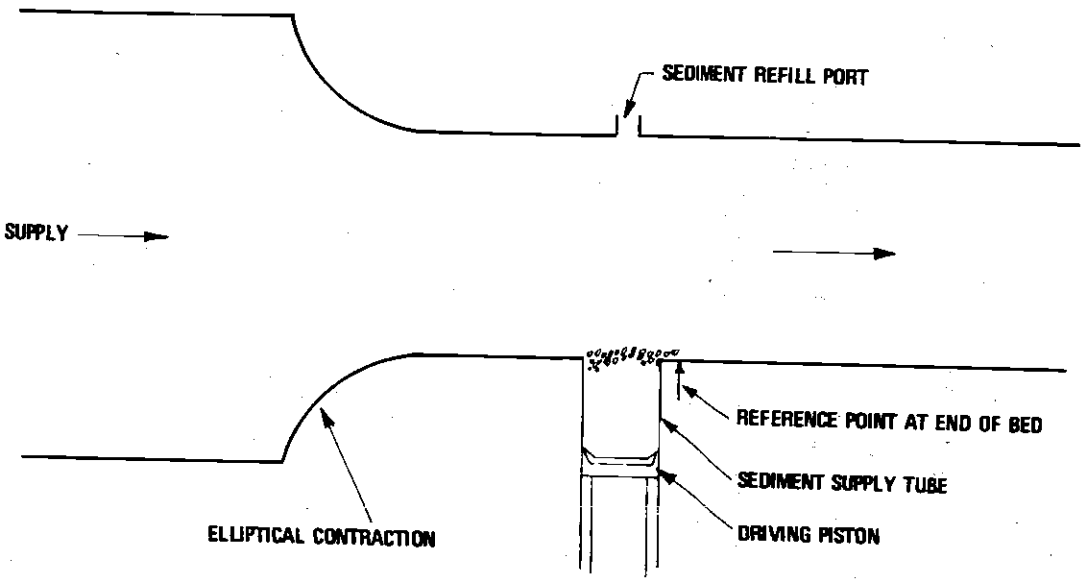

Figure 4. Definitive Sketch of Test Section

Table 1. Properties of Sediment

Sediment (1)	Material (2)	Specific gravity, s (3)	Diameter D_g in mm (4)	Standard deviation (5)	Angle of Repose, Φ in degrees (6)
1	nickel	8.75	0.570	1.10	24.7
2	sand	2.62	0.585	1.04	34.0
3	sand	2.63	0.185	1.24	34.0*
4	glass	2.47	0.297	1.08	24.7*
5	glass	2.46	0.106	1.05	24.7
6	Lucite	1.20	0.250	1.31	30.0

*Determined from the side slope of a scour hole which developed as a result of oscillatory flow past a vertical pile.

3) until the pickup velocity, u_e, was just equal to the piston velocity, that is, an equilibrium reference condition prevailed. The reference condition was a slightly mounded condition over the end of the sediment-supply tube. In every run the mound was just high enough to allow a single layer of particles to rest on the smooth tube wall in the wake of the mound. This layer of stationary particles extended to a visible reference mark about $\frac{1}{8}$-inch downstream from the sediment-supply tube outlet as shown in Figure 4. The mound height could not be directly measured. The only visible indication of a mound was the stationary particles in the wake. The length of this bed extension was very sensitive to water discharge thereby providing a satisfactory reference con-

dition for each of the 84 runs. After the water discharge was adjusted to achieve the reference condition, the head on the weir was measured by means of a hook gage and the water temperature was measured.

Special Experiments

Two special series of experiments were performed in order to determine the flow condition of incipient motion and to determine the velocity distribution of the flow approaching the sediment bed.

Incipient-Motion Tests-- Prior to the initial-motion tests, the bed at the sediment-supply-tube outlet was established at the reference condition, the water velocity was reduced until the bed was stationary, and the sediment feeder was stopped. Then the water velocity was increased in steps until an appreciable number of particles were swept from the bed. The flow condition corresponding to the beginning of movement of an appreciable number of particles was defined as the incipient-motion condition even though a few isolated particles had been moved at slightly lesser velocity. Values of the mean velocity, U, are listed in Table 2.

Velocity-Distribution Tests-- In order to determine the velocity distribution in the test section, the sediment-supply tube was removed and replaced with a movable stagnation tube as shown in Figure 5. The location of the 0.0275-in.-diameter (outside diameter) stagnation tube was measured by means of a cathetometer which was sighted on the reference mark on the stem of the stagnation-tube support. A wall piezometer was located in the top of the pipe directly over the tip of the stagnation tube. A constant-displacement differential manometer with water as the manometric fluid was used to determine the pressure difference be-

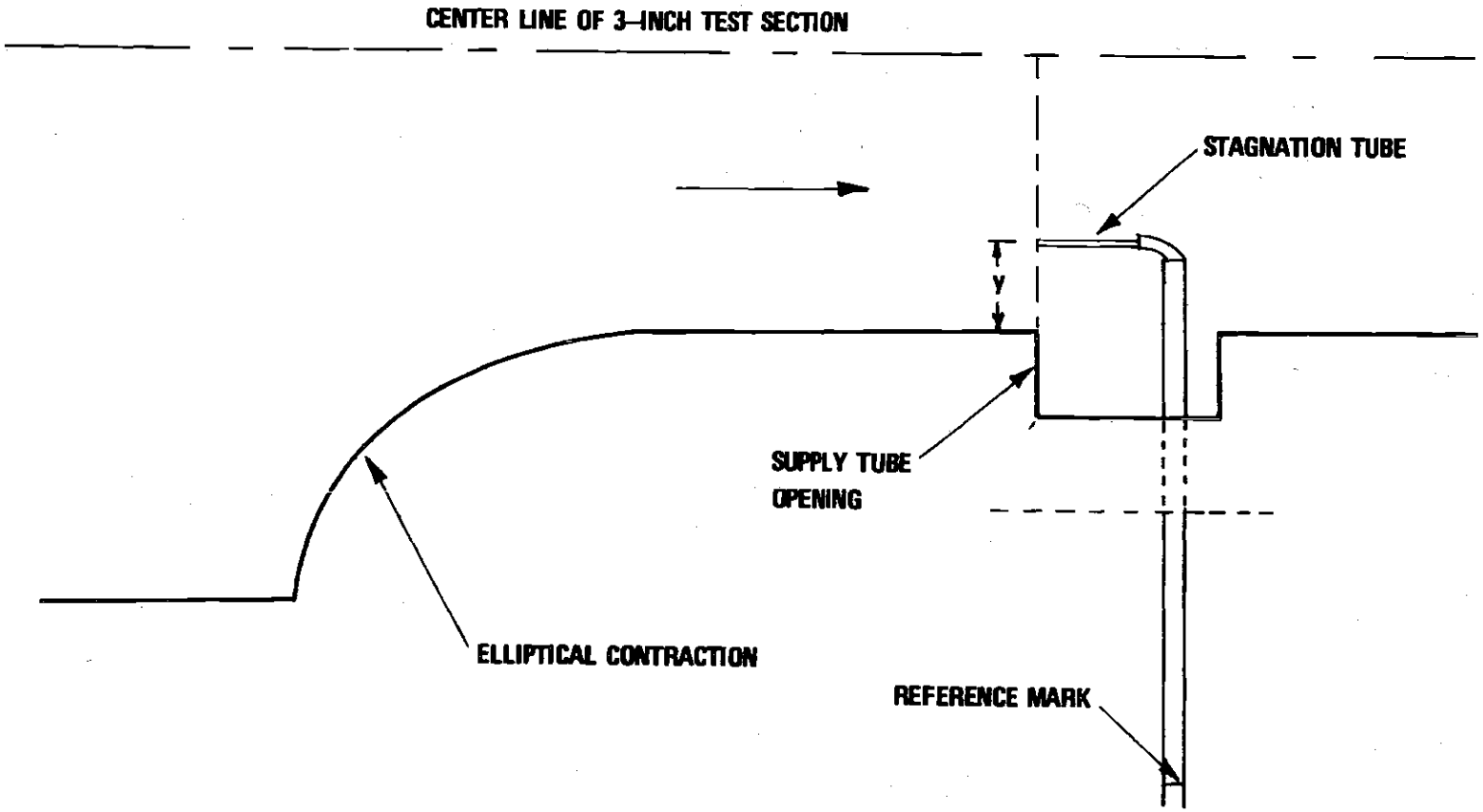

Figure 5. Velocity-Measuring Apparatus

Table 2. Flow Condition at Incipient Motion

Sediment (See Table 1)	Water Temperature in °F	Mean Velocity, U, in fps
1	-	1.30
2	71	0.63
3	73	0.70
4	73	0.60
5	75	0.63
6	-	0.29

tween the stagnation tube and the wall piezometer to the nearest 0.001 in.

For convenience of instrumentation, air rather than water was forced through the test section during the two runs in which velocity-distribution data were obtained. Analogous to the treatment of velocity-distribution data along a flat plate, the velocity-distribution data are shown in Figure 6 in dimensionless form of u/U as a function of $y\sqrt{U/\nu x}$ in which U is the mean velocity, ν is kinematic viscosity, and x is the distance from the virtual origin of the laminar boundary layer. The velocity-distribution parameters calculated from experimental data superposed as shown in Figure 6 with a value of x of 0.41 ft. Inasmuch as the Reynolds numbers, Ux/ν of the sediment-transport runs with water are in the same range as the air-flow runs, the velocity distribution shown in Figure 6 is used in analyzing the sediment-transport runs.

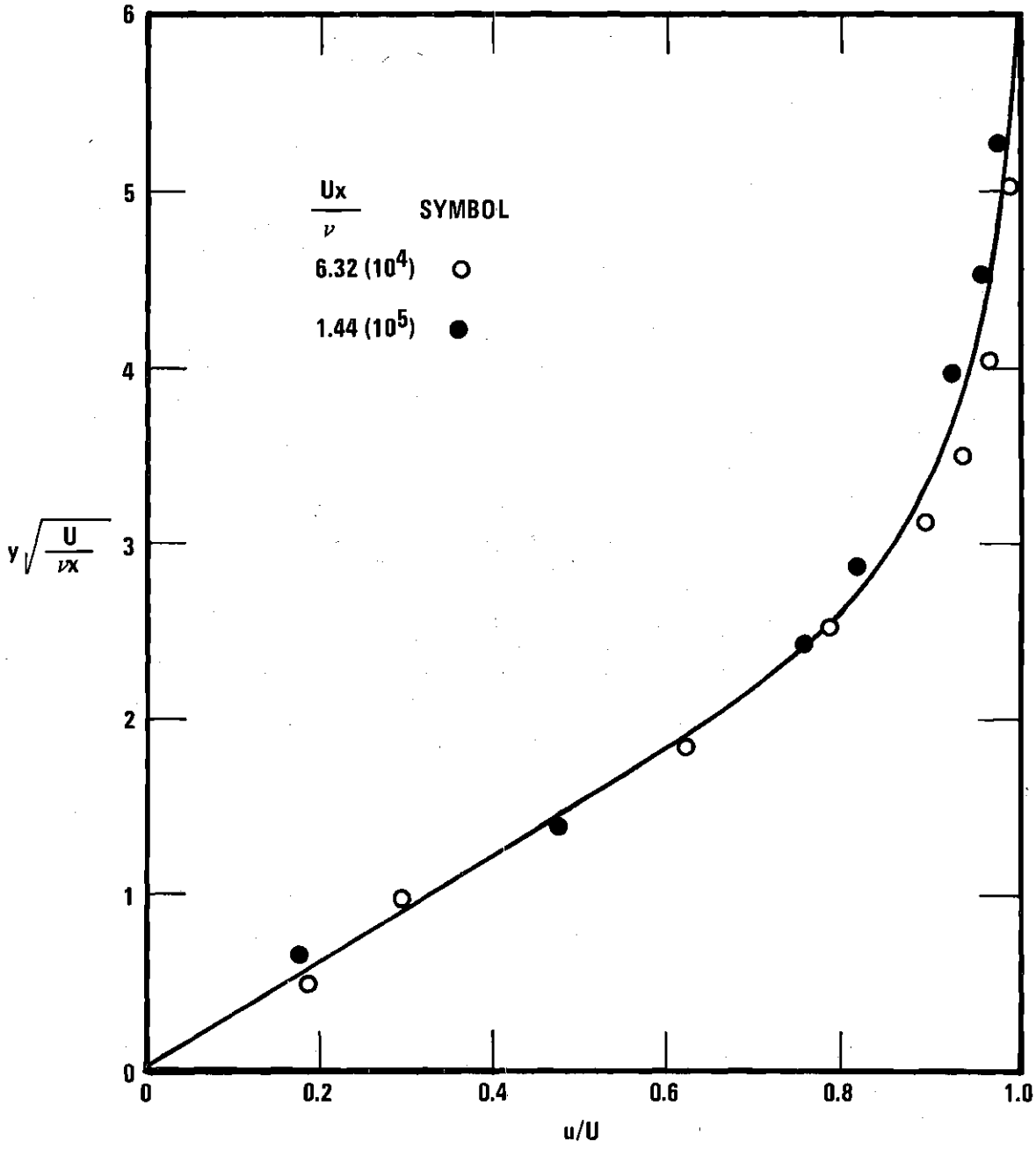

Figure 6. Velocity Distribution in the Test Section

Analysis of Experimental Results

Prior to reduction of the transport data into the functional form of Equation 12, the following questions have to be answered:

1. What is the velocity, u, at particle level?
2. What is the value of the angle of repose, Φ?
3. What is the bed slope?

Velocity, u

As mentioned previously, the sediment was pushed up into the water flowing through the test section forming a small mound which was so small that direct measurements of height were not possible. The effect of the small mound is pronounced upon the velocity in the vicinity of the particles which are being removed from the bed. The incipient-motion results, Table 2, were utilized to obtain a measure of the mound height. For each sediment a critical velocity, u_c, was computed from Equation 8. The value of C_D' for sediments 1, 4 and 5 (Table 1) was evaluated for spherical particles and for sediments 2, 3 and 6 was evaluated for natural sand particles having a shape factor of 0.7 as given by Albertson, Barton, and Simons (4). The ratio of computed critical velocity, u_c, to the observed mean velocity at incipient motion as listed in Table 2 is a value of u/U with which to estimate protrusion into the flow from Figure 6. The values of protrusion height computed in this manner varied from 1.6 D_g to 2.8 D_g. These values appeared to be reasonable considering that the $\frac{1}{2}$-in. long bed extension in the wake of the mound appeared to be a single layer of particles. In the absence of any recognizable trend in the computed protrusion height, the assumption is that the variation is an

indication of the accuracy of the experimental observations of incipient motion which were qualitative. Consequently a mean value of protrusion height of 2.2 D_g was used in all subsequent calculations of the velocity, u. Specifically the procedure was to calculate the value of U from the measured value of Q, to calculate the value of $y\sqrt{U/\nu x}$ using $y = 2.2\ D_g$ and x = 0.41 ft., to determine u/U from Figure 6, and finally to calculate u.

Angle of Repose, Φ

The angle of repose, Φ, is a simple concept but is difficult to determine inasmuch as Φ is a function of the gradation of the particles, σ_g, packing (porosity), particle shape, and the angularity of the material. Values of Φ for sediments 3 and 4, Table 1, were determined from the geometry of scour holes which develop around a single vertical pile subjected to oscillatory flow. The difference in the value Φ of these two sands is primarily that of particle shape since the glass beads, sediment 4, are nearly spherical whereas the Ottawa "banding" sand, sediment 3, is well rounded but is not spherical having a shape factor of about 0.7. Since the particles of sediments, 1 and 5, Table 1, are nearly spherical, the measured value of Φ = 24.7 degrees determined for sediment 4 was selected for all sediments of spherical particles.

Bed Slope

Since the mound is only about two grain diameters in height, the bed slope was taken as zero in the computation of the dimensionless independent variable -- the expression within parentheses on the right side of Equation 12.

Sediment Pickup Rate

The experimental results in dimensionless form are shown in Figure 7. Based on these results the rate of sediment pickup, except for the nickel particles, can be expressed as follows:

$$\frac{u_e}{u} = 1\ (10^{-3}) \left(\frac{C_D'}{8.2 \cos \alpha} \frac{u^2}{(s-1) g D_g} - \tan \alpha - \tan \Phi \right)^{5/2} \qquad (13)$$

No satisfactory explanation could be found for the untypical results obtained with the nickel particles. The explanation of another independent parameter, density ratio, is not convincing inasmuch as the results obtained with the Lucite particles were similar to those obtained with quartz particles.

Discussion

The most difficult of all flow phenomena to analyze are those occurring at the interface between a bed of particles and the overlying flowing fluid. The flow region close to the bed is complicated enough without considering the effects of particle pickup, deposition, and transport. The complexity of the phenomena in this region has precluded theoretical work of much utility. Similarly the large number of independent physical variables has precluded a systematic experimental approach, for example, the systematic experiments which have defined the functional relationship of the boundary-drag coefficient in a circular pipe. Because of these blocked paths to progress, the researcher turns to the alternative of attempting to analyze simpler sub-systems in the hope that these sub-systems can be combined (preferably) in a linear com-

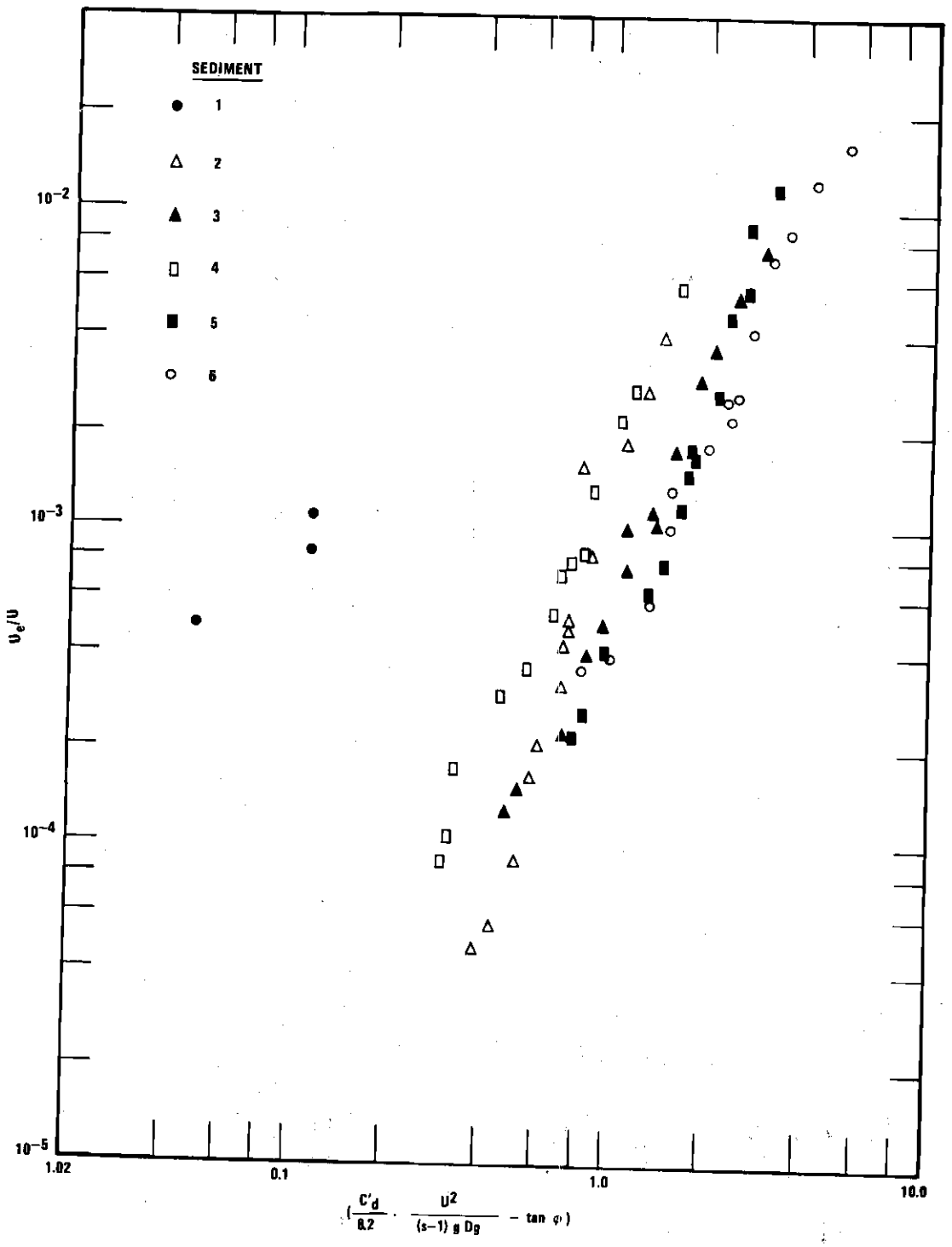

Figure 7. Sediment-Pickup Rate

bination) in order to ultimately analyze practical problems of interest. The sediment-pickup function is a sub-system of sediment transport.

The sub-system of immediate concern is that of the rate of sediment pickup without the complication of deposition simultaneously occurring at the same location on the bed. The ratio of the velocity of scour of the bed, u_e, to the fluid velocity, u, in the vicinity of the bed particles is expressed in terms of a single independent dimensionless variable. The independent variable is formulated assuming that the rate of removal of particles from the bed is proportional to the force ratio of the forces acting on a typical particle in a direction parallel to the bed and of the forces acting normal to the bed. The sub-system, sediment-pickup function, is expressed in terms of the velocity, u, in the vicinity of the particle in order that the sediment-pickup function can be used without regard to the particular flow situation from which the velocity at particle level developed. In other words the determination of u is considered to be an independent problem.

The concept of sub-systems of pickup rate and deposition rate which can be linearly combined into the equation of continuity of sediment has been pursued at the Georgia Tech Hydraulics Laboratory for several years. The first effort involved analysis of the development of a scour hole around a horizontal cylinder lying on the bed under oscillatory flow (5). In fact, the paucity of reported experimental studies from which to formulate a sediment-pickup function led to the study reported herein. Currently the same approach is being followed in a study of scour-hole development around a single vertical pile under oscillatory flow. As his graduate research study, Neilson (6) used the sediment-

pickup function in a theoretical analysis of two-dimensional dunes under oscillatory flow. In this situation, Neilson utilized irrotational flow analysis in order to determine the velocity, u, along the upstream face of the dune.

Summary

A function expressing the rate of removal of bed has been presented in terms of the following variables: coefficient of drag, particle diameter, bed slope, angle of repose, and fluid density in the vicinity of the particle. The variables of the function were established by consideration of the forces acting on a typical surface particle. The functional relationship was established by the results of an experimental study. The sediment-pickup function has been formulated as a local rate of bed removal in order to be able to incorporate the function in the differential form of the equation of continuity.

Acknowledgments

The experimental study reported herein to establish a sediment-pickup function was a portion of the first-writer's research study executed in partial fulfillment of the requirements for the degree of Doctor of Philosophy and presented to the Georgia Institute of Technology in 1965. The current research study involving scour around a vertical pile under oscillatory flow is sponsored by the U.S. Army Coastal Engineering Research Center, Contract No. DACW72-67-0017.

REFERENCES OF

APPENDIX

1. Simons, Dayrl B., and Albertson, Maurice, L., "Uniform Water Conveyance Channels in Alluvial Material," Transactions, American Society of Civil Engineers, Vol. 128, Part I, 1963, Figure 12 p. 97.

2. Chepil, W. S., "The Use of Evenly Spaced Hemispheres to Evaluate Aerodynamic Forces on a Soil Surface," Transactions, American Geophysical Union, Vol. 39, No. 3, June 1958, pp. 397-404.

3. Carstens, M. R., Neilson, F. M., and Altinbilek, H. D., "Bed Forms Generated in the Laboratory Under an Oscillatory Flow: Analytical and Experimental Study," Tech. Memo. No. 28, U.S. Army Coastal Engineering Research Center, Washington, D.C., June 1969, 105 pp.

4. Albertson, Maurice L., Barton, James R., and Simons, Dayrl B., Fluid Mechanics for Engineers, Prentice-Hall Inc., Englewood Cliffs, New Jersey, 1960, Figure 9-2, p. 399.

5. Carstens, M. R., "Part II -- Localized Scour Around a Horizontal Cylinder," Final Report (Contract No. N600(24)-59885) U.S. Navy Mine Defense Laboratory, Panama City, Florida, June 1967.

6. Neilson, F. M., "The Geometry of Stable Bed Forms Under Oscillatory Flow," Thesis presented to the Georgia Institute of Technology, Atlanta, Georgia, in 1968, in partial fulfillment of the requirements for the degree of Doctor of Philosophy.

NOTATION OF

APPENDIX

The following symbols are used in this paper:

C_D = coefficient of drag on a particle lying on the surface of the bed;

C'_D = coefficient of drag on a particle falling in a quiescent fluid;

C_L = coefficient of lift on a particle lying on the surface of the bed;

D_g = geometric mean diameter of sediment particles;

F_D = drag force on a typical particle lying on the surface of the bed;

F_L = lift force on a typical particle lying on the surface of the bed;

F_N = summation of the external forces on a particle in a direction normal to the bed (+ downward);

F_T = summation of the external forces on a particle in a direction parallel to the bed (+ in direction of flow);

g = magnitude of the acceleration of gravity;

K = $2\ k_3/k_1k_2$;

k_1, k_2 = particle-shape coefficients (projected area);

k_3 = particle-shape coefficient (volume);

k_4 = C_D/C'_D;

s = specific-weight ratio, γ_s/γ;

U = mean velocity in the test section;

u = velocity of particle level;

u_c = value of u at beginning of particle motion;

u_d = deposit velocity, that is, the velocity that the bed surface moves due to deposition;

u_e = pickup velocity, that is, the velocity that the bed surface moves due to scour;

u_t = velocity of bed movement, $u_d - u_e$;

W = submerged weight of a typical particle;

x = distance from the sediment-supply tube to the virtual origin of the laminar boundary layer;

y = coordinate normal to bed (+ upward);

α = angle of inclination of the bed from the horizontal;

γ = specific weight of the fluid;

γ_s = specific weight of the bed material;

ν = kinematic viscosity;

ρ = fluid density;

σ_g = geometric standard deviation of bed material as to size;

τ = boundary shear stress; and

Φ = angle of repose

VITA

Hilmi Dogan Altinbilek was born in Isparta, Turkey, on February 19, 1944. He graduated from Ataturk High School, Ankara, Turkey, in 1961. He graduated from the Middle East Technical University, Ankara, Turkey, with a Bachelor of Science in Civil Engineering in June of 1965. He was employed by the Middle East Technical University as a student research assistant during the school year of 1964-1965 and as a research engineer during the summer of 1965. He attended the graduate school at Georgia Institute of Technology from September 1965 to the present. In June 1966 he was awarded the degree of Master of Science in Civil Engineering with a major in hydrology.

During the school year of 1965-1966 he was a recipient of a World Student Fund Scholarship of Georgia Tech. During the period 1966-1968 he was employed as a research assistant and as such, participated in two projects of the Engineering Experiment Station of the Georgia Institute of Technology. While in graduate school, he served as vice president of International Student Organization and as a dormitory counselor. He was awarded the Outstanding International Student Award in 1968.

Mr. Altinbilek, is a member of the honorary societies Sigma Xi and Chi Epsilon; a member of the International Association for Hydraulics Research; and a student member of the American Geophysical Union; and an associate member of the American Society of Civil Engineers.

He is single.